

BOUNDARY LAYER STAGNATION POINT  
FLOW TOWARDS AN EXPONENTIALLY  
STRETCHING/SHRINKING SHEET



MASTER OF SCIENCE (MATHEMATICS)  
UNIVERSITI MALAYSIA PAHANG

UNIVERSITI MALAYSIA PAHANG

**DECLARATION OF THESIS AND COPYRIGHT**

Author's full name : SAYED QASIM ALAVI  
Date of birth : 12 AUGUST 1982  
Title : BOUNDARY LAYER STAGNATION POINT FLOW  
TOWARDS AN EXPONENTIALLY STRETCHING/  
SHRINKING SHEET

Academic Session : 2015/2016

I declare that this thesis is classified as:

- CONFIDENTIAL** (contains confidential information under the official secret Act 1972)\*
- RESTRICTED** (contains restricted information as specified by the organization where research was done)\*
- OPEN ACCESS** I agree that my thesis to be published as online open access (Full text)

I acknowledge the Universiti Malaysia Pahang reserve the right as follows:

1. The thesis is the property of University Malaysia Pahang.
2. The library of University Malaysia Pahang has the right to make copies for purpose of research only.
3. The library has the right to make copies of the thesis for academic exchange.

Certified By:

\_\_\_\_\_  
(Student's Signature)

ST 027146

New IC/ Passport Number

Date: 01 October 2015

\_\_\_\_\_  
(Signature of Supervisor)

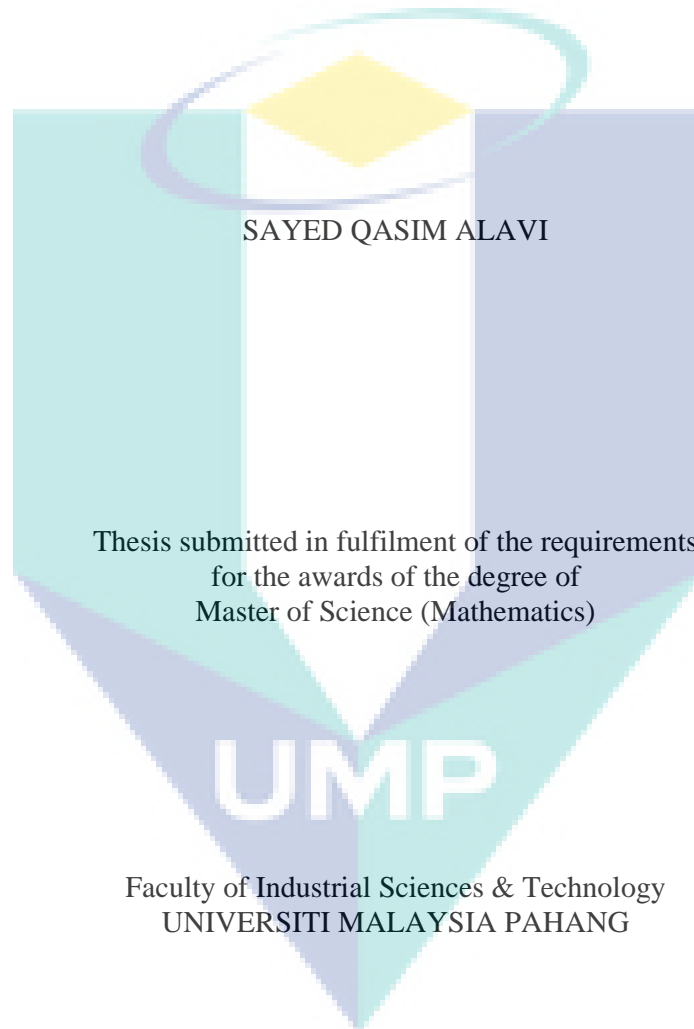
ASSOC. PROF. DR. MOHD ZUKI SALLEH

(Name of Supervisor)

Date: 01 October 2015

**NOTES** : \* If the thesis is CONFIDENTIAL or RESTRICTED, please attach with the letter from the organization with period and reasons for confidentiality or restriction.

BOUNDARY LAYER STAGNATION POINT FLOW TOWARDS  
AN EXPONENTIALLY STRETCHING/SHRINKING SHEET



October 2015

## SUPERVISOR'S DECLARATION

We hereby declare that we have checked this thesis and in our opinion, this thesis is adequate in term of scope and quality for the award of the degree of Master of Science (Mathematics).

Signature

Name of Supervisor:

DR. MOHD ZUKI BIN SALLEH

Position:

ASSOC. PROF

Date:

07/10/2015

Signature

Name of Co-supervisor:

DR. NORHAYATI BINTI ROSLI

Position:

SENIOR LECTURER

Date:

07/10/2015

Signature

Name of Co-supervisor:

DR. ABDUL RAHMAN BIN MOHD KASIM

Position:

SENIOR LECTURER

Date:

07/10/2015

The logo of Universiti Malaysia Perlis (UMP) is centered on the page. It features a stylized yellow diamond shape at the top, with a blue and green circular swoosh around it. Below this, the letters 'UMP' are written in a large, bold, white font. The background of the logo is a light blue and green gradient.

UMP

### STUDENT'S DECLARATION

I hereby declare that the work in this thesis is my own except for quotations and summaries which have been duly acknowledged. The thesis has not been accepted for any degree and is not concurrently submitted for award of other degree.

Signature :  
Name : SAYED QASIM ALAVI  
ID Number : MSE13001  
Date : 07/10/2015





## ACKNOWLEDGEMENT

Alhamdulillah, thanks to almighty Allah for giving me strength, success and good health to complete my master thesis properly and on time. First of all, my deepest thanks to my honourable supervisor Assoc. Prof. Dr. Mohd Zuki bin Salleh, my honourable co-supervisor Dr. Norhayati binti Rosli and Dr. Abdul Rahman bin Mohd Kasim, for their useful and valuable guidance, time and support throughout this research. It is mentionable that from the beginning of this investigation, I was not familiar on conducting research. By continuous help, support and encouragement from my dear supervisors, I had the confidence to do my research as scheduled.

I also would like to express my appreciation to the Ministry of Education (MOE) of Malaysia and Research and Innovation Department of University Malaysia Pahang (UMP) for sponsoring and funding my research articles, which have been submitted to conferences and journals, through Vote: RDU 121302 (RACE) and RDU 140111(FRGS).

Also my sincere appreciation is owed to the Ministry of Higher Education (MOHE) of Afghanistan for giving me a scholarship through World Bank funding. Besides, special thanks to Bamyán University (BU) for my study leave and sending me overseas to Malaysia to pursue my master degree and to upgrade my academic qualification.

Special thanks to my beloved mother, wife and children, for their constant support and encouragement throughout my duration of my study. I really appreciate their kindness, since they have encountered with lots of life difficulties, but still they sent me to university.

Last but never least, my heartfelt appreciation is presented to my best friends who supported, helped and guided me throughout this study. A world of thanks is dedicated to Applied & Industrial Mathematics research group for their helpful and useful discussions.

## ABSTRACT

The problem of boundary layer flow has many applications in industries and engineering field. Some of these applications are drawing of plastic films, glass fiber production, hot rolling and many others in industrial manufacturing processes. The final product characteristics requested depends on the cooling liquid used and the rate of stretching. Four common boundary conditions are used in modelling of convective boundary layer flow problems, which are constant or prescribed wall temperature, constant or prescribed surface heat flux, Newtonian heating and convective boundary conditions. In this thesis, the mathematical modelling for the effects of radiation and MHD on stagnation point flow and heat transfer over an exponentially stretching/shrinking sheet is investigated. In this study, the governing boundary layer equations are first transformed using an appropriate similarity transformation, which are then solved numerically by using Keller-box method. MATLAB software is used as a tool in order to obtain the numerical solution. Five parameters are investigated in this problem, which are Prandtl number  $Pr$ , velocity ratio parameter  $v$ , conjugate parameter  $\chi$ , magnetic parameter  $M$  and thermal radiation parameter  $N_R$ . In conclusion, there are dual solution when velocity ratio parameter  $v$  satisfies  $-1.487068 \leq v \leq -0.9734$ , unique solution for  $v > -0.9734$  and no solution exist for  $v < -1.487068$ . To get a physically acceptable value in second solution, the value of Prandtl number  $Pr$  must be smaller than a critical value  $Pr_c$ . It depends on conjugate parameter  $\chi$ . While, the values of conjugate parameter  $\chi$  must be greater than some critical values  $\chi_c$  which also depends on the Prandtl number  $Pr$ . Furthermore, increasing values of Prandtl number  $Pr$  and velocity ratio parameter  $v$  has led to decrease in temperature profile while the increasing in radiation parameter  $N_R$  and magnetic parameter  $M$  has enhanced the temperature profiles.

## ABSTRAK

Permasalahan aliran lapisan sempadan banyak diaplikasikan dalam industri dan kejuruteraan. Aplikasi ini adalah pelakaran filem plastik, penghasilan gentian kaca, pengelekan panas dan pelbagai proses dalam industri pembuatan. Ciri-ciri produk akhir bergantung kepada cecair pendingin yang digunakan dan kadar perengangan. Kebiasaannya, terdapat empat syarat sempadan digunakan untuk pemodelan olakan aliran lapisan sempadan, antaranya adalah suhu dinding malar atau tetap, fluks haba malar atau tetap, pemanasan Newtonian dan syarat sempadan olakan. Dalam tesis ini, pemodelan matematik bagi kesan-kesan sinaran termal dan MHD ke atas aliran titik genangan pemindahan haba melepasi lapisan meregang/mengecut secara eksponen dikaji. Dalam kajian ini, persamaan menakluk lapisan sempadan pertama sekali dijemakan dengan menggunakan kaedah penjelmaan setara yang sesuai, kemudiannya diselesaikan secara berangka dengan menggunakan kaedah kotak Keller. Perisian MATLAB digunakan sebagai program komputer untuk pengekodan berangka. Lima parameter digunakan dalam permasalahan ini, iaitu nombor Prandtl  $Pr$ , parameter nisbah halaju  $v$ , parameter konjugat  $\chi$ , parameter magnetik  $M$  dan parameter sinaran terma  $N_R$ . Kesimpulannya, permasalahan ini mempunyai dwi penyelesaian iaitu apabila parameter nisbah halaju  $v$  memenuhi ketaksamaan  $-1.487068 \leq v \leq -0.9734$ , penyelesaian unik bagi  $v > -0.9734$  dan ketidakwujudan penyelesaian persamaan bagi  $v < -1.487068$ . Bagi memperoleh nilai fizikal yang boleh diterima untuk penyelesaian kedua, nilai  $Pr$  mestilah lebih kecil daripada nilai kritikal  $Pr_c$  dan ia bergantung kepada nilai  $\chi$ , manakala nilai parameter konjugat  $\chi$  mestilah lebih besar daripada nilai kritikal  $\chi_c$ , yang juga bergantung kepada nilai  $Pr$ . Tambahan lagi, peningkatan nombor Prandtl  $Pr$  dan parameter nisbah halaju  $v$  memberi kesan kepada penyusutan suhu profil manakala peningkatan parameter sinaran terma  $N_R$  and parameter magnetik  $M$  meningkatkan suhu profil.

## TABLE OF CONTENTS

	<b>Page</b>
<b>SUPERVISOR'S DECLARATION</b>	ii
<b>STUDENT'S DECLARATION</b>	iii
<b>DEDICATION</b>	iv
<b>ACKNOWLEDGEMENT</b>	v
<b>ABSTRACT</b>	vi
<b>ABSTRAK</b>	vii
<b>TABLE OF CONTENTS</b>	viii
<b>LIST OF TABLES</b>	xi
<b>LIST OF FIGURES</b>	xiii
<b>LIST OF SYMBOLS</b>	xvii
<b>LIST OF ABBREVIATIONS</b>	xix
<b>CHAPTER 1                    PRELIMINERIES</b>	
1.1            Introduction	1
1.2            Boundary Layer Theory	2
1.3            Boundary Conditions	3
1.3.1    Constant/Prescribed Wall Temperature	3
1.3.2    Constant/Prescribed Surface Heat Flux	4
1.3.3    Convective Boundary Conditions	5
1.4            Keller-Box Method	6
1.5            Stagnation Point	7
1.6            Research Objective	8
1.7            Research Scope	8
1.8            Literature Review	8
1.8.1    Boundary Layer Stagnation Point Flow over a Stretching/Shrinking Sheet	8
1.8.2    Boundary Layer Stagnation Point Flow over an Exponentially Stretching/Shrinking Sheet	12
1.8.3    Radiation Effects on MHD of the Boundary Layer Stagnation Point Flow over an Exponentially Stretching/Shrinking Sheet	14

1.9	Significant of the Research	16
1.10	Thesis Outline	17
<b>CHAPTER 2</b>	<b>METHODOLOGY</b>	
2.1	Introduction	19
2.2	Governing Equations/Problem Formulation	19
	2.2.1 Similarity Transformation	21
2.3	Numerical Method: Keller-Box Method	28
	2.3.1 Finite Difference Method	28
	2.3.2 Newton's Method	32
	2.3.3 The Block Elimination Technique	36
	2.4.4 Starting Conditions	43
<b>CHAPTER 3</b>	<b>STAGNATION POINT FLOW AND HEAT TRANSFER TOWARDS AN EXPONENTIALLY STRETCHING/SHRINKING SHEET</b>	
3.1	Introduction	48
3.2	Mathematical Formulation	49
3.3	Result and Discussions	52
	3.3.1 Prescribed Wall Temperature (PWT)	52
	3.3.2 Prescribed Surface Heat Flux (PHF)	55
	3.3.3 Convective Boundary Conditions (CBC)	59
	3.3.4 Conclusion	66
<b>CHAPTER 4</b>	<b>RADIATION EFFECT ON MHD STAGNATION- POINT FLOW AND HEAT TRANSFER TOWARDS AN EXPONENTIALLY STRETCHING SHEET</b>	
4.1	Introduction	68
4.2	Mathematical Formulation	68
4.3	Results and Discussions	75
	4.3.1 Prescribed Wall Temperature (PWT)	75
	4.3.2 Prescribed Surface Heat Flux (PHF)	83
	4.3.3 Convective Boundary Conditions (CBC)	88

4.3.4	Conclusion	97
-------	------------	----

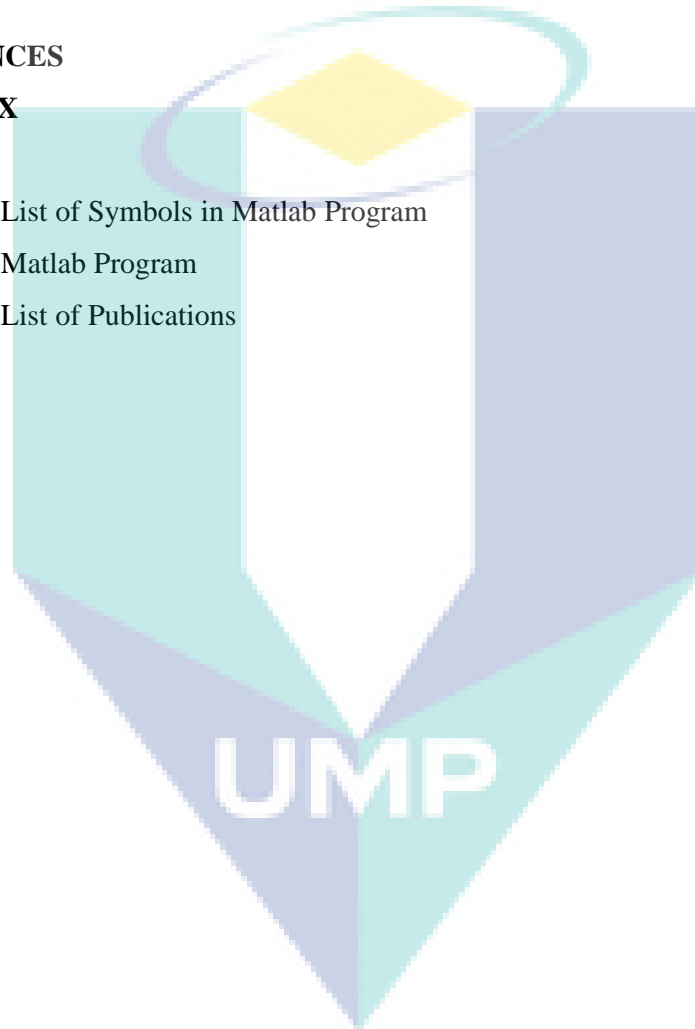
## **CHAPTER 5 CONCLUSION**

5.1	Summary and Conclusion	99
5.2	Suggestion for Future Studies	101

<b>REFERENCES</b>		103
-------------------	--	-----

## **APPENDIX**

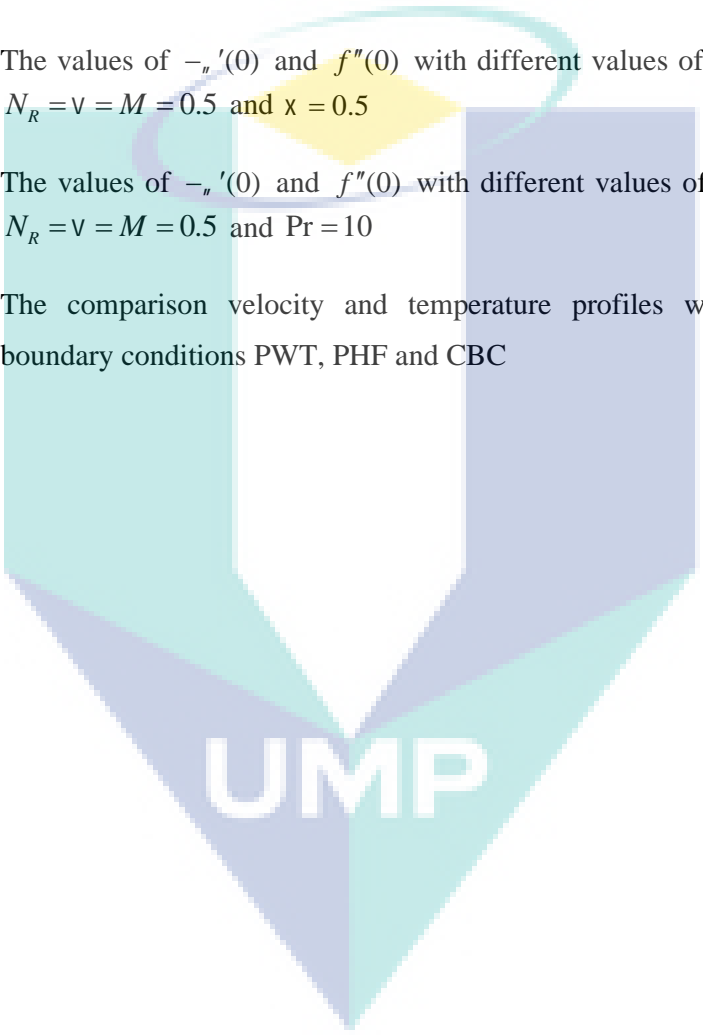
A	List of Symbols in Matlab Program	111
B	Matlab Program	112
C	List of Publications	116



## LIST OF TABLES

Table No	Title	Page
3.1	The various value the reduced Nusselt number $-n'(0)$ with different value of Pr and $\nu$	53
3.2	The comparison velocity and temperature profiles with three boundary conditions PWT, PHF and CBC	67
4.1	The comparison heat transfer coefficient $-n'(0)$ when $\nu = 0$	77
4.2	Comparison the reduced skin friction coefficient $f''(0)$ when $M = 0$	78
4.3	Values of the reduced skin friction coefficient $f''(0)$ and heat transfer coefficient $-n'(0)$ for several values of $M$ when $Pr = N_R = 1$ and $\nu = 0.2$	78
4.4	Values of the reduced skin friction coefficient $f''(0)$ and heat transfer coefficient $-n'(0)$ for different values of $N_R$ when $Pr = M = 1$ and $\nu = 0.2$	79
4.5	Values of the reduced skin friction coefficient $f''(0)$ and heat transfer coefficient $-n'(0)$ for various values of Pr when $N_R = M = 1$ and $\nu = 0.5$	79
4.6	Values of the reduced skin friction coefficient $f''(0)$ and heat transfer coefficient $-n'(0)$ with various values of $\nu$ when $N_R = M = 1$ and $Pr = 1$	80
4.7	Various values of the reduced Nusselt number for various values of $\nu$ and $N_R$ when $M = 1$ and $Pr = 1$	84
4.8	Various values of the reduced Nusselt number for various values of Pr and $M$ when $N_R = 1$ and $\nu = 0.5$	85
4.9	The comparison of $-n'(0)$ with various values of $N_R, M$ and Pr when $\nu = 0$ and $\chi \rightarrow \infty$	91

- 4.10 The values of  $-u'(0)$  and  $f''(0)$  with different values of  $M$  when  $v = \chi = N_R = 0.5$  and  $Pr = 10$  91
- 4.11 The values of  $-u'(0)$  and  $f''(0)$  with different values of  $N_R$  when  $v = \chi = M = 0.5$  and  $Pr = 10$  92
- 4.12 The values of  $-u'(0)$  and  $f''(0)$  with different values of  $v$  when  $N_R = \chi = M = 0.5$  and  $Pr = 10$  92
- 4.13 The values of  $-u'(0)$  and  $f''(0)$  with different values of  $Pr$  when  $N_R = v = M = 0.5$  and  $\chi = 0.5$  93
- 4.14 The values of  $-u'(0)$  and  $f''(0)$  with different values of  $\chi$  when  $N_R = v = M = 0.5$  and  $Pr = 10$  93
- 4.15 The comparison velocity and temperature profiles with three boundary conditions PWT, PHF and CBC 98

The logo of UMP (Universitas Muhammadiyah Purwokerto) is a large, stylized shield shape. It is divided into four quadrants by a white vertical line and a white horizontal line that meet at the center. The top-left quadrant is light blue, the top-right is light purple, the bottom-left is light green, and the bottom-right is light blue. The letters 'UMP' are written in a bold, white, sans-serif font across the center of the shield.

UMP

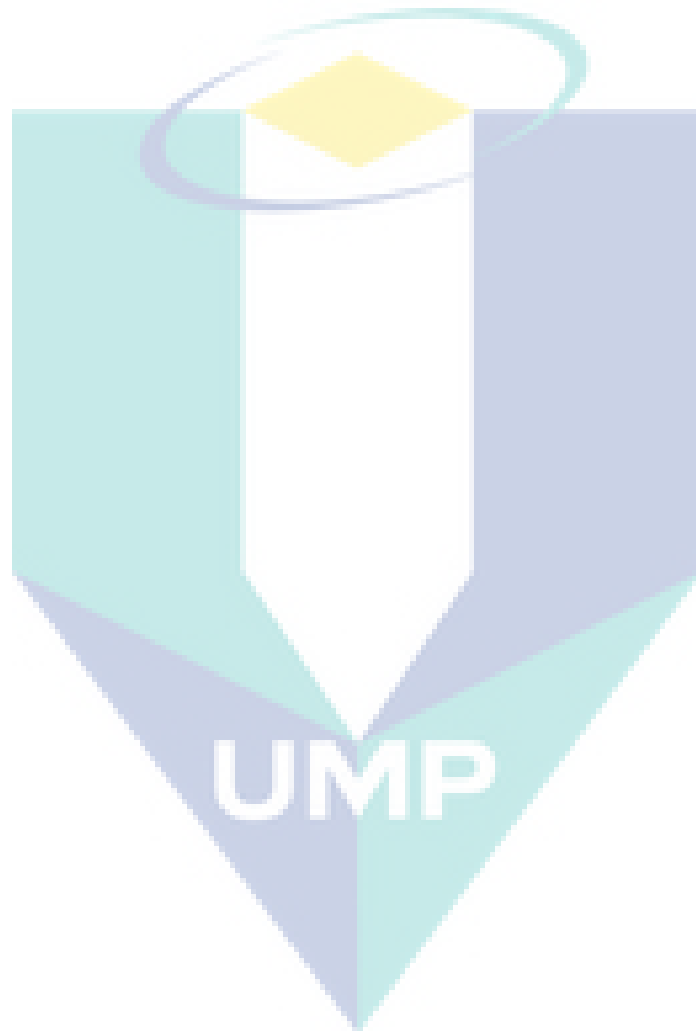
## LIST OF FIGURES

Figure No	Title	Page
1.1	Velocity and thermal boundary layer	2
2.1	Physical model and coordinate system	20
2.2	Net rectangle for difference approximations	29
2.3	Flow diagram for the Keller-box method	46
3.1	Comparison of the reduced skin friction coefficient $f''(0)$ with different values of $\nu$	53
3.2	Comparison of the reduced Nusselt number $- \theta'(0)$ with different values of $\nu$ when $Pr = 0.2$	54
3.3	Variation of temperature profile $\theta(y)$ with different values of $Pr = 0.2, 1, 3, 7, 10$ when $\nu = 0.5$	54
3.4	Variation of temperature profile $\theta(y)$ with different values of $\nu = -0.7, 0.7, 3, 7, 10$ when $Pr = 0.2$	55
3.5	The value of $Nu_x / Re_x^{1/2}$ with $\nu$	56
3.6	Variation of velocity profiles $f'(y)$ with various values of $\nu$ when $Pr = 0.2$	57
3.7	Variation of temperature profiles $\theta(y)$ with different values of $\nu = 3, 5, 7, 9$ when $Pr = 0.7$	57
3.8	Variation of temperature profile $\theta(y)$ with different values of $Pr = 0.3, 0.5, 0.7, 1, 3$ when $\nu = 3$	58
3.9	Variation of velocity profile $f'(y)$ with different values of $\nu = 3, 5, 7, 10$ when $Pr = 0.7$	58
3.10	Variation of velocity profile $f'(y)$ with different values of $\nu = -0.7, -0.3, 0.3, 0.7$ when $Pr = 0.7$	59

3.11	Variation of the reduced skin friction coefficient $f''(0)$ with $\nu$ when $\text{Pr} = 0.2$ and $\chi = 0.5$	61
3.12	Comparison of the reduced Nusselt number $- \theta'(0)$ with different values of $\nu$ when $\text{Pr} = 0.2$ and $\chi \rightarrow \infty$	61
3.13	Variation of the temperature $\theta(0)$ with $\nu$ when $\text{Pr} = 0.2$ and $\chi = 0.5$	62
3.14	Variation of the temperature $\theta(0)$ with $\text{Pr}$ when $\chi = 0.5, 1$ and $\nu = -1.2$	62
3.15	Variation of the temperature $\theta(0)$ with $\chi$ when $\text{Pr} = 0.2$ and $\nu = -1.2$	63
3.16	Temperature profile $\theta(y)$ for various values of $\nu = -1.1, -1.2, -1.3$ when $\text{Pr} = 0.2$ and $\chi = 0.5$	63
3.17	Temperature profile $\theta(y)$ for various values of $\text{Pr} = 0.1, 0.2, 0.25$ when $\nu = -1.2$ and $\chi = 0.5$	64
3.18	Temperature profile $\theta(y)$ for various values of $\chi = 0.5, 1, 2$ when $\text{Pr} = 0.2$ and $\nu = -1.2$	64
3.19	Velocity profiles $f'(y)$ for different values of $\nu = -1.1, -1.2, -1.3$ when $\text{Pr} = 0.2$ and $\chi = 0.5$	65
3.20	Velocity profiles $f'(y)$ for different values of $\nu = -0.2, 0.3, 0.7, 1.0, 1.3, 1.7, 2.2$ when $\text{Pr} = 0.2$ and $\chi = 0.5$	65
4.1	Physical model and coordinate system	69
4.2	The velocity profile $f'(y)$ with $y$ for different values of $\nu = 0, 0.5, 1, 1.5, 2$ when $\text{Pr} = N_R = 1$ and $M = 0.1$	80
4.3	The velocity profile $f'(y)$ with $y$ for different values of $M = 0, 0.5, 1$ when $\nu = 0.1, 2$ and $\text{Pr} = N_R = 1$	81
4.4	The temperature profile $\theta(y)$ with $y$ for different values of $\nu = 0.1, 0.5, 1, 2, 4$ when $\text{Pr} = N_R = 1$ and $M = 1$	81
4.5	The temperature profile $\theta(y)$ with $y$ for different values of $\text{Pr} = 0.5, 1, 2, 4, 7$ when $\nu = N_R = 1$ and $M = 1$	82

4.6	The temperature profile $\theta(y)$ with $y$ for different values of $N_R = 0.5, 1, 2, 4$ when $Pr = \nu = 1$ and $M = 1$	82
4.7	The temperature profile $\theta(y)$ with $y$ for different values of $M = 0, 1, 2, 4$ when $Pr = N_R = 1$ and $\nu = 0.2$	83
4.8	The temperature profile $\theta(y)$ with $y$ for different values of $\nu = 0.1, 0.5, 1, 2$ when $Pr = N_R = 1$ and $M = 1$	85
4.9	The temperature profile $\theta(y)$ with $y$ for different values of $Pr = 0.5, 1, 2, 4, 7$ when $N_R = \nu = 1$ and $M = 1$	86
4.10	The temperature profile $\theta(y)$ with $y$ for different values of $M = 0, 1, 2, 4$ when $Pr = N_R = 1$ and $\nu = 0.2$	86
4.11	The temperature profile $\theta(y)$ with $y$ for different values of $N_R = 0.5, 1, 2, 4$ when $Pr = \nu = 1$ and $M = 1$	87
4.12	The velocity profile $f'(y)$ with $y$ for different values of $\nu = 0.3, 0.5, 0.7, 1.3, 1.5, 1.7$ when $Pr = N_R = 1$ and $M = 0.5$	87
4.13	The velocity profile $f'(y)$ with $y$ for different values of $M = 0.0, 0.3, 0.5, 0.7, 0.9$ when $\nu = 0.2, 2$ and $Pr = N_R = 1$	88
4.14	The temperature profiles $\theta(y)$ for several values of $M = 0, 2, 0.5, 1, 2$ when $Pr = N_R = \nu = 0.5$ and $\chi = 0.5$	94
4.15	The temperature profiles $\theta(y)$ for several values of $N_R = 0.2, 0.5, 1, 2$ when $Pr = M = \nu = 0.5$ and $\chi = 0.5$	94
4.16	The temperature profiles $\theta(y)$ for several values of $\chi = 0, 2, 0.5, 1, 2$ when $Pr = M = \nu = 0.5$ and $N_R = 0.5$	95
4.17	The temperature profiles $\theta(y)$ for several values of $Pr = 0, 2, 0.5, 1, 2$ when $N_R = M = \nu = 0.5$ and $\chi = 0.5$	95
4.18	The temperature profiles $\theta(y)$ for several values of $\nu = 0, 2, 0.5, 1, 2$ when $N_R = M = Pr = 0.5$ and $\chi = 0.5$	96
4.19	The velocity profiles $f'(y)$ for several values of $\nu = 0, 0.4, 0.8, 1.3, 1.6, 2.0$ when $N_R = M = Pr = 0.5$ and $\chi = 0.5$	96

- 4.20 The velocity profiles  $f'(y)$  for several values of  $M = 0.2, 0.5, 1, 2$  when  $N_R = \kappa = \text{Pr} = 0.5$  and  $\nu = 0.5, 1.7$  97



## LIST OF SYMBOLS

$a, b, c$	Constant
$B_0$	Uniform magnetic field
$C_f$	Local skin friction coefficient
$C_{fx}$	The reduced skin friction coefficient
$f$	Dimensionless stream function
$F_x, F_y$	Body force in $x, y$ direction, respectively
$h$	Heat transfer coefficient
$h_f$	Heat transfer coefficient for convective boundary conditions
$k$	Thermal conductivity
$k^*$	Mean absorption coefficient
$L$	Length of plate surface
$M$	Magnetic parameter
$N_R$	Radiation parameter
$Nu_x$	Local Nusselt number
$Pr$	Prandtl number
$Pr_c$	Critical value of Prandtl number
$q_w$	Surface heat flux
$Re$	Reynolds number
$Re_x$	Critical value of Reynolds number
$T$	Temperature
$T_f$	Fluid temperature
$T_w$	Wall temperature
$T_\infty$	Ambient temperature
$u, v$	Velocity component in $x, y$ direction, respectively
$U_e$	External velocity
$U_w$	Stretching velocity

$U$	Free stream velocity
$x, y$	Cartesian coordinate

### Greek Symbol

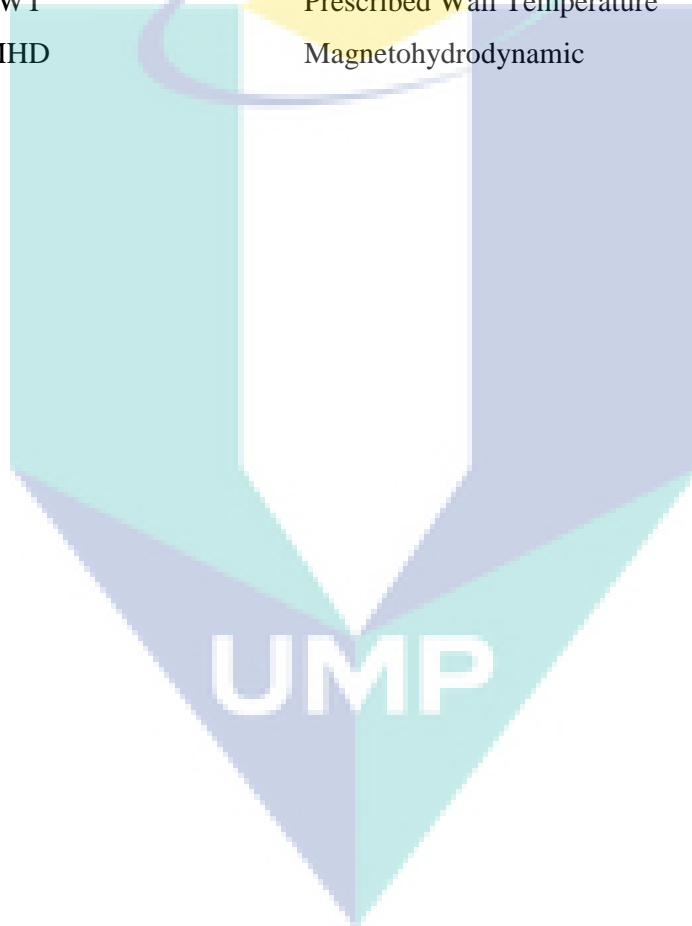
$\Gamma$	Thermal diffusivity coefficient
$\beta$	Thermal expansion coefficient
$\delta$	Boundary layer thickness
$\nu$	Stretching/shrinking parameter
$\lambda$	Conjugate parameter for convective boundary conditions
$\lambda_c$	Critical value of conjugate parameter convective boundary conditions
$\eta$	Dimensionless similarity variable
$\mu$	Dynamic viscosity
$\nu$	Kinematic viscosity
$\rho$	Fluid density
$\sigma$	Electric conductivity
$\sigma^*$	Stefan-Boltzman constant
$\theta$	Dimensionless temperature
$\psi$	Stream function

### Subscript

$\infty$	Outer boundary layer conditions
----------	---------------------------------

**LIST OF ABBREVIATIONS**

CBC	Convective Boundary Conditions
CHF	Constant Surface Heat Flux
CWT	Constant Wall Temperature
NH	Newtonian Heating
PHF	Prescribed Surface Heat Flux
PWT	Prescribed Wall Temperature
MHD	Magnetohydrodynamic



## CHAPTER 1

### PRELIMINARIES

#### 1.1 INTRODUCTION

Heat transfer is defined as the thermal energy transfer from a hotter object to a cooler object. The transition can be made by conduction, radiation and convection. Heat transfer by direct molecular contact which takes place without significant molecules being moved in solids is called conduction. Conduction heat transfer can also take place through direct contact of two bodies with different temperatures. Radiation heat transfer takes place by the transition of heat through electromagnetic waves. Electromagnetic waves can pass through a vacuum and also go through materials. In this study, convection heat transfer will be considered. The transition of heat from one place to another, through the physical movement of fluids and which, usually takes place between a solid surface and fluid molecules through physical contact. Liquids and gases are fervently used for dominant form of heat transfer. The convective mode of heat transfer basically occurs into three elementary processes, which are free, forced and mixed convection (Baehr and Stephan, 1994).

Forced convection happens when fluid motion is generated mechanically by external forced like a fan, blower, nozzle or jet. Fluid motion related to a surface can be generated by moving an object, such as a missile, through a fluid. Otherwise, the free convection happens when the fluid motion is generated by gravitational field. Occurrence of free convection requires fluid density change. In free convection, temperature changes are primarily due to variations in density. Fluid flow and heat transfer link to each other because of this continuity process from buoyancy to a difference in temperature. An increase in the rate of heat exchange normally uses forced

convection. Heat radiator systems and regulatory temperature systems in the body's circulatory system, are examples of forced convection (Merkin and Pop, 2011).

Convective heat transfer can also be classified as having either internal or external flow. Free, forced and mixed convection processes may be divided into having an external flow over immersed body such as flat plates, cylinder, sphere or an internal flow in ducts such as pipes, channels and enclosures. The resultant flow can further be categorized as laminar (stable) or turbulent (unstable) flow. Laminar flow is smooth, with a particle of fluid moving steadily in a smooth line parallel to a surface, while on the other hand, turbulent flow is described as chaotic of fluid moving unsteadily (Incropera, 2011).

## 1.2 BOUNDARY LAYER THEORY

The Ludwig Prandtl (1875-1953) on August 1904, introduced and developed the boundary layer theory which states that a thin layer (region) sticks to a surface that is embedded in a fluid motion field. This region (thin layer) near the surface is called the boundary layer (Schlichting, 1979). Figure 1.1 considers the fluid flow on a flat plate which introduces the concept of the boundary layer which states that the boundary layer is the thin layer near the flat plate surface where its viscosity should not be neglected. Also, in the boundary layer, the frictional force must be considered while outside the boundary layer, the frictional force is too small and can be neglected (Schlichting, 1979).

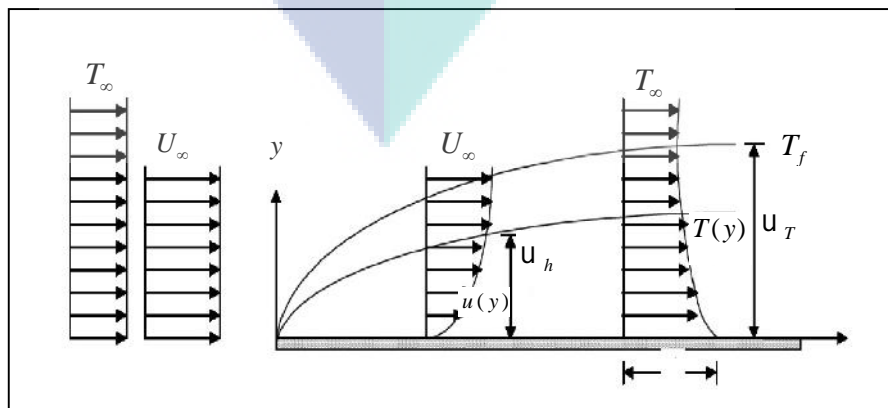


**Figure 1.1:** Velocity and thermal boundary (Mohamed, 2013)

Boundary layer equations can be derived by setting a few assumptions on the boundary layer flow which are (Ahmad, 2009);

- (i) The viscous effects are limited in a boundary layer only. The viscous effects outside of the boundary layer are not important.
- (ii) The boundary layer is smaller than the flat plate surface. If  $\delta$  is the boundary layer thickness and  $L$  is the length of flat plate surface, then  $\delta/L \leq 1$ . Also,  $x = O(L)$  and  $y = O(\delta)$ .
- (iii) The fluid obeys the no slip condition on a plate surface while the free stream velocity at the outside of the boundary, when  $u(x,0) = 0$ ,  $v(x,0) = 0$ ,  $u(x,\infty) = U_\infty$  and  $v(x,\infty) = 0$  where  $u$  and  $v$  are velocity component in  $x$  and  $y$  direction, respectively, also  $U_\infty$  is free stream velocity.
- (iv) In the boundary layer, let  $u = O(U_\infty)$ .

### 1.3 BOUNDARY CONDITIONS

Generally, there are four common heating processes specifying the wall-to-ambient temperature distributions (Merkin, 1994). These are the constant/prescribed wall temperature (CWT/PWT), the constant/prescribed surface heat flux (CHF/PHF), the Newtonian heating (NH) and the convective boundary conditions (CBC). In this research, three types of boundary conditions are considered namely the prescribed wall temperature (PWT), the prescribed surface heat flux (PHF) and the convective boundary conditions (CBC). The precise mathematical form of the boundary conditions depends on the specific problem.

#### 1.3.1 Constant/Prescribed Wall Temperature

Usually, constant wall temperature and prescribed surface heat flux are applied as boundary conditions in modelling natural convection flow. A constant wall temperature is the thermal boundary condition which can be imposed at the inside wall

of the duct. For constant wall temperature, the temperature  $T_w$  is constant, and boundary condition is

$$T_w = T_\infty + T_0 e^{\frac{x}{2L}}, \quad (1.1)$$

where  $T_\infty$  is the stream temperature assumed to be constant,  $T_0$  is a constant which measures the rate of temperature increase along the sheet,  $L$  is the reference length, In addition, the heat transfer coefficient in the laminar flow is strongly dependent on the thermal boundary conditions. In laminar flow, the thermal boundary layer has the biggest effects on the heat transfer coefficient. This boundary condition is approximated in condensers, evaporators and liquids to the gas heat exchangers with high velocity liquid flows (Kakac et al., 2013).

A number of researches on the boundary layer flow on exponentially stretching with constant wall temperature have been done. For example, Sajid and Hayat (2008) and Bidin and Nazar (2009) have solved analytically and numerically the effect of radiation on the boundary layer flow and heat transfer over an exponentially stretching sheet, respectively. Moreover, the effect of radiation on MHD flow and heat transfer on an exponentially stretching sheet with constant wall temperature was solved numerically and analytically by Ishak (2011) and Mabood et al. (2014), respectively. Further, Ishak (2011) studied MHD flow and heat transfer over an exponentially stretching sheet with radiation effects with constant wall temperature.

### 1.3.2 Constant/Prescribed Surface Heat Flux

For constant surface heat flux  $q_w$  we first note that it is a simple matter to determine the heat transfer coefficient and the boundary condition is

$$-k \frac{\partial T}{\partial y} = q_w, \quad (1.2)$$

where  $q_w(x) = q_{w_0} \sqrt{a/2\nu L} e^{x/L}$  is the variable surface heat flux and  $k$  is thermal conductivity in the laminar flow over a flat plate, the heat transfer coefficient on a plate

is constantly maintained. There are many practical applications of constant surface heat flux over the surface, for example; electric resistance heating, nuclear heating and in a counter flows heat exchanger with equal thermal capacity rates. It is well-established that convective heat transfer depends on the form of the thermal boundary conditions imposed, with it being usual to take either a prescribed temperature or a prescribed surface heat flux on the boundary surface. However, in many problems, particularly those involving the cooling of electrical and nuclear components, the wall heat flux is known (Shu and Pop, 1998).

In addition, heat transfer from a stretching surface with constant surface heat flux is investigated by Shu and Pop (1998). Kumari et al. (1990) studied MHD flow and heat transfer over a stretching sheet with prescribed wall temperature and heat flux. Elbashbeshy and Aldawody (2010) studied the unsteady boundary layer flow and heat transfer on a stretching sheet with heat flux in the presence of a heat source or sink. Some other researchers also drew attention to investigate the boundary layer problem with the case of constant surface heat flux. For example; Pavithra and Gireesha (2014) numerically studied the unsteady boundary layer flow and heat transfer of a quiescent fluid over an exponentially stretching sheet. Boundary layer flow and heat transfer over an exponentially stretching porous sheet with the surface heat flux was investigated by Mandal and Mukhopadhyay (2013).

### 1.3.3 Convective Boundary Conditions

Recent trends and demands in heat transfer engineering have forced researchers to develop various new types of compact and light-weight heat transfer equipment with superior performance and efficiency. Consider a fluid over a sheet along the  $x$ -axis. The lower face of the sheet is in contact with another fluid a temperature  $T_f$ . The sheet is stretched and the fluid starts moving, this situation is called convective boundary condition and the boundary condition is,

$$-k \frac{\partial T}{\partial y} = h_f (T_f - T), \quad (1.3)$$

where  $T_f$  is the temperature of the hot fluid and  $h_f$  is the heat transfer coefficient. Due to the increase in the need for small-size units, the focus has been casted on the effects of the interaction between developments of the thermal boundary layer in both fluid streams, and of axial wall conduction, which usually affects heat exchange performance (Salleh et al., 2010a, 2010b).

Since an early paper written by Luikov et al. (1971), many researchers have studied the topics of conjugate heat transfer. In addition, the laminar flow and thermal boundary layer over the flat plate in a uniform stream of fluid with convective boundary condition was studied by Aziz (2009). Recently, Makinde and Aziz (2010) and Ishak (2010) investigated the MHD mixed convection flow and steady laminar boundary layer flow over a flat plate and vertical plate with convective boundary conditions, respectively. Furthermore, the stagnation point flow and heat transfer over a stretching/shrinking sheet with convective boundary condition was studied by Bachok et al. (2013).

#### **1.4 KELLER-BOX METHOD**

Keller (1970) introduced the Keller-box to solve differential equation problems. This method is implicit finite difference method used with Newton's method for linearization. It is suitable to solve parabolic partial differential equations and can also be modified to solve a problem in any order. This method has been used widely since it is flexible, fast, and easy to be programmed (Keller and Cebeci, 1972). The Keller-box that is used in this study is based on the explanation by Na (1979) and Cebeci and Cousteix (2005).

Kumari and Nath (1989), Nazar et al. (2002) and Ishak et al. (2008b) solved boundary layer problems using the Keller-box method. Recently, other researchers had used the Keller-box in solving the boundary layer problems including Salleh et al. (2010a), Anwar et al. (2012) and Mohamed et al. (2013). A solution by the Keller-box method involves the following four steps:

- (i) The ordinary differential equation in reducing to a first-order system.
- (ii) Writing the differential equations using the central differences.

- (iii) The resulting algebraic equations from step 2 are linearised using Newton's method and rewritten in matrix-vector form.
- (iv) The linear system is solved by using the block triadiagonal elimination technique.

The detailed procedure for the Keller-box method will be discussed in Section 2.7.

## 1.5 STAGNATION POINT

Throughout the past decades, many researchers have been interested to investigate the stagnation point flow because of the industrial scientific applicability. For example, its application in the cooling of fans electronic devices, the cooling of nuclear reactors during emergency shutdowns, the solar central receivers exposed to wind currents, and hydrodynamic processes. At a stagnation point the speed of the fluid is zero and all of the kinetic energy has been converted to internal energy and is added to the local static enthalpy. In problems of fluid mechanics, the point in the flow field where the local velocity of the fluid becomes zero is called a stagnation-point. This point exists at the surface of the object where the fluid is brought to be at rest because of a force exerted by the object. The Bernoulli equation shows that the total pressure in terms of static pressure is called stagnation where the pressure is at maximum value when the fluid velocity is zero (Jafar et al., 2011).

The stagnation point marks the location in the fluid flow where the approaching flow divides and passes on both sides along a surface. The stagnation point flow exists everywhere in the sense that, it certainly appears as a component of more complicated flow fields. For example, in some situations, the flow is stagnated by a solid wall while in others, there is a line interior to a homogeneous fluid domain or the interface between two immiscible fluids (Tilley and Weidman, 1998). There are several types of stagnations-point flows such as viscous or inviscid, steady or unsteady, two-dimensional or three dimensional, orthogonal or oblique, and forward or rear (Lok, 2008). The two dimensional stagnation point which flows moving towards a stationary plate was first studied by Hiemenz (1911), using similarity transformation to reduce the Navier-Stokes equations to nonlinear ordinary differential equations.

## 1.6 RESEARCH OBJECTIVE

This research embarks on the following objectives:

- (i) To analyse the mathematical models for the following problems:
  - a. The boundary layer stagnation point boundary layer flow and heat transfer towards an exponentially stretching/shrinking sheet.
  - b. Effects of radiation on MHD boundary layer stagnation point flow towards and exponentially stretching/shrinking sheet.
- (ii) To carry out mathematical formulation and analyses of these problems.
- (iii) To develop numerical algorithms for the computations of these problems.
- (iv) To provide theoretical predictions and mathematical formulations that will help to explain and verify experimental results in the future.

## 1.7 RESEARCH SCOPE

The flow is considered to be two-dimensional, Newtonian, incompressible and laminar. The boundary conditions are prescribed wall temperature, prescribed surface heat flux and convective boundary conditions. The Keller-box method with appropriate numerical algorithm is used to solve the set of ordinary differential equations in related problems.

## 1.8 LITERATURE REVIEW

### 1.8.1 Boundary Layer Stagnation Point Flow over a Stretching/Shrinking Sheet

During the last few decades, the viscous flow and heat transfer in the boundary layer region due to a stretching sheet has attracted a considerable attention for many researchers. In fact, it has several theoretical and technical applications in industrial manufacturing processes. Some of the applications are the aerodynamic extrusion of plastic sheets, hot rolling, wire drawing, glass-fibre production, the cooling and drying of paper and textiles (Nadeem and Lee, 2012). The two-dimensional flow of a fluid near a stagnation point is a classical problem in fluid mechanics. It was first examined by

Hiemenz (1911), who demonstrated that the Navier-Stokes equations governing flow can be reduced to an ordinary differential equation using similarity transformation. Later, Sakiadis (1961) introduced the concept of the boundary layer flow due to ambient fluid on a continuous moving surface with a constant speed.

Then, Tsou et al. (1967) certified that the Sakiadis's theoretical predictions for Newtonian fluids by means of experimental studies. In this problem, the analytical and experimental nature of the laminar and turbulent boundary layer flow and heat transfer on a continuous moving surface was investigated. An exact solution of a steady two-dimensional boundary layer flow over a linearly stretching surface was first considered by Crane (1970). Gupta and Gupta (1977) investigated two-dimensional heat and mass transfer over a stretching sheet subject to suction or blowing. In the same way, Chen and Char (1988) studied the laminar boundary layer heat transfer flow over a linearly stretching and moving plate with suction consideration, blowing and constant surface heat flux. It was found that the thermal boundary layer thickness and wall temperature reduces with increase in values of Prandtl number. The work of Hiemenz (1911) and Crane (1970) was developed by Chiam (1994), who studied the stagnation point flow towards a stretching surface.

The stagnation point flows have many applications in industrial science and engineering. Because of that many researchers have examined the two-dimensional stagnation point flow. Such as, Wang (2008) was the first to investigate the two-dimensional and axisymmetric stagnation flow towards a shrinking sheet and analysed using similarity transformation which reduces the Navier-Stokes equations to a set of nonlinear ordinary differential equations. The results of this problem showed that the unique solution exists for stretching/shrinking ( $\gamma \geq -1$ ), as well as that the boundary layer thickness becomes thinner as shrinking is decreased. Ishak et al. (2006) studied the steady mixed convection boundary layer flow near the stagnation point flow over a stretching vertical sheet immersed in an incompressible viscous fluid. In this study, the Keller-box method was used to solve for the nonlinear ordinary differential. For assisting flow, it showed that the value of the skin friction coefficient and the local Nusselt number were increasing when the buoyancy parameter increases. Meanwhile, by increasing the values of Pr, the local Nusselt number increases but the skin friction

coefficient decreases. For opposing flow, by increasing the values of the Prandtl number, both of the skin friction coefficient and the local Nusselt number have increased, but by increasing the values of the buoyancy parameter, both led decreased.

Nazar et al. (2004) studied the unsteady boundary layer on stagnation point over a stretching sheet. The governing equations were solved numerically using the Keller-box method. The numerical solutions were compared with analytical solutions, small and large time solution. Salleh et al. (2009) considered the forced convection boundary layer flow near the stagnation point with Newtonian heating. The transformed governing equations were solved by using the Keller-box method. The results showed increase in the values of Prandtl number has led to increase the temperature distribution in all cases constant wall temperature (CWT), constant surface heat flux (CHF) and Newtonian heating (NH). An increment of Prandtl number enhanced the heat transfer in case of CHF, while the wall temperature and heat transfer were decreased in both cases of CHF and NH, respectively.

In addition, there are some references of stagnation point flow that has dual solution. Ishak et al. (2010) investigated the problem of steady two-dimensional stagnation point flow of an incompressible micropolar fluid flow towards a shrinking sheet. The dual solutions were found for the shrinking sheet. In another study, Bhattacharyya (2011b) studied the similarity solutions of mass transfer and chemical reactions in the boundary layer stagnation point flows on stretching/shrinking. The results revealed the effects of the velocity ratio parameter of the dual solution for velocity field and concentration distribution. The boundary thickness for the second solution was always thicker than the first solution. Moreover, the steady two-dimensional stagnation point and heat transfer flow over a linearly stretching/shrinking sheet in a porous medium was investigated by Rosali et al. (2011). The governing equations were solved by using the Keller-box method. The solution is unique and exists for all values of the stretching/shrinking parameter for the stretching case. However, for the shrinking case, the solution is dual and exists only for the critical values of the stretching/shrinking parameter.

Recently, Bhattacharyya (2013) studied the numerical solutions of heat transfer in unsteady boundary layer stagnation point flow over a stretching/shrinking sheet. The problem was solved numerically by using the shooting method. The results showed the lower branch and upper branch. Bachok et al. (2013) investigated the dual similarity of solutions of the boundary layer stagnation point flow of nanofluid, namely, copper-water over a permeable stretching/shrinking sheet. It was found that the unique solution exists for the stretching case and dual solution for the shrinking case. Furthermore, steady axisymmetric stagnation point flows and heat transfer of an incompressible fluid over a non-linearly moving flat plate in a parallel free stream with partial slip velocity was discussed by Ro ca et al. (2014). The `bvp4c` Matlab program was used to solve the transformed self-similar equations. In this work, a two branch solution was found for the suction and opposing flow, an upper branch and lower branch solution.

The heat flux is one of the heating processes which are being considered in this study. Besides other investigations, Lin and Chen (1998) introduced an exact solution of heat transfer from a continuously stretching surface with constant temperature heat flux. The steady mixed convection boundary layer flow of incompressible and electrically conducting fluid on a vertical plate with variable continuously surface heat flux fixed in a porous medium was investigated by Elbashbeshy and Bazid (2002). The method used in this study is called the implicit finite difference method. The velocity and temperature increases with a mixed convection parameter, while they decrease with an exponent of temperature. The heat transfer and laminar flow of an incompressible micropolar fluid over a stretching surface with heat flux was examined by Ishak et al. (2008a). It was found that, with increasing values of the Prandtl number, the Nusselt number also increased.

Lastly, Elbashbeshy and Aldawody (2010) have reported the unsteady two-dimensional laminar boundary layer flow of incompressible fluid over an unsteady stretching surface with variable flux in the presence of a heat source or sink. Suali et al. (2012) have analysed the numerical solutions of the unsteady two-dimensional stagnation point flow and heat transfer towards a stretching/shrinking sheet with prescribed surface heat flux. They used the shooting method to solve the transformed nonlinear ordinary differential equations. This leads to an increase in the Prandtl

number and stretching/shrinking parameter as the values of velocity and temperature increase, but the surface temperature is reduced.

### **1.8.2 Boundary Layer Stagnation Point Flow over an exponentially Stretching/Shrinking Sheet**

Much research has been done in the boundary layer flow over a linear stretching/shrinking sheet, but not more research was done in boundary layer flow over an exponentially stretching/shrinking sheet. There are some references about the exponentially stretching surface that have been done by researchers. Firstly, Magyari and Keller (1999) investigated the similarity in the solutions of the flow and thermal boundary layer over an exponentially stretching surface. Moreover, Elbashbeshy (2001) investigated the laminar boundary layer flow and heat transfer towards an exponentially stretching continuous surface subject to suction. The exact solution of ordinary differential equations was found in this problem. This shows that increasing the values of the Prandtl number can reduce the thermal boundary layer thickness. The skin friction coefficient increases as the values of the suction parameter decreases.

In addition, the heat transfer and boundary layer flow over an exponentially stretching surface immersed in viscoelastic fluid was analysed by Khan and Sanjayanand (2005). The problem was solved analytically and numerically by employing the Runge-Kutta fourth order method with the shooting technique. The skin friction coefficient reduces by increasing the values of viscoelastic parameter and Reynolds number. The temperature distribution in the flow region reduces as Prandtl number increases, but it increases with viscoelastic parameter. Bhattacharyya (2011a) has analysed the numerical solution of the boundary layer flow and heat transfer towards an exponentially shrinking sheet. He used the shooting method to solve non-linear ordinary differential equations. The dual solutions were obtained for the velocity profile and temperature distributions. The temperature and thermal boundary layer thickness were reduced by increasing the values of the Prandtl number in both solutions.

Furthermore, Bhattacharyya (2012) investigated the steady two-dimensional boundary layer and reaction of mass transfer towards an exponentially stretching

continuous surface with an exponential stream. Fourth order Runge-Kutta method was used to solve ordinary differential equations numerically. The thickness of the viscous boundary layer in this type of flow was significantly thinner than the linear stagnation point flow over a linearly stretching sheet, due to an increase in the velocity ratio parameter where, the mass transfer enhances from the sheet, but the viscous and solute boundary layer thicknesses are reduced. Nadeem and Lee (2012) performed the steady boundary layer flow over an exponentially stretching surface in nanofluid by using a homotopy analysis method.

Bachok et al. (2012) investigated the steady two-dimensional stagnation point and heat transfer flow of nanofluid past an exponentially stretching/shrinking sheet. In this study, three nanofluids, namely Cu-water,  $\text{Al}_2\text{O}_3$ -water, and  $\text{TiO}_2$ -water were discussed. It was also found that, when the range of the shrinking/stretching parameter in the similar solution of exponentially stretching/shrinking sheets exists was larger than the linear stretching/shrinking case, that for the Cu-water nanofluid, the skin friction coefficient and local Nusselt number are higher than for the others. The two-dimensional stagnation point flow and heat transfer towards an exponentially shrinking sheet was studied by Bhattacharyya and Vajravelu (2012). The dual solution exists for shrinking sheet case. The boundary layer thickness for the second solution was always thicker than the first solution.

Recently, the analytical solutions of the boundary layer stagnation point flow past an exponentially stretching sheet with nonuniform heat generation/absorption in nanofluid was investigated by Malvandi et al. (2013). The ordinary differential equations were solved analytically by using the homotopy analysis method. Pramanik (2014) studied the boundary layer flow of a non-Newtonian fluid accompanied by heat transfer toward an exponentially stretching surface in the presence of suction or blowing at the surface. The thermal boundary layer thickness increases as the Casson parameter increases, but the momentum boundary layer thickness decreases. The dimensionless skin friction was lower for blowing than for that of suction. Also, the radiation parameter increases as the temperature increased.

In this thesis, the two-dimensional stagnation point flow over an exponentially stretching/shrinking sheet is considered. Three boundary conditions are considered namely prescribed wall temperature, prescribed surface heat flux and convective boundary conditions. This problem has not been presented and published previously.

### **1.8.3 Radiation Effects on Magnetohydrodynamic of the Boundary Layer Stagnation Point Flow over an Exponentially Stretching/Shrinking Sheet**

The thermal radiation or radiation on heat transfer has been used for a long time and in many ways. The most important result of the study of radiation heat transfer is the black body radiation spectral relationship that was a useful tool for analysing of radiation heat transfer, which was first presented by Max Planck in year 1900. The transfer of heat from one surface to another through an intervening space is called thermal radiation. Thermal radiation is the energy associated with photons emitted from, or absorbed by, a material (Rolle, 2014; Makinde, 2010).

Sajid and Hayat (2008) studied the exact solution for two dimensional boundary layer flow over an exponentially stretching sheet with the effect of radiation and Bidin and Nazar (2009) investigated this problem numerically. The thermal boundary layer thickness decreases by increasing the values of the Prandtl number, but the values of the Eckert number and radiation parameter decreases. The problem of the radiation effect on unsteady mixed convection boundary layer flow and heat transfer of viscous fluids in the presence of a magnetic field and internal heat generation or absorption over an exponentially stretching sheet was considered by Elbashbeshy et al. (2012). For a solution to this problem, the authors used NDSolve subroutine in Mathematica. The values of the skin friction coefficient decreased by increasing in values of the Prandtl number, the unsteadiness, the section and the magnetic parameters. While, when increasing the values of the dimensionless coordinate, the thermal radiation, the heat generation/absorption, and the permeability parameters, the value of skin friction coefficient also had increased.

In 1918, the MHD flow gained interest, when the electromagnetic pump was invented by Hartmann. In recent years, many researchers studied the non-uniform

transverse magnetic field because of its applications in the loads of engineering systems (Davidson, 2001). For example, its application in the polymer industry using hydro magnetic techniques was employed by the cooling of continuous strips or filaments by drawing them through a quiescent fluid (Hamad, 2011).

There are some literatures about the MHD flows. Mahapatra and Gupta (2001) studied numerically the steady two-dimensional MHD stagnation point flow of incompressible viscoelastic fluids over a stretched surface. The MHD boundary layer stagnation point flow of a micropolar fluid due to a nonlinear stretching surface was investigated by Hayat et al. (2009) using Homotopy analysis method. It was found that, when the stretching/shrinking parameter increases the momentum boundary layer thickness decreases.

In addition, Aman et al. (2013) investigated the effects of slip on the MHD stagnation point flow due to a stretching/shrinking sheet. The two dimensional MHD stagnation point flow over a linear stretching surface was investigated by Ishak et al. (2009). Abd El-Aziz (2009) studied the boundary layer flow of micropolar fluid over an exponentially stretching sheet with cooling by mixed convection flow. The coupled differential equations were solved numerically using the shooting technique with the fifth-order Runge-Kutta-Fehlberg integration scheme. Mukhopadhyay (2013) studied the MHD flow and heat transfer over an exponentially stretching sheet embedded in a thermally stratified medium and solved numerically using the shooting method. The heat transfer coefficient increases with increasing in the values of the stratification parameter, while, it decreases with the section parameter. One more important result is that, with a stronger magnetic field, fluid velocity is reduced.

Ishak (2011) investigated the effect of radiation on the MHD flow over an exponentially stretching sheet. The results showed that by increasing the values of the magnetic parameter, the temperature increases, while the velocity profile decreases. Moreover, the temperature increases as increasing the values of radiation parameter, meanwhile, the values of Prandtl number decreases. This problem was also solved analytically using Homotopy analysis method by Mabood et al. (2014).

In this thesis, the radiation effects on MHD stagnation point flow over an exponentially stretching/shrinking sheet are considered. Three boundary conditions are considered namely prescribed wall temperature, prescribed surface heat flux and convective boundary conditions. This problem was solved numerically using the Keller-box method. This problem has not been solved before.

## 1.9 SIGNIFICANCE OF THE RESEARCH

This thesis depicts the stagnation point flow over an exponentially stretching/shrinking sheet. A stagnation flow explains that the fluid motion near the stagnation region exists on a solid body where the fluid moves towards it. The stagnation region encounters the highest pressure and the highest heat transfer. It has several theoretical and technical applications in industrial manufacturing processes such as the aerodynamic extrusion of plastic sheets, hot rolling, wire drawing, glass-fiber production, and the cooling and drying of paper and textiles. Such types of flow are quite important in polymer extrusion, stretching of plastic films, cable coating, cooling of plastic strips and filaments.

The thermal radiation effect with MHD is significant in processes involving high temperature such as gas turbines, thermal energy storage and nuclear power plants. This effect is also important with power generators, MHD accelerators, the design of heat exchanges and electrostatic filters. In this thesis the radiation effects and MHD stagnation point flow are solved theoretically and numerically. Hope that our theoretical prediction and mathematical formulation will help to explain and verify experiments. For example, the engineers need some theoretical results in the form of correlation for better measure and compare their experimental data. This will consequently helps in the improvement of the existing labs and experimental facilities in the industries and will eventually increase efficiency.

## 1.10 THESIS OUTLINE

This thesis has five (5) chapters. Chapter 1 should be regarded as preliminaries with a general introduction, the boundary layer theory, boundary conditions, stagnation point, research objective, research scope, literature review and significance of the studies.

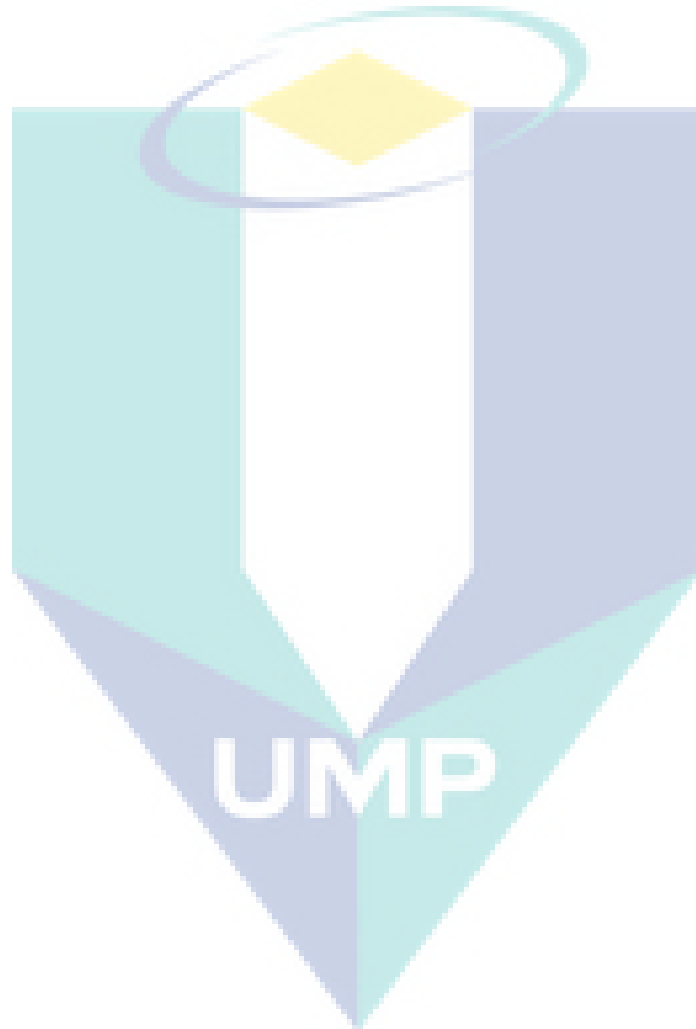
The methodology is discussed in Chapter 2, which is the derivation of governing equations, similarity transformation and the numerical method used to solve the problem of boundary layer stagnation point flows and heat transfer over an exponentially stretching/shrinking sheet with a prescribed wall temperature. This chapter will be divided into three sections. Introduction is considered in section one. The derivation of governing equation is discussed in section two. In section three, the details of the numerical method namely Keller-box are discussed. This section concerns the finite difference method, Newton's method and the block elimination technique. The Keller-box method is a suitable method to solve the problem of ordinary differential equations numerically and MATLAB software is used in order to solve using the Keller-box method.

The first problem in the stagnation point flow and heat transfer towards an exponentially stretching/shrinking sheet is discussed in Chapter 3. This problem is studied with three boundary conditions, namely prescribed wall temperature, prescribed surface heat flux and convection boundary conditions. In addition, this chapter includes four sections introduction, mathematical formulation, result and discussion and the conclusion.

Chapter 4 discusses about the second problem which is the magnetohydrodynamic stagnation point flow and heat transfer over an exponentially stretching sheet with radiation effects. This problem is also discussed with prescribed wall temperature, prescribed surface heat flux and convective boundary conditions. This chapter consists of four sections which are introduction, mathematical formulation with derivation of governing equation for second problem and derivation of reduced skin friction coefficient and reduced local Nusselt number, result and discussion and finally

conclusion. Similar to Chapter 3, this problem also considered three cases of boundary conditions.

Chapter 5 contains a summary of research and some suggestions for future research. Figures and tables discussed in previous chapter will be used in order to make comparisons in extended research by either numerical calculation or experimental study.



## CHAPTER 2

### METHODOLOGY

#### 2.1 INTRODUCTION

This chapter discusses the derivation of boundary layer equations for first problem, similarity transformation and the Keller-box as the numerical method to solve the problem. This chapter begins with a detailed discussion on the governing equations including the derivation of governing equation and the similarity in transformation. The formulation of the governing equation of the boundary layer stagnation point flow and heat transfer towards an exponentially stretching sheet with prescribed wall temperature, prescribed surface heat flux and convective boundary conditions are considered. Lastly, a detailed discussion on the algorithm of a numerical method, which is known as the Keller-box method and it used to solve all the problems in this study.

#### 2.2 GOVERNING EQUATIONS / PROBLEM FORMULATION

Consider the problem of stagnation point boundary layer flow and heat transfer over an exponentially stretching/shrinking sheet as shown in Figure 2.1. The Cartesian coordinate system is used in such a way that the  $x$ -axis is along the surface of the sheet and the  $y$ -axis is normal to it. It is assumed that  $U_e = a \exp(x/L)$  is the free stream velocity and  $a > 0$  is the straining velocity rate, the velocity stretching/shrinking sheet is  $U_w = b \exp(x/L)$ ,  $b$  is the stretching/shrinking velocity rate with  $b > 0$  for stretching and  $b < 0$  shrinking and  $T_w = T_\infty + T_0 \exp(x/2L)$  is the surface temperature,  $T_\infty$  is the stream temperature assumed to be constant,  $T_0$  is a constant which measures the rate of temperature increase along the sheet and  $L$  is the reference length. (Yacob et al., 2011).

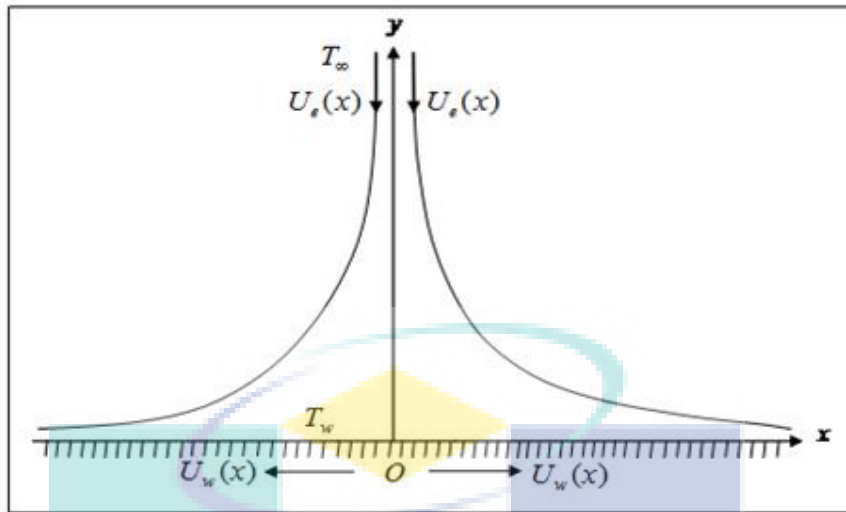


**Figure 2.1:** Physical model and coordinate system

The boundary layer equations are written as

$$\frac{\partial u}{\partial x} + \frac{\partial v}{\partial y} = 0, \quad (2.1)$$

$$u \frac{\partial u}{\partial x} + v \frac{\partial u}{\partial y} = U_e \frac{dU_e}{dx} + \epsilon \frac{\partial^2 u}{\partial y^2}, \quad (2.2)$$

$$u \frac{\partial T}{\partial x} + v \frac{\partial T}{\partial y} = \Gamma \frac{\partial^2 T}{\partial y^2}. \quad (2.3)$$

where  $u$  and  $v$  are the components of velocity in  $x$ - and  $y$ - axes, respectively.  $T$  is the temperature,  $\epsilon$  is the kinematic fluid viscosity and  $\Gamma$  is the thermal diffusivity of the fluid. The boundary conditions are given by:

$$u = U_w(x), \quad v = 0, \quad \text{at } y = 0, \quad (2.4)$$

$$T = T_w = T_\infty + T_0 e^{\frac{x}{2L}} \text{ (PWT)}, \quad \text{at } y = 0, \quad (2.5)$$

$$\frac{\partial T}{\partial y} = -\frac{q_w}{k} \text{ (PHF)} \quad \text{at } y = 0, \quad (2.6)$$

$$-k \frac{\partial T}{\partial y} = h(T_f - T) \text{ (CBC)}, \quad \text{at } y = 0, \quad (2.7)$$

$$u = U_e(x), \quad T \rightarrow T_\infty \quad \text{as } y \rightarrow \infty. \quad (2.8)$$

where  $q_w(x) = q_{w_0} \sqrt{a/2\nu L} e^{x/L}$  is the variable surface heat flux.

### 2.2.1 Similarity Transformation

We consider the stream function  $\mathbb{E} = \mathbb{E}(x, y)$  related to the velocities  $u$  and  $v$ , according to the equations,

$$u = \frac{\partial \mathbb{E}}{\partial y}, \quad (2.9)$$

$$v = -\frac{\partial \mathbb{E}}{\partial x}. \quad (2.10)$$

A particularly useful similarity transformation is adopted from Sajid and Hayat (2008);

$$\mathbb{E} = \sqrt{(2avL)} e^{\frac{x}{2L}} f(y), \quad (2.11)$$

$$y = y \sqrt{\left(\frac{a}{2\nu L}\right)} e^{\frac{x}{2L}}, \quad (2.12)$$

$$\theta(y) = \frac{T - T_\infty}{T_w - T_\infty} \quad (\text{PWT}), \quad (2.13)$$

$$\theta(y) = \left(\frac{k}{q_w}\right) (T - T_\infty) \sqrt{\left(\frac{a}{2\nu L}\right)} e^{\frac{x}{2L}} \quad (\text{PHF}), \quad (2.14)$$

$$\theta(y) = \frac{T - T_\infty}{T_f - T_\infty} \quad (\text{CBC}), \quad (2.15)$$

where  $y$  is the similarity variable,  $f(y)$  is the dimensionless stream function and  $\theta(y)$  is the dimensionless temperature. Using Eq. (2.9), the velocity component  $u$  derives as

$$\begin{aligned} u &= \frac{\partial}{\partial y} \left( \sqrt{(2avL)} e^{\frac{x}{2L}} f(y) \right), \\ &= \left( \sqrt{(2avL)} e^{\frac{x}{2L}} f'(y) \right) \left( \sqrt{\frac{a}{2\nu L}} e^{\frac{x}{2L}} \right), \end{aligned}$$

$$= a e^{\frac{x}{L}} f'(y). \quad (2.16)$$

By using Eq. (2.10) the velocity component  $v$  derives as

$$\begin{aligned} v &= -\frac{\partial}{\partial x} \left( \sqrt{(2avL)} e^{\frac{x}{2L}} f(y) \right), \\ &= -\sqrt{(2avL)} \left( \frac{1}{2L} e^{\frac{x}{2L}} f(y) + \frac{y}{2L} e^{\frac{x}{2L}} f'(y) \right), \\ v &= -\sqrt{\frac{va}{2L}} e^{\frac{x}{2L}} \{f(y) + y f'(y)\}. \end{aligned} \quad (2.17)$$

Using the similarity variable (2.12) and the velocity components Eqs. (2.16) and (2.17) can be written as

$$\frac{\partial u}{\partial x} = \frac{a}{L} e^{\frac{x}{L}} f'(y) + e^{\frac{x}{L}} f''(y) \frac{ya}{2L}, \quad (2.18)$$

$$\frac{\partial v}{\partial y} = -\sqrt{\frac{va}{2L}} e^{\frac{x}{2L}} \{2f'(y) + y f''(y)\},$$

$$\frac{\partial y}{\partial y} = \sqrt{\frac{a}{2vL}} e^{\frac{x}{2L}},$$

$$\frac{\partial v}{\partial y} = \frac{\partial v}{\partial y} \frac{\partial y}{\partial y} = \frac{a}{2vL} e^{\frac{x}{L}} \{2f'(y) + y f''(y)\}. \quad (2.19)$$

Substituting Eqs.(2.18) and (2.19) into Eq. (2.1), the continuity equation can be derives as

$$\frac{a}{L} e^{\frac{x}{L}} f'(y) + e^{\frac{x}{L}} f''(y) \frac{ya}{2L} - \sqrt{\frac{va}{2L}} e^{\frac{x}{2L}} \{2f'(y) + y f''(y)\} \sqrt{\frac{a}{2vL}} e^{\frac{x}{2L}} = 0,$$

$$\frac{a}{L} e^{\frac{x}{L}} f'(y) + e^{\frac{x}{L}} f''(y) \frac{ya}{2L} - \frac{a}{2L} e^{\frac{x}{L}} \{2f'(y) + y f''(y)\} = 0,$$

$$\frac{a}{L} e^{\frac{x}{L}} f'(y) + e^{\frac{x}{L}} f''(y) \frac{ya}{2L} - \frac{a}{L} e^{\frac{x}{L}} f'(y) - e^{\frac{x}{L}} f''(y) \frac{ya}{2L} = 0.$$

This proves that the continuity equation is satisfied. For the derivation of momentum equation, the stretching velocity  $U_w$  and straining velocity  $U_e$  are written as

$$U_w = be^{\frac{x}{L}}, \quad (2.20)$$

$$U_e = ae^{\frac{x}{L}}, \quad (2.21)$$

By using the similarity transformation from Eqs. (2.12), (2.16) and the straining velocity Eq. (2.21), the results are as follows,

$$\frac{dU_e}{dx} = \frac{a}{L} e^{\frac{x}{L}}, \quad (2.22)$$

$$\frac{\partial u}{\partial y} = \frac{\partial u}{\partial y} \frac{\partial y}{\partial y} = ae^{\frac{x}{L}} f''(\mathcal{Y}) \sqrt{\frac{a}{2vl}} e^{\frac{x}{2L}}, \quad (2.23)$$

$$\begin{aligned} \frac{\partial^2 u}{\partial y^2} &= \frac{\partial}{\partial y} \left( \frac{\partial u}{\partial y} \right) = \frac{\partial}{\partial y} \left( ae^{\frac{x}{L}} f''(\mathcal{Y}) \sqrt{\frac{a}{2vl}} e^{\frac{x}{2L}} \right) \frac{\partial y}{\partial y}, \\ &= \left( ae^{\frac{x}{L}} f'''(\mathcal{Y}) \sqrt{\frac{a}{2vl}} e^{\frac{x}{2L}} \right) \left( \sqrt{\frac{a}{2vl}} e^{\frac{x}{2L}} \right), \\ &= \frac{a^2}{2vl} e^{\frac{2x}{L}} f'''(\mathcal{Y}), \end{aligned} \quad (2.24)$$

By substituting the Eqs. (2.16), (2.17) and Eqs. (2.22) to (2.24) into momentum Eq. (2.2), then

$$\begin{aligned} &ae^{\frac{x}{L}} f'(\mathcal{Y}) \left( \frac{a}{L} e^{\frac{x}{L}} f'(\mathcal{Y}) + e^{\frac{x}{L}} f''(\mathcal{Y}) \frac{ya}{2L} \right) - \sqrt{\frac{va}{2L}} e^{\frac{x}{2L}} \{ f(\mathcal{Y}) + \mathcal{Y} f'(\mathcal{Y}) \} \\ &\left( ae^{\frac{x}{L}} f''(\mathcal{Y}) \sqrt{\frac{a}{2vl}} e^{\frac{x}{2L}} \right) = ae^{\frac{x}{L}} \frac{a}{L} e^{\frac{x}{L}} + \epsilon \frac{a^2}{2vl} e^{\frac{2x}{L}} f'''(\mathcal{Y}), \\ &2 \frac{a^2}{2L} e^{\frac{2x}{L}} (f'(\mathcal{Y}))^2 - \frac{a^2}{2L} e^{\frac{2x}{L}} f(\mathcal{Y}) f''(\mathcal{Y}) = 2 \frac{a^2}{2L} e^{\frac{2x}{L}} + \frac{a^2}{2L} e^{\frac{2x}{L}} f'''(\mathcal{Y}), \\ &2f'^2 - ff'' = 2 + f''', \\ &f''' + f'f'' - 2f'^2 + 2 = 0, \end{aligned} \quad (2.25)$$

From combine the boundary conditions (2.5) and Eq. (2.13) for case prescribed wall temperature,

$$T = T_\infty + T_0 e^{\frac{x}{2L}} (\text{PWT}), \quad (2.26)$$

Using the similarity variable Eq. (2.12) to Eq. (2.15), the results are,

a. Prescribed wall temperature (PWT)

$$\begin{aligned}
 \frac{\partial T}{\partial x} &= \frac{T_0}{2L} \theta''(\eta), \\
 \frac{\partial T}{\partial y} &= \frac{\partial T}{\partial \eta} \frac{\partial \eta}{\partial y} = T_0 e^{\frac{x}{2L}} \theta'(\eta) \sqrt{\frac{a}{2\nu L}} e^{\frac{x}{2L}}, \\
 \frac{\partial^2 T}{\partial y^2} &= \frac{\partial}{\partial \eta} \left( T_0 e^{\frac{x}{2L}} \theta'(\eta) \sqrt{\frac{a}{2\nu L}} e^{\frac{x}{2L}} \right) \frac{\partial \eta}{\partial y}, \\
 &= \left( T_0 e^{\frac{x}{2L}} \theta''(\eta) \sqrt{\frac{a}{2\nu L}} e^{\frac{x}{2L}} \right) \left( \sqrt{\frac{a}{2\nu L}} e^{\frac{x}{2L}} \right).
 \end{aligned} \tag{2.27}$$

b. Prescribed surface heat flux (PHF)

$$\begin{aligned}
 \frac{\partial T}{\partial x} &= \frac{q_{w_0}}{k} \frac{1}{2L} \theta''(\eta) e^{\frac{x}{2L}}, \\
 \frac{\partial T}{\partial y} &= \frac{\partial T}{\partial \eta} \frac{\partial \eta}{\partial y} = \frac{q_{w_0}}{k} e^{\frac{x}{2L}} \theta'(\eta) \sqrt{\frac{a}{2\nu L}} e^{\frac{x}{2L}}, \\
 \frac{\partial^2 T}{\partial y^2} &= \frac{\partial}{\partial \eta} \left( \frac{q_{w_0}}{k} e^{\frac{x}{2L}} \theta'(\eta) \sqrt{\frac{a}{2\nu L}} e^{\frac{x}{2L}} \right) \frac{\partial \eta}{\partial y}, \\
 &= \left( \frac{q_{w_0}}{k} e^{\frac{x}{2L}} \theta''(\eta) \sqrt{\frac{a}{2\nu L}} e^{\frac{x}{2L}} \right) \left( \sqrt{\frac{a}{2\nu L}} e^{\frac{x}{2L}} \right), \\
 \frac{\partial^2 T}{\partial y^2} &= \frac{q_{w_0}}{k} e^{\frac{3x}{2L}} \theta''(\eta) \frac{a}{2\nu L}.
 \end{aligned} \tag{2.28}$$

c. Convective boundary condition (CBC)

For this case  $T_w = T_f = T_\infty + T_0 e^{\frac{x}{2L}}$

$$\begin{aligned}
 \frac{\partial T}{\partial x} &= \frac{T_0}{2L} e^{\frac{x}{2L}} \theta''(\eta), \\
 \frac{\partial T}{\partial y} &= \frac{\partial T}{\partial \eta} \frac{\partial \eta}{\partial y} = T_0 e^{\frac{x}{2L}} \theta'(\eta) \sqrt{\frac{a}{2\nu L}} e^{\frac{x}{2L}}, \\
 \frac{\partial^2 T}{\partial y^2} &= \frac{\partial}{\partial \eta} \left( \frac{\partial T}{\partial \eta} \right) = T_0 e^{\frac{x}{2L}} \theta''(\eta) \frac{a}{2\nu L}.
 \end{aligned} \tag{2.29}$$

By substituting velocity components equations and Eqs. (2.27) to (2.29) into Eq. (2.3), the energy equation for cases of prescribed wall temperature (PWT), prescribed surface heat flux and convective boundary condition respectively, can be derives as,

a. Prescribed wall temperature

$$\begin{aligned} & \left( ae^{\frac{x}{L}} f'(\eta) \right) \left( \frac{T_0}{2L} \eta''(\eta) \right) - \sqrt{\frac{va}{2L}} e^{\frac{x}{2L}} \{ f(\eta) + \eta f'(\eta) \}, \\ & T_0 e^{\frac{x}{2L}} \eta''(\eta) \sqrt{\frac{a}{2vL}} = r \frac{aT_0}{2vL} e^{\frac{3x}{2L}} \eta''(\eta), \end{aligned} \quad (2.30)$$

b. Prescribed surface heat flux

$$\begin{aligned} & \left( ae^{\frac{x}{L}} f'(\eta) \right) \left( \frac{q_{w_0}}{k} \frac{1}{2L} \eta''(\eta) e^{\frac{x}{2L}} \right) - \sqrt{\frac{va}{2L}} e^{\frac{x}{2L}} \{ f(\eta) + \eta f'(\eta) \}, \\ & \frac{q_{w_0}}{k} e^{\frac{x}{2L}} \eta''(\eta) \sqrt{\frac{a}{2vL}} = r \frac{q_{w_0}}{k} e^{\frac{3x}{2L}} \eta''(\eta) \frac{a}{2vL}, \end{aligned} \quad (2.31)$$

c. Convective boundary condition

$$\begin{aligned} & \left( ae^{\frac{x}{L}} f'(\eta) \right) \left( \frac{T_0}{2L} e^{\frac{x}{2L}} \eta''(\eta) \right) - \sqrt{\frac{va}{2L}} e^{\frac{x}{2L}} \{ f(\eta) + \eta f'(\eta) \} \\ & \left( T_0 e^{\frac{x}{2L}} \eta''(\eta) \sqrt{\frac{a}{2vL}} \right) = r T_0 e^{\frac{x}{2L}} \eta''(\eta) \frac{a}{2vL} e^{\frac{x}{2L}}, \end{aligned} \quad (2.32)$$

The energy equation from Eqs. (2.30) to (2.32) is yield,

$$\eta'' + \text{Pr} (f'' - f' \eta') = 0. \quad (2.33)$$

where  $\text{Pr} = \frac{\nu}{r}$  is the Prandtl number.

From the boundary conditions (2.4) and similarity transformation (2.17), the results are

$$-\sqrt{\frac{va}{2L}} e^{\frac{x}{2L}} \{ f(\eta) + \eta f'(\eta) \} = 0,$$

$$\begin{aligned}
 f(0) + 0f'(0) &= 0, \\
 f(0) &= 0.
 \end{aligned}
 \tag{2.34}$$

By substituting Eq. (2.20) into the boundary conditions (2.4), then compares with Eq. (2.16), the boundary condition becomes

$$\begin{aligned}
 be^{\frac{x}{L}} &= ae^{\frac{x}{L}}f'(y), \\
 f'(y) &= \frac{b}{a}, \\
 f'(0) &= v.
 \end{aligned}
 \tag{2.35}$$

By using the similarity transformations (2.13) to (2.15), the thermal boundary condition Eq. (2.5) to (2.7) yields

$$\begin{aligned}
 T_{\infty} + T_0 e^{\frac{x}{2L}} \theta''(y) &= T_{\infty} + T_0 e^{\frac{x}{2L}}, \\
 \theta''(y) &= 1, \\
 \theta''(0) &= 1 \text{ (PWT)}.
 \end{aligned}
 \tag{2.36}$$

$$\begin{aligned}
 \frac{\partial T}{\partial y} &= \frac{q_{w_0}}{k} e^{\frac{x}{2L}} \theta''(y) \sqrt{\frac{a}{2\nu L}} e^{\frac{x}{2L}}, \\
 -\frac{q_{w_0}}{k} \sqrt{\frac{a}{2\nu L}} e^{\frac{x}{L}} &= \frac{q_{w_0}}{k} \sqrt{\frac{a}{2\nu L}} \theta''(y) e^{\frac{x}{L}}, \\
 \theta''(y) &= -1, \\
 \theta''(0) &= -1 \text{ (PHF)}.
 \end{aligned}
 \tag{2.37}$$

$$\begin{aligned}
 T_0 e^{\frac{x}{L}} \theta''(y) \sqrt{\frac{a}{2\nu L}} &= -\frac{h}{k} \left( T_0 e^{\frac{x}{2L}} - T_0 e^{\frac{x}{2L}} \theta''(y) \right), \\
 T_0 e^{\frac{x}{L}} \theta''(y) \sqrt{\frac{a}{2\nu L}} &= -\frac{h}{k} T_0 e^{\frac{x}{2L}} (1 - \theta''(y)), \\
 \theta''(y) &= -\chi (1 - \theta''(y)), \\
 \theta''(0) &= -\chi (1 - \theta''(0)) \text{ (CBC)}.
 \end{aligned}
 \tag{2.38}$$

where  $\chi = hk^{-1} e^{\frac{x}{2L}} \sqrt{\frac{2\nu L}{a}}$  is the conjugate parameter.

By substituting Eq. (2.21) into the boundary conditions (2.8), then compares with Eq. (2.16), the boundary condition becomes

$$\begin{aligned} a e^{\frac{x}{L}} f'(y) &= a e^{\frac{x}{L}}, \\ f'(y) &\rightarrow \frac{a}{a}, \\ f'(\infty) &\rightarrow 1, \end{aligned} \tag{2.39}$$

where  $v = b/a$  is the stretching/shrinking parameter, can be noted that  $v < 0$  is for shrinking,  $v > 0$  is valid for stretching. By using the similarity transformation Eqs. (2.13) to (2.15), the thermal boundary condition Eq. (2.8) yields,

$$\begin{aligned} \theta(y) &= \frac{T_w - T_\infty}{T_w - T_\infty} \text{ (PWT)}, \\ \theta(y) &= \left( \frac{k}{q_{w0}} \right) (T_\infty - T_w) \exp\left( \frac{x}{2L} \right) \text{ (PHF)}, \\ \theta(y) &= \frac{T_w - T_\infty}{T_0 e^{\frac{x}{2L}}} \text{ (CBC)}, \\ \theta(y) &\rightarrow 0, \\ \theta(\infty) &\rightarrow 0. \end{aligned} \tag{2.40}$$

The boundary conditions (2.4)-(2.8) can be reduced as

$$\begin{aligned} f(0) &= 0, \quad f'(0) = v \text{ at } y = 0, \\ \theta(0) &= 1 \text{ (PWT) at } y = 0, \\ \theta'(0) &= 1 \text{ (PHF) at } y = 0, \\ \theta'(0) &= -x (1 - \theta(0)) \text{ (PWT) at } y = 0, \\ f'(y) &\rightarrow 1, \quad \theta(y) = 0 \text{ as } y \rightarrow \infty. \end{aligned} \tag{2.41}$$

Further discussion is in Chapter 3.

## 2.3 NUMERICAL METHOD: KELLER-BOX METHOD

The detail of the numerical scheme which is the Keller-box method is discussed in this section. Keller (1970) introduced the finite difference method for solving the parabolic partial differential equations. This method is found to be the most efficient and flexible to solve the boundary layer flow problems. This method is the implicit finite difference method used with Newton's method for linearization. Furthermore, the Keller-box method is adaptable to solve equations of any order (Na, 1979). Thus, in this section Eqs. (2.25) and (2.33) with boundary conditions (2.41) are solved for case of prescribed wall temperature by using the Keller-box method.

This section is divided into four sub-sections. Sub-section 2.7.1 discussed on the finite difference method in which the nonlinear ordinary differential equations are reduced to first order, and then written as finite difference forms using central difference. Sub-section 2.7.2 shows the Newton's method. It is used to linearise the resulting nonlinear equations before the result into matrix vector form. Finally, the linear system of ordinary differential equations with boundary conditions is solved using the block-elimination method which comes into under sub-section 2.7.3. Sub-section 2.7.4 discussed about the initial profiles.

### 2.3.1 Finite Difference Method

The Eqs. (2.25) and (2.33) are subjected to the boundary conditions (2.41) are written as a first order differential equation. For this purpose,  $f(y)$ ,  $u(y)$ ,  $v(y)$ ,  $t(y)$  and  $s(y)$  are introduced as new dependent variables, and  $s(y)$  is replaced by  $\theta(y)$  as the temperature's variable. The first order equations are as follows:

$$f' = u, \quad (2.42)$$

$$u' = v, \quad (2.43)$$

$$s' = t, \quad (2.44)$$

where  $\theta = s = s(y)$ ,  $u = u(y)$ ,  $v = v(y)$ ,  $t = t(y)$  and (') is derivative with respect to  $y$ . Subject to this definition, the Eqs. (2.25) and (2.33) can be written as

$$v' + fv - 2u^2 + 2 = 0, \quad (2.45)$$

$$\frac{1}{\text{Pr}} t' + ft - us = 0. \quad (2.46)$$

The boundary conditions are,

$$\begin{aligned} f(0) = 0, \quad u(0) = v, \quad s(0) = 1, \\ u(y) \rightarrow 1, \quad s(y) \rightarrow 0, \quad \text{as } y \rightarrow \infty. \end{aligned} \quad (2.47)$$

Figure 2.2 presents the net rectangle in the  $y$  plane. The net points are defined as,

$$\begin{aligned} y_0 = 0, \quad y_j = y_{j-1} + h_j, \quad j = 1, 2, \dots, J \\ y_j \equiv y_\infty, \end{aligned} \quad (2.48)$$

where  $h_j$  is the  $\Delta y_j$ -spacing. Here  $n$  and  $j$  are just the sequence of numbers that indicate the coordinate location, not tensor indices or exponents.

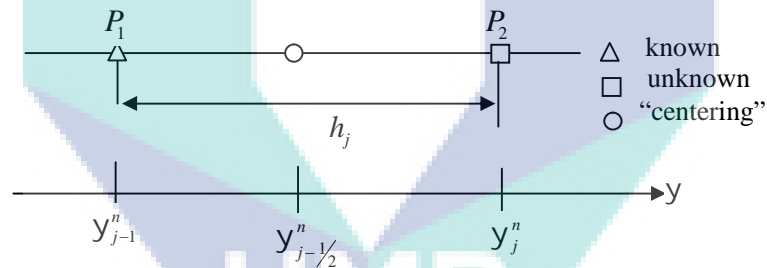


**Figure 2.2:** Net rectangle for difference approximations

The finite difference form for any points is

$$(\cdot)_{j-\frac{1}{2}}^n = \frac{1}{2} [(\cdot)_j^n + (\cdot)_{j-1}^n], \quad (2.49)$$

$$\left( \frac{\partial u}{\partial y} \right)_{j-\frac{1}{2}}^{n-\frac{1}{2}} = \frac{u_j^{n-\frac{1}{2}} - u_{j-1}^{n-\frac{1}{2}}}{h_j}. \quad (2.50)$$

We start by writing the finite difference form of Eqs. (2.42) to (2.44) by considering a mesh rectangle as shown in Figure 2.2. The approximate of finite

difference for ordinary differential Eqs. (2.42) to (2.44) are written for mid-point  $y_{j-1/2}^n$  of the segment  $P_1P_2$  by using the central difference. Hence, the following are obtained,

$$\frac{f_j^n - f_{j-1}^n}{h_j} = \frac{u_j^n + u_{j-1}^n}{2} = u_{j-1/2}^n, \quad (2.51)$$

$$\frac{u_j^n - u_{j-1}^n}{h_j} = \frac{v_j^n + v_{j-1}^n}{2} = v_{j-1/2}^n, \quad (2.52)$$

$$\frac{s_j^n - s_{j-1}^n}{h_j} = \frac{t_j^n + t_{j-1}^n}{2} = t_{j-1/2}^n. \quad (2.53)$$

The ordinary differential Eqs. (2.45) and (2.46) are stated in finite difference method by centering about the mid-point  $y_{j-1/2}$  for the line  $P_1P_2$ . The terms on the left hand side Eqs. (2.45) and (2.46) can be denoted as  $L_1$  and  $L_2$ , respectively. Then, the finite difference equation for Eqs. (2.45) and (2.46) are

$$(L_1)_{j-1/2}^{n-1/2} = 0. \quad (2.54)$$

$$(L_2)_{j-1/2}^{n-1/2} = 0. \quad (2.55)$$

Following the Eqs. (2.45) and (2.46), can be written as

$$(L_1)_{j-1/2}^n + (L_1)_{j-1/2}^{n-1} = 0, \quad (2.56)$$

$$(L_2)_{j-1/2}^n + (L_2)_{j-1/2}^{n-1} = 0, \quad (2.57)$$

$$\begin{aligned} (L_1)_{j-1/2}^n &= [v' + fv - 2u^2 + 2]_{j-1/2}^n \\ &= \frac{v_j^n - v_{j-1}^n}{h_j} + f_{j-1/2}^n v_{j-1/2}^n - 2(u_{j-1/2}^n)^2 + 2v^2 - Mu_{j-1/2}^n, \end{aligned} \quad (2.58)$$

$$\begin{aligned}
(L_2)_{j-\frac{1}{2}}^n &= \left[ \frac{1}{\text{Pr}} t' + ft - su \right]_{j-\frac{1}{2}}^n \\
&= \frac{1}{\text{Pr}} \frac{t_j^n - t_{j-1}^n}{h_j} + f_{j-\frac{1}{2}}^n t_{j-\frac{1}{2}}^n - s_{j-\frac{1}{2}}^n u_{j-\frac{1}{2}}^n.
\end{aligned} \tag{2.59}$$

By substituting Eqs. (2.58) and (2.59) into Eqs. (2.56) and (2.57), respectively

$$\begin{aligned}
\frac{v_j^n - v_{j-1}^n}{h_j} + f_{j-\frac{1}{2}}^n v_{j-\frac{1}{2}}^n - 2(u_{j-\frac{1}{2}}^n)^2 + 2 + (L_1)_{j-\frac{1}{2}}^{n-1} &= 0, \\
\frac{v_j^n - v_{j-1}^n}{h_j} + f_{j-\frac{1}{2}}^n v_{j-\frac{1}{2}}^n - 2(u_{j-\frac{1}{2}}^n)^2 + 2 &= -(L_1)_{j-\frac{1}{2}}^{n-1}.
\end{aligned} \tag{2.60}$$

$$\begin{aligned}
\frac{1}{\text{Pr}} \frac{t_j^n - t_{j-1}^n}{h_j} + f_{j-\frac{1}{2}}^n t_{j-\frac{1}{2}}^n - s_{j-\frac{1}{2}}^n u_{j-\frac{1}{2}}^n + (L_2)_{j-\frac{1}{2}}^{n-1} &= 0, \\
\frac{1}{\text{Pr}} \frac{t_j^n - t_{j-1}^n}{h_j} + f_{j-\frac{1}{2}}^n t_{j-\frac{1}{2}}^n - s_{j-\frac{1}{2}}^n u_{j-\frac{1}{2}}^n &= -(L_2)_{j-\frac{1}{2}}^{n-1}.
\end{aligned} \tag{2.61}$$

where

$$\begin{aligned}
(L_1)_{j-\frac{1}{2}}^{n-1} &= \frac{v_j^{n-1} - v_{j-1}^{n-1}}{h_j} + f_{j-\frac{1}{2}}^{n-1} v_{j-\frac{1}{2}}^{n-1} - 2(u_{j-\frac{1}{2}}^{n-1})^2 + 2, \\
(L_2)_{j-\frac{1}{2}}^{n-1} &= \frac{1}{\text{Pr}} \frac{t_j^{n-1} - t_{j-1}^{n-1}}{h_j} + f_{j-\frac{1}{2}}^{n-1} t_{j-\frac{1}{2}}^{n-1} - s_{j-\frac{1}{2}}^{n-1} u_{j-\frac{1}{2}}^{n-1}.
\end{aligned}$$

By multiplying the Eqs. (2.51) to (2.53) with  $h_j$ , therefore

$$f_j^n - f_{j-1}^n = \frac{h_j}{2} (u_j^n + u_{j-1}^n), \tag{2.62}$$

$$u_j^n - u_{j-1}^n = \frac{h_j}{2} (v_j^n + v_{j-1}^n), \tag{2.63}$$

$$s_j^n - s_{j-1}^n = \frac{h_j}{2} (t_j^n + t_{j-1}^n). \tag{2.64}$$

Next, the Eqs. (2.60) and (2.61) are multiplied with  $h_j$  then yield

$$v_j^{n-1} - v_{j-1}^{n-1} + h_j f_{j-\frac{1}{2}}^{n-1} v_{j-\frac{1}{2}}^{n-1} - 2h_j (u_{j-\frac{1}{2}}^{n-1})^2 + 2h_j = (R_1)_{j-\frac{1}{2}}^{n-1}, \quad (2.65)$$

$$(t_j^n - t_{j-1}^n) + \text{Pr } h_j f_{j-\frac{1}{2}}^n t_{j-\frac{1}{2}}^n - \text{Pr } h_j s_{j-\frac{1}{2}}^n u_{j-\frac{1}{2}}^n = (R_2)_{j-\frac{1}{2}}^{n-1}. \quad (2.66)$$

where

$$(R_1)_{j-\frac{1}{2}}^{n-1} = -h_j (L_1)_{j-\frac{1}{2}}^{n-1},$$

$$(R_2)_{j-\frac{1}{2}}^{n-1} = -h_j (L_2)_{j-\frac{1}{2}}^{n-1}.$$

The Eqs. (2.62) to (2.66) are imposed for  $j = 1, 2, \dots, J$  at the given  $n$ . Also, the boundary condition (2.47) become

$$f_0^n = 0, u_0^n = v, s_0^n = 1, u_J^n = 1 \text{ and } s_J^n = 0. \quad (2.67)$$

### 2.3.2 Newton's Method

If  $f_j^{n-1}, u_j^{n-1}, v_j^{n-1}, s_j^{n-1}, t_j^{n-1}$  are supposed to be known for  $0 \leq j \leq J$ , then they should define the solution of the unknown variable as  $(f_j^n, u_j^n, v_j^n, s_j^n, t_j^n)$ ,  $j = 0, 1, \dots, J$ . To simplify the writing, the unknown variable  $x = x^i$ ,  $(f_j^n, u_j^n, v_j^n, s_j^n, t_j^n)$  are written as  $(f_j, u_j, v_j, s_j, t_j)$  (Nazar, 2003). The system of Eqs. (2.62) to (2.66) can be written as

$$f_j - f_{j-1} - \frac{h_j}{2}(u_j + u_{j-1}) = 0, \quad (2.68)$$

$$u_j - u_{j-1} - \frac{h_j}{2}(v_j + v_{j-1}) = 0, \quad (2.69)$$

$$s_j - s_{j-1} - \frac{h_j}{2}(t_j + t_{j-1}) = 0, \quad (2.70)$$

$$v_j - v_{j-1} + \frac{h_j}{4}(f_j + f_{j-1})(v_j + v_{j-1}) - \frac{h_j}{2}(u_j + u_{j-1})^2 + 2h_j = (R_1)_{j-\frac{1}{2}}^{n-1}, \quad (2.71)$$

$$\begin{aligned} & (t_j - t_{j-1}) + \frac{h_j}{4} \Pr(f_j + f_{j-1})(t_j + t_{j-1}) - \\ & \frac{h_j}{4} \Pr(s_j + s_{j-1})(u_j + u_{j-1}) = (R_2)_{j-\frac{1}{2}}^{n-1}. \end{aligned} \quad (2.72)$$

where

$$\begin{aligned} (R_1)_{j-\frac{1}{2}}^{n-1} &= -h_j \left[ \frac{v_j - v_{j-1}}{h_j} + f_{j-\frac{1}{2}} v_{j-\frac{1}{2}} - 2(u_{j-\frac{1}{2}})^2 + 2 \right]^{n-1}, \\ (R_2)_{j-\frac{1}{2}}^{n-1} &= -h_j \left[ \frac{1}{\Pr} \frac{t_j - t_{j-1}}{h_j} + f_{j-\frac{1}{2}} t_{j-\frac{1}{2}} - s_{j-\frac{1}{2}} u_{j-\frac{1}{2}} \right]^{n-1}, \end{aligned}$$

For the Newton's method, following iterates are introduced to linearise the nonlinear system as

$$\begin{aligned} f_j^{(i+1)} &= f_j^{(i)} + u f_j^{(i)}, \\ u_j^{(i+1)} &= u_j^{(i)} + u u_j^{(i)}, \\ v_j^{(i+1)} &= v_j^{(i)} + u v_j^{(i)}, \\ s_j^{(i+1)} &= s_j^{(i)} + u s_j^{(i)}, \\ t_j^{(i+1)} &= t_j^{(i)} + u t_j^{(i)}, \end{aligned} \quad (2.73)$$

Substitute the iteration (2.73) into the system of Eqs. (2.68) to (2.72), then

$$(f_j^{(i)} + u f_j^{(i)}) - (f_{j-1}^{(i)} + u f_{j-1}^{(i)}) - \frac{h_j}{2} (u_j^{(i)} + u u_j^{(i)} + u_{j-1}^{(i)} + u u_{j-1}^{(i)}) = 0, \quad (2.74)$$

$$(u_j^{(i)} + u u_j^{(i)}) - (u_{j-1}^{(i)} + u u_{j-1}^{(i)}) - \frac{h_j}{2} (v_j^{(i)} + u v_j^{(i)} + v_{j-1}^{(i)} + u v_{j-1}^{(i)}) = 0, \quad (2.75)$$

$$(s_j^{(i)} + u s_j^{(i)}) - (s_{j-1}^{(i)} + u s_{j-1}^{(i)}) - \frac{h_j}{2} (t_j^{(i)} + u t_j^{(i)} + t_{j-1}^{(i)} + u t_{j-1}^{(i)}) = 0, \quad (2.76)$$

$$\begin{aligned} & (v_j^{(i)} + u v_j^{(i)}) - (v_{j-1}^{(i)} + u v_{j-1}^{(i)}) + \frac{h_j}{4} [(f_j^{(i)} + u f_j^{(i)}) + (f_{j-1}^{(i)} + u f_{j-1}^{(i)})] \\ & \left[ (v_j^{(i)} + u v_j^{(i)}) + (v_{j-1}^{(i)} + u v_{j-1}^{(i)}) \right] - \frac{h_j}{2} [(u_j^{(i)} + u u_j^{(i)}) + (u_{j-1}^{(i)} + u u_{j-1}^{(i)})]^2 \\ & + 2h_j = (R_1)_{j-\frac{1}{2}}^{n-1}, \end{aligned} \quad (2.77)$$

$$\begin{aligned}
& \left( (t_j^{(i)} + u t_j^{(i)}) - (t_{j-1}^{(i)} + u t_{j-1}^{(i)}) \right) + \frac{h_j}{4} \Pr \left[ (f_j^{(i)} + u f_j^{(i)}) + (f_{j-1}^{(i)} + u f_{j-1}^{(i)}) \right] \\
& \left[ (t_j^{(i)} + u t_j^{(i)}) + (t_{j-1}^{(i)} + u t_{j-1}^{(i)}) \right] - \frac{h_j}{4} \Pr \left[ (s_j^{(i)} + u s_j^{(i)}) + (s_{j-1}^{(i)} + u s_{j-1}^{(i)}) \right] \\
& \left[ (u_j^{(i)} + u u_j^{(i)}) + (u_{j-1}^{(i)} + u u_{j-1}^{(i)}) \right] = (R_2)_{j-\frac{1}{2}}^{n-1}.
\end{aligned} \tag{2.78}$$

The superscript  $i$  is dropped for simplicity. After a few steps of algebra the higher order terms as in  $u f_j^{(i)}, u u_j^{(i)}, u v_j^{(i)}, u s_j^{(i)}, u t_j^{(i)}$  are also dropped. The system of equation are becomes as follows,

$$u f_j - u f_{j-1} - \frac{1}{2} h_j (u u_j + u u_{j-1}) = f_{j-1} - f_j + h_j u_{j-\frac{1}{2}}, \tag{2.79}$$

$$u u_j - u u_{j-1} - \frac{1}{2} h_j (u v_j + u v_{j-1}) = u_{j-1} - u_j + h_j v_{j-\frac{1}{2}}, \tag{2.80}$$

$$u s_j - u s_{j-1} - \frac{1}{2} h_j (u t_j + u t_{j-1}) = s_{j-1} - s_j + h_j t_{j-\frac{1}{2}}, \tag{2.81}$$

$$\begin{aligned}
& u v_j \left[ 1 + \frac{1}{4} h_j (f_j + f_{j-1}) \right] + u v_{j-1} \left[ -1 + \frac{1}{4} h_j (f_j + f_{j-1}) \right] + \\
& u f_j \left[ \frac{1}{4} h_j (v_j + v_{j-1}) \right] + u f_{j-1} \left[ \frac{1}{4} h_j (v_j + v_{j-1}) \right] + u u_j \left[ -\frac{1}{2} h_j (u_j + u_{j-1}) \right] \\
& + u u_{j-1} \left[ -\frac{1}{2} h_j (u_j + u_{j-1}) \right] = -v_j + v_{j-1}
\end{aligned} \tag{2.82}$$

$$-h_j \left[ \frac{1}{4} (f_j + f_{j-1})(v_j + v_{j-1}) - \frac{1}{2} (u_j + u_{j-1})^2 - \frac{1}{2} (u_j + u_{j-1}) \right] - 2h_j + (R_1)_{j-\frac{1}{2}}^{n-1},$$

$$\begin{aligned}
& u t_j \left[ 1 + \frac{1}{4} h_j \Pr(f_j + f_{j-1}) \right] + u t_{j-1} \left[ -1 + \frac{1}{4} h_j \Pr(f_j + f_{j-1}) \right] + \\
& u f_j \left[ \frac{1}{4} h_j \Pr(t_j + t_{j-1}) \right] + u f_{j-1} \left[ \frac{1}{4} h_j \Pr(t_j + t_{j-1}) \right] + u s_j \left[ -\frac{1}{4} h_j \Pr(u_j + u_{j-1}) \right] + \\
& u s_{j-1} \left[ -\frac{1}{4} h_j \Pr(u_j + u_{j-1}) \right] + u u_j \left[ -\frac{1}{4} h_j \Pr(s_j + s_{j-1}) \right] + \\
& u u_{j-1} \left[ \frac{1}{4} h_j \Pr(s_j + s_{j-1}) \right] = (-t_j + t_{j-1}) -
\end{aligned} \tag{2.83}$$

$$h_j \Pr \left[ \frac{1}{4} (f_j + f_{j-1})(t_j + t_{j-1}) \right] + h_j \Pr \left[ \frac{1}{4} (s_j + s_{j-1})(u_j + u_{j-1}) \right] + (R_2)_{j-\frac{1}{2}}^{n-1},$$

The simple form of the system of Eqs. (2.80) to (2.83) are

$$u f_j - u f_{j-1} - \frac{1}{2} h_j (u u_j + u u_{j-1}) = (r_1)_{j-\frac{1}{2}}, \quad (2.84)$$

$$u u_j - u u_{j-1} - \frac{1}{2} h_j (u v_j + u v_{j-1}) = (r_2)_{j-\frac{1}{2}}, \quad (2.85)$$

$$u s_j - u s_{j-1} - \frac{1}{2} h_j (u t_j + u t_{j-1}) = (r_3)_{j-\frac{1}{2}}, \quad (2.86)$$

$$\begin{aligned} & (a_1)_j u v_j + (a_2)_j u v_{j-1} + (a_3)_j u f_j + \\ & (a_4)_j u f_{j-1} + (a_5)_j u u_j + (a_6)_j u u_{j-1} = (r_4)_{j-\frac{1}{2}}, \end{aligned} \quad (2.87)$$

$$\begin{aligned} & (b_1)_j u t_j + (b_2)_j u t_{j-1} + (b_3)_j u f_j + (b_4)_j u f_{j-1} + \\ & (b_5)_j u s_j + (b_6)_j u s_{j-1} + (b_7)_j u u_j + (b_8)_j u u_{j-1} = (r_5)_{j-\frac{1}{2}}, \end{aligned} \quad (2.88)$$

where

$$\begin{aligned} (a_1)_j &= 1 + \frac{1}{2} h_j f_{j-\frac{1}{2}}, \\ (a_2)_j &= -1 + \frac{1}{2} h_j f_{j-\frac{1}{2}} = (a_1)_j - 2, \\ (a_3)_j &= \frac{1}{2} h_j v_{j-\frac{1}{2}}, \\ (a_4)_j &= (a_3)_j, \\ (a_5)_j &= -h_j u_{j-\frac{1}{2}}, \\ (a_6)_j &= (a_5)_j, \\ (b_1)_j &= 1 + \frac{1}{2} h_j \text{Pr} f_{j-\frac{1}{2}}, \\ (b_2)_j &= -1 + \frac{1}{2} h_j \text{Pr} f_{j-\frac{1}{2}} = (b_1)_j - 2, \\ (b_3)_j &= \frac{1}{2} h_j \text{Pr} t_{j-\frac{1}{2}}, \\ (b_4)_j &= (b_3)_j, \\ (b_5)_j &= -\frac{1}{2} h_j \text{Pr} u_{j-\frac{1}{2}}, \\ (b_6)_j &= (b_5)_j, \end{aligned} \quad (2.89)$$

$$\begin{aligned}
(b_7)_j &= -\frac{1}{2}h_j \text{Pr } s_{j-\frac{1}{2}}, \\
(b_8)_j &= (b_7)_j,
\end{aligned} \tag{2.90}$$

$$\begin{aligned}
(r_1)_{j-\frac{1}{2}} &= f_{j-1} - f_j + \frac{1}{2}h_j u_{j-\frac{1}{2}}, \\
(r_2)_{j-\frac{1}{2}} &= u_{j-1} - u_j + \frac{1}{2}h_j v_{j-\frac{1}{2}}, \\
(r_3)_{j-\frac{1}{2}} &= s_{j-1} - s_j + \frac{1}{2}h_j t_{j-\frac{1}{2}},
\end{aligned} \tag{2.91}$$

$$\begin{aligned}
(r_4)_{j-\frac{1}{2}} &= -v_j + v_{j-1} - h_j \left[ f_{j-\frac{1}{2}} v_{j-\frac{1}{2}} - 2 \left( u_{j-\frac{1}{2}} \right)_{j-\frac{1}{2}} + 2 \right] + (R_1)_{j-\frac{1}{2}}, \\
(r_5)_{j-\frac{1}{2}} &= (-t_j + t_{j-1}) - h_j \left[ \text{Pr } f_{j-\frac{1}{2}} t_{j-\frac{1}{2}} \right] + h_j \left[ \text{Pr } s_{j-\frac{1}{2}} u_{j-\frac{1}{2}} \right] + (R_2)_{j-\frac{1}{2}}.
\end{aligned}$$

To complete the system of Eqs. (2.84) to (2.88) with boundary condition (2.67) which can be satisfied exactly with no iteration (Cebeci and Bradshaw, 1988). So, to maintain these correct values in all the iterates, we take

$$u f_0 = 0, u u_0 = 0, u s_0 = 0 \quad \text{and} \quad u u_J = 0, u s_J = 0. \tag{2.92}$$

### 2.3.3 The Block Elimination Technique

The linearised difference Eqs. (2.84) to (2.88) are in the structure of a block-tridiagonal system (Na, 1979).

Usually, the three diagonal block structure consists of variables or constants, but here in Keller-box method is different because it consists of block matrices. In order to solve the linearise difference Eqs. (2.84) to (2.88) by using the block elimination technique, the elements of block matrices from Eqs. (2.84) to (2.88) must be defined by considering three different cases which is when  $j = 1$ ,  $j = 2, \dots, j = J - 1$  and  $j = J$ . When  $j = 1$ , the linearised scheme in Eqs. (2.84) to (2.88) become

$$u f_1 - u f_0 - \frac{1}{2} h_1 (u u_1 + u u_0) = (r_1)_{1-\frac{1}{2}},$$

$$u u_1 - u u_0 - \frac{1}{2} h_1 (u v_1 + u v_0) = (r_2)_{1-\frac{1}{2}},$$

$$u s_1 - u s_0 - \frac{1}{2} h_1 (u t_1 + u t_0) = (r_3)_{1-\frac{1}{2}},$$

$$(a_1)_1 u v_1 + (a_2)_1 u v_0 + (a_3)_1 u f_1 + (a_4)_1 u f_0 + (a_5)_1 u u_1 + (a_6)_1 u u_0 = (r_4)_{1-\frac{1}{2}},$$

$$(b_1)_1 u t_1 + (b_2)_1 u t_0 + (b_3)_1 u f_1 + (b_4)_1 u f_0 + (b_5)_1 u s_1 + (b_6)_1 u s_0 + (b_7)_1 u u_1 + (b_8)_1 u u_0 = (r_5)_{1-\frac{1}{2}}.$$

The corresponding matrix form with boundary conditions (2.92) is as follows,

$$\begin{bmatrix} 0 & 0 & 1 & 0 & 0 \\ -1/2 h_1 & 0 & 0 & -1/2 h_1 & 0 \\ 0 & -1/2 h_1 & 0 & 0 & -1/2 h_1 \\ (a_2)_1 & 0 & (a_3)_1 & (a_1)_1 & 0 \\ 0 & (b_2)_1 & (b_3)_1 & 0 & (b_1)_1 \end{bmatrix} \begin{bmatrix} u v_0 \\ u t_0 \\ u f_1 \\ u v_1 \\ u t_1 \end{bmatrix} + \begin{bmatrix} -1/2 h_1 & 0 & 0 & 0 & 0 \\ 1 & 0 & 0 & 0 & 0 \\ 0 & 1 & 0 & 0 & 0 \\ (a_5)_1 & 0 & 0 & 0 & 0 \\ (b_7)_1 & (b_5)_1 & 0 & 0 & 0 \end{bmatrix} \begin{bmatrix} u u_1 \\ u s_1 \\ u f_2 \\ u v_2 \\ u t_2 \end{bmatrix} = \begin{bmatrix} (r_1)_{1-\frac{1}{2}} \\ (r_2)_{1-\frac{1}{2}} \\ (r_3)_{1-\frac{1}{2}} \\ (r_4)_{1-\frac{1}{2}} \\ (r_5)_{1-\frac{1}{2}} \end{bmatrix}.$$

Hence, for the values of  $j = 1$ , it can be written as

$$[A_1][u_1] + [C_1][u_2] = [r_1]. \quad (2.93)$$

Next, we can write the linear system of Eqs. (2.84) to (2.88) for  $j = 2, \dots, J-1$  as

$$u f_{j-1} - u f_{j-2} - \frac{1}{2} h_{j-1} (u u_{j-1} + u u_{j-2}) = (r_1)_{(j-1)-\frac{1}{2}},$$

$$\begin{aligned}
& uu_{j-1} - uu_{j-2} - \frac{1}{2}h_{j-1}(uv_{j-1} + uv_{j-2}) = (r_2)_{(j-1)-\frac{1}{2}}, \\
& us_{j-1} - us_{j-2} - \frac{1}{2}h_{j-1}(ut_{j-1} + ut_{j-2}) = (r_3)_{(j-1)-\frac{1}{2}}, \\
& (a_1)_{j-1}uv_{j-1} + (a_2)_{j-1}uv_{j-2} + (a_3)_{j-1}uf_{j-1} + \\
& (a_4)_{j-1}uf_{j-2} + (a_5)_{j-1}uu_{j-1} + (a_6)_{j-1}uu_{j-2} = (r_4)_{(j-1)-\frac{1}{2}}, \\
& (b_1)_{j-1}ut_{j-1} + (b_2)_{j-1}ut_{j-2} + (b_3)_{j-1}uf_{j-1} + (b_4)_{j-1}uf_{j-2} + \\
& (b_5)_{j-1}us_{j-1} + (b_6)_{j-1}us_{j-2} + (b_7)_{j-1}uu_{j-1} + (b_8)_{j-1}uu_{j-2} = (r_5)_{(j-1)-\frac{1}{2}},
\end{aligned}$$

$$\begin{aligned}
& \begin{bmatrix} 0 & 0 & -1 & 0 & 0 \\ 0 & 0 & 0 & -1/2h_{j-1} & 0 \\ 0 & 0 & 0 & 0 & -1/2h_{j-1} \\ 0 & 0 & (a_4)_{j-1} & (a_2)_{j-1} & 0 \\ 0 & 0 & (b_4)_{j-1} & 0 & (b_2)_{j-1} \end{bmatrix} \begin{bmatrix} uu_{j-3} \\ us_{j-3} \\ uf_{j-2} \\ uv_{j-2} \\ ut_{j-2} \end{bmatrix} + \\
& \begin{bmatrix} -1/2h_{j-1} & 0 & 1 & 0 & 0 \\ -1 & 0 & 0 & -1/2h_{j-1} & 0 \\ 0 & -1 & 0 & 0 & -1/2h_{j-1} \\ (a_6)_{j-1} & 0 & (a_3)_{j-1} & (a_1)_{j-1} & 0 \\ (b_8)_{j-1} & (b_6)_{j-1} & (b_3)_{j-1} & 0 & (b_1)_{j-1} \end{bmatrix} \begin{bmatrix} uu_{j-2} \\ us_{j-2} \\ uf_{j-1} \\ uv_{j-1} \\ ut_{j-1} \end{bmatrix} + \\
& \begin{bmatrix} -1/2h_{j-1} & 0 & 0 & 0 & 0 \\ 1 & 0 & 0 & 0 & 0 \\ 0 & 1 & 0 & 0 & 0 \\ (a_5)_{j-1} & 0 & 0 & 0 & 0 \\ (b_7)_{j-1} & (b_5)_{j-1} & 0 & 0 & 0 \end{bmatrix} \begin{bmatrix} uu_{j-1} \\ us_{j-1} \\ uf_j \\ uv_j \\ ut_j \end{bmatrix} = \begin{bmatrix} (r_1)_{(j-1)-\frac{1}{2}} \\ (r_2)_{(j-1)-\frac{1}{2}} \\ (r_3)_{(j-1)-\frac{1}{2}} \\ (r_4)_{(j-1)-\frac{1}{2}} \\ (r_5)_{(j-1)-\frac{1}{2}} \end{bmatrix}.
\end{aligned}$$

Hence, for the values of  $j = 2, \dots, J - 1$ , can be written as

$$[B_j][u_{j-1}] + [A_j][u_j] + [C_j][u_{j+1}] = [r_{j-1}]. \quad (2.94)$$

Lastly, we can write the linear system Eqs. (2.84) to (2.88) for  $j = J$  as below

$$uf_j - uf_{j-1} - \frac{1}{2}h_j(uu_j + uu_{j-1}) = (r_1)_{j-\frac{1}{2}},$$

$$\begin{aligned}
uu_j - uu_{j-1} - \frac{1}{2}h_j(uv_j + uv_{j-1}) &= (r_2)_{j-\frac{1}{2}}, \\
us_j - us_{j-1} - \frac{1}{2}h_j(ut_j + ut_{j-1}) &= (r_3)_{j-\frac{1}{2}}, \\
(a_1)_j uv_j + (a_2)_j uv_{j-1} + (a_3)_j uf_j + \\
(a_4)_j uf_{j-1} + (a_5)_j uu_j + (a_6)_j uu_{j-1} &= (r_4)_{j-\frac{1}{2}}, \\
(b_1)_j ut_j + (b_2)_j ut_{j-1} + (b_3)_j uf_j + (b_4)_j uf_{j-1} + \\
+ (b_5)_j us_j + (b_6)_j us_{j-1} + (b_7)_j uu_j + (b_8)_j uu_{j-1} &= (r_5)_{j-\frac{1}{2}},
\end{aligned}$$

$$\begin{bmatrix} 0 & 0 & -1 & 0 & 0 \\ 0 & 0 & 0 & -1/2h_j & 0 \\ 0 & 0 & 0 & 0 & -1/2h_j \\ 0 & 0 & (a_4)_j & (a_2)_j & 0 \\ 0 & 0 & (b_4)_j & 0 & (b_2)_j \end{bmatrix} \begin{bmatrix} uu_{j-2} \\ us_{j-2} \\ uf_{j-1} \\ uv_{j-1} \\ ut_{j-1} \end{bmatrix} +$$

$$\begin{bmatrix} -1/2h_j & 0 & 1 & 0 & 0 \\ -1 & 0 & 0 & -1/2h_j & 0 \\ 0 & -1 & 0 & 0 & -1/2h_j \\ (a_6)_j & 0 & (a_3)_j & (a_1)_j & 0 \\ (b_8)_j & (b_6)_j & (b_3)_j & 0 & (b_1)_j \end{bmatrix} \begin{bmatrix} uu_{j-1} \\ us_{j-1} \\ uf_j \\ uv_j \\ ut_j \end{bmatrix} = \begin{bmatrix} (r_1)_{j-\frac{1}{2}} \\ (r_2)_{j-\frac{1}{2}} \\ (r_3)_{j-\frac{1}{2}} \\ (r_4)_{j-\frac{1}{2}} \\ (r_5)_{j-\frac{1}{2}} \end{bmatrix}.$$

Hence, for the values of  $j = J$ , it can be written as

$$[B_J][u_{j-1}] + [A_J][u_j] = [r_j]. \quad (2.95)$$

Therefore, in overall, for  $j = 1, 2, 3, \dots, J-1, J$ , we have,

$$\begin{aligned}
j=1 & : [A_1][u_1] + [C_1][u_2] = [r_1], \\
j=2 & : [B_2][u_1] + [A_2][u_2] + [C_2][u_3] = [r_2], \\
& \vdots \\
j=J-1 & : [B_3][u_2] + [A_3][u_3] + [C_3][u_4] = [r_3], \\
j=J & : [B_J][u_{j-1}] + [A_J][u_j] = [r_j].
\end{aligned}$$

Now, we write the above system in matrix vector form as



$$[u_1] = \begin{bmatrix} uv_0 \\ ut_0 \\ uf_1 \\ uv_1 \\ ut_1 \end{bmatrix}, [u_j] = \begin{bmatrix} uu_{j-1} \\ us_{j-1} \\ uf_1 \\ uv_1 \\ ut_1 \end{bmatrix}, 2 \leq j \leq J, \quad (2.101)$$

$$[r_j] = \begin{bmatrix} (r_1)_{j-\frac{1}{2}} \\ (r_2)_{j-\frac{1}{2}} \\ (r_3)_{j-\frac{1}{2}} \\ (r_4)_{j-\frac{1}{2}} \\ (r_5)_{j-\frac{1}{2}} \end{bmatrix}, 2 \leq j \leq J. \quad (2.102)$$

In Eq. (2.96), the matrix  $A$  coefficient is known as a tridiagonal matrix with zero elements. According the block-elimination method, we solve the Eq. (2.96) by assuming that matrix  $A$  is nonsingular (Na, 1979). Matrix  $A$  can be factorized into lower matrix  $[L]$  and upper matrix  $[U]$  as

$$[A] = [L][U], \quad (2.103)$$

$$[L] = \begin{bmatrix} [r_1] & & & & \\ [B_2] & [r_2] & & & \\ & \ddots & \ddots & & \\ & & \ddots & \ddots & \\ & & & [r_{j-1}] & \\ & & & [B_j] & [r_j] \end{bmatrix},$$

and

$$[U] = \begin{bmatrix} [I] & [\Gamma_1] & & & \\ & [I] & [\Gamma_2] & & \\ & & \ddots & \ddots & \\ & & & [I] & [\Gamma_j] \\ & & & & [I] \end{bmatrix},$$

where  $[I]$  is the identity matrix of order 5 and  $[r_i]$  and  $[\Gamma_i]$  are  $5 \times 5$  matrices which elements are determined by the following equations

$$[r_1] = [A_1], \quad (2.104)$$

$$[A_1][\Gamma_1] = [C_1], \quad (2.105)$$

$$[r_j] = [A_j] - [B_j][\Gamma_{j-1}], \quad j = 2, 3, \dots, J, \quad (2.106)$$

$$[r_j][\Gamma_j] = [C_j], \quad j = 2, 3, \dots, J-1. \quad (2.107)$$

then, Eq. (2.103) is substituted into Eq. (2.96) such that

$$[L][U][u] = [r]. \quad (2.108)$$

If

$$[U][u] = [W], \quad (2.109)$$

then, the Eq. (2.108) becomes

$$[L][W] = [r], \quad (2.110)$$

where

$$[W] = \begin{bmatrix} [W_1] \\ [W_2] \\ \vdots \\ [W_{J-1}] \\ [W_J] \end{bmatrix}.$$

$[W_j]$  are  $5 \times 1$  column matrices. The elements  $[W]$  can be solved from Eq. (2.109)

$$[r_1][W_1] = [r_1], \quad (2.111)$$

$$[r_j][W_j] = [r_j] - [B_j][W_{j-1}], \quad 2 \leq j \leq J. \quad (2.112)$$

The step in which  $[\Gamma_j]$ ,  $[r_j]$  and  $[W_j]$  are calculated is referred to as the forward sweep. Once the elements of  $[W]$  are found, Eq. (2.109) then gives the solution  $[u]$  in the so-called backward sweep, in which the elements are obtained by the following relations:

$$[u_j] = [W_j], \quad (2.113)$$

$$[u_j] = [W_j] - [\Gamma_j][u_{j+1}], \quad 1 \leq j \leq J-1, \quad (2.114)$$

Since the elements of  $[ ]$  are found. Eqs. (2.84) to (2.88) then can be used to find  $(i+1)^{\text{th}}$  iteration for Eq. (2.73). These calculations are repeated until some convergence criterion is satisfied. In laminar boundary layer calculations, the wall shear stress parameter  $v(0)$  is commonly used as convergence criterion (Cebeci and Bradshaw, 1988). Calculations are stopped when

$$|u v_0^{(i)}| < v_1, \quad (2.115)$$

where  $v_1$  is a too small fixed value. In this study,  $v_1 = 0.00001$  which gives the precise values until four decimal places, as suggested by Cebeci and Bradshaw (1988).

#### 2.7.4 Starting Conditions

The suitable step size  $\Delta y$  and boundary layer thickness  $y_\infty$  must be determined in numerical computation. This is usually done by trial and error approach. We can start with small value of  $y_\infty$  and move to a large value until the suitable values is obtained. Sometime, too small or too large value of  $y_\infty$  is found through trial and error, which may give rise to the convergence difficulties. For most laminar boundary layer flows, the transformed boundary layer thickness ( $y$ ) is constant (Cebeci and Bradshaw, 1988) and typically lies between 5 to 10. In this study, the suitable boundary layer starts from 5 to 10 to provide accurate numerical results depending on the problems involved.

A step size ( $\Delta y$ ) of 0.02 to 0.04 is sufficient for the accurate numerical results (Nazar, 2003). Moreover, Lok (2008) successfully used a step size of 0.1, and a step size 0.01 is used in this study. The appropriate value of step size  $\Delta y$  must not affect the converged results appreciably, for example, the value of skin friction coefficient must be free from the value of step size  $\Delta y$  chosen. An overly small values of  $\Delta y$  may increase

a waiting time in calculations, while an overly large values of  $\Delta y$  can be calculated quickly but may produce inaccurate results (Ahmad, 2009).

Choosing an appropriate initial guesses for the function  $f$ ,  $u$ ,  $v$ ,  $s$  and  $t$  are necessary in numerical computation of boundary layer flow. We start the initial guesses with velocity  $u$  and temperature  $s$  at  $y = 0$  to  $y = y_\infty$ . After that, by differentiation and integration in respect to  $y$ , other functions  $f$ ,  $v$  and  $t$  also can be defined. There are a few possibilities in the selection of distribution curves, as long as they satisfy the boundary conditions (2.45). For the problem considered here, one possibility distribution curves for  $u$  and  $s$  is suggested by Bejan (1984), Burmeister (1983) and Bejan and Kraus (2003) are

$$u(y) = \frac{\partial f}{\partial y} = \left(\frac{y}{y_\infty}\right) + v \left(1 - \frac{y}{y_\infty}\right), \quad (2.116)$$

$$s(y) = t(y) = \left(1 - \frac{y}{y_\infty}\right)^2. \quad (2.117)$$

By integrating the Eq. (2.116) with respect to  $y$  produce

$$f(y) = \int_{y=0}^{y=y_\infty} u dy = y \left( v + \frac{1}{2} \frac{y}{y_\infty} (1-v) \right). \quad (2.118)$$

Differentiating the Eqs. (2.116) and (2.117) gives

$$v(y) = \frac{du}{dy} = \frac{1}{y_\infty} (1-v), \quad (2.119)$$

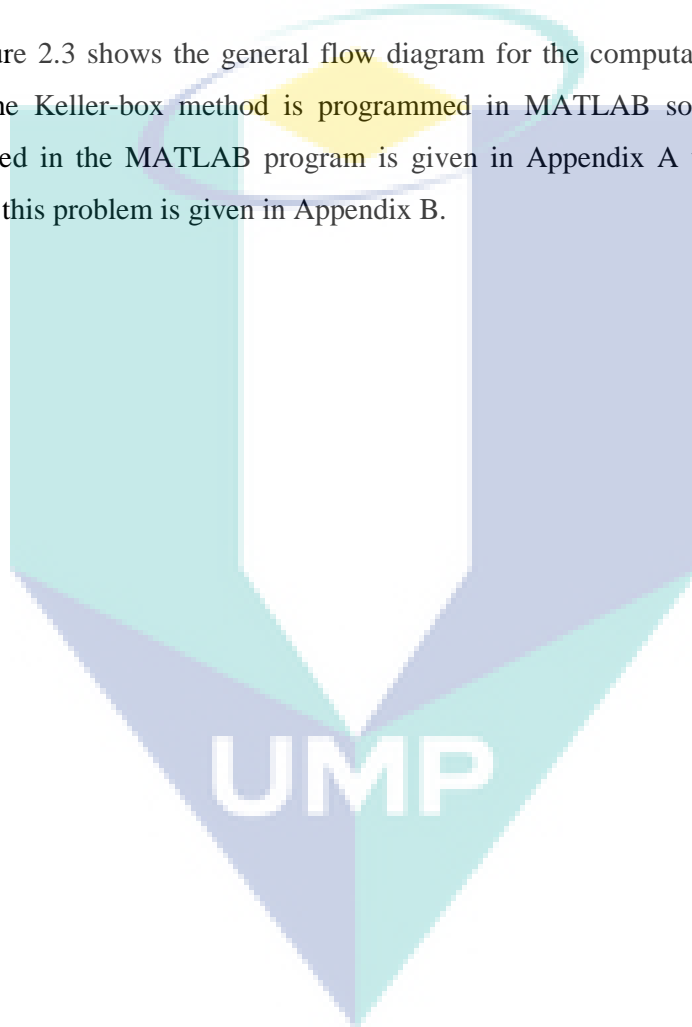
and

$$t(y) = \frac{ds}{dy} = -2 \left(\frac{1}{y_\infty}\right) \left(1 - \frac{y}{y_\infty}\right), \quad (2.120)$$

respectively.

Note that the complete solution for the problem is discussed in this chapter 3 which is the problem of the stagnation point flow and heat transfer towards an exponentially stretching sheet with prescribed wall temperature, prescribed surface heat flux and convective boundary conditions. From the numerical results, it is found that the Keller-box method is suitable to provide an accurate result of the convection in an incompressible viscous fluid problem.

Figure 2.3 shows the general flow diagram for the computations of Keller-box method. The Keller-box method is programmed in MATLAB software. The list of symbols used in the MATLAB program is given in Appendix A while the complete program of this problem is given in Appendix B.



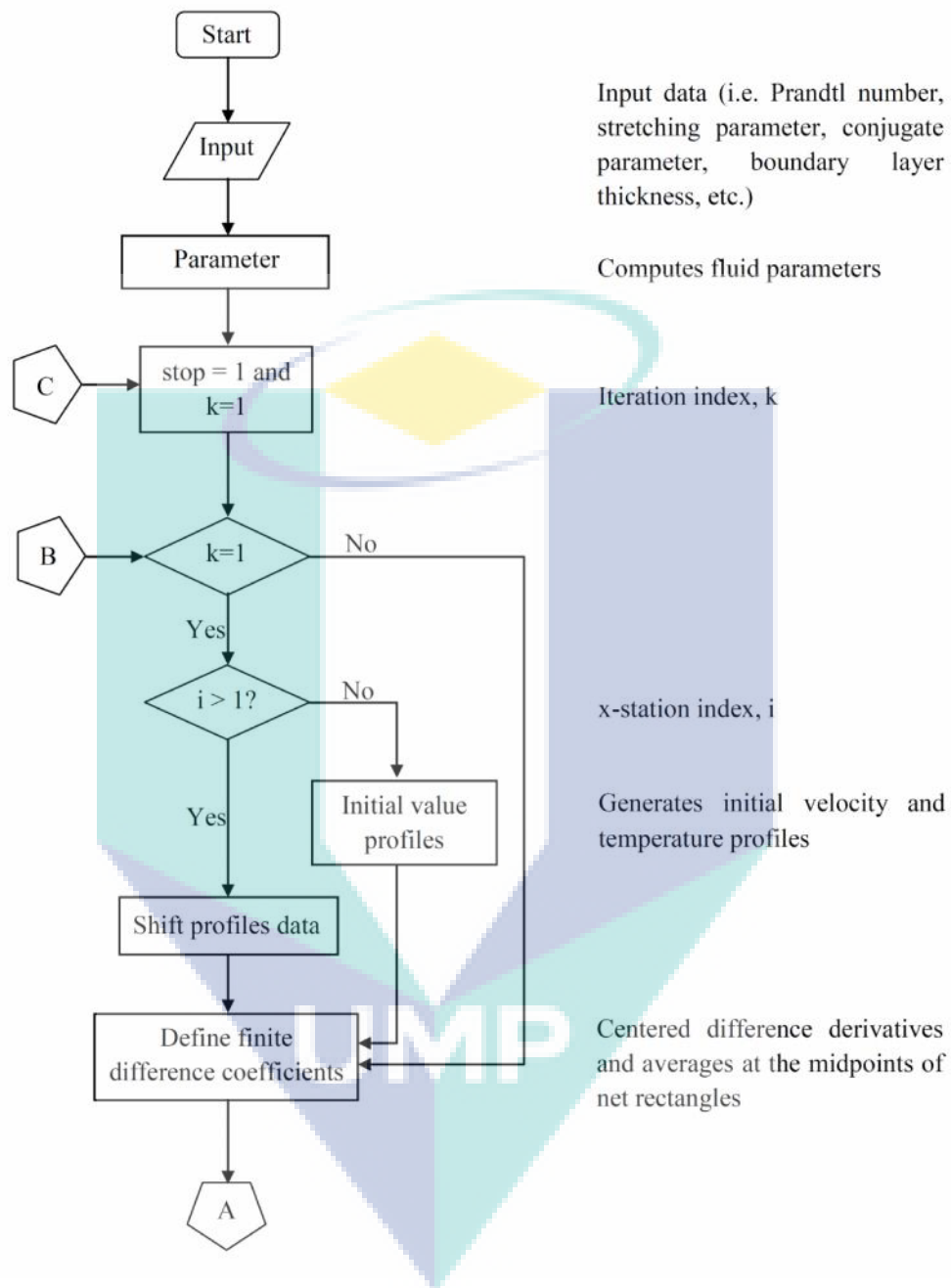


**Figure 2.3:** Flow diagram for the Keller-box method

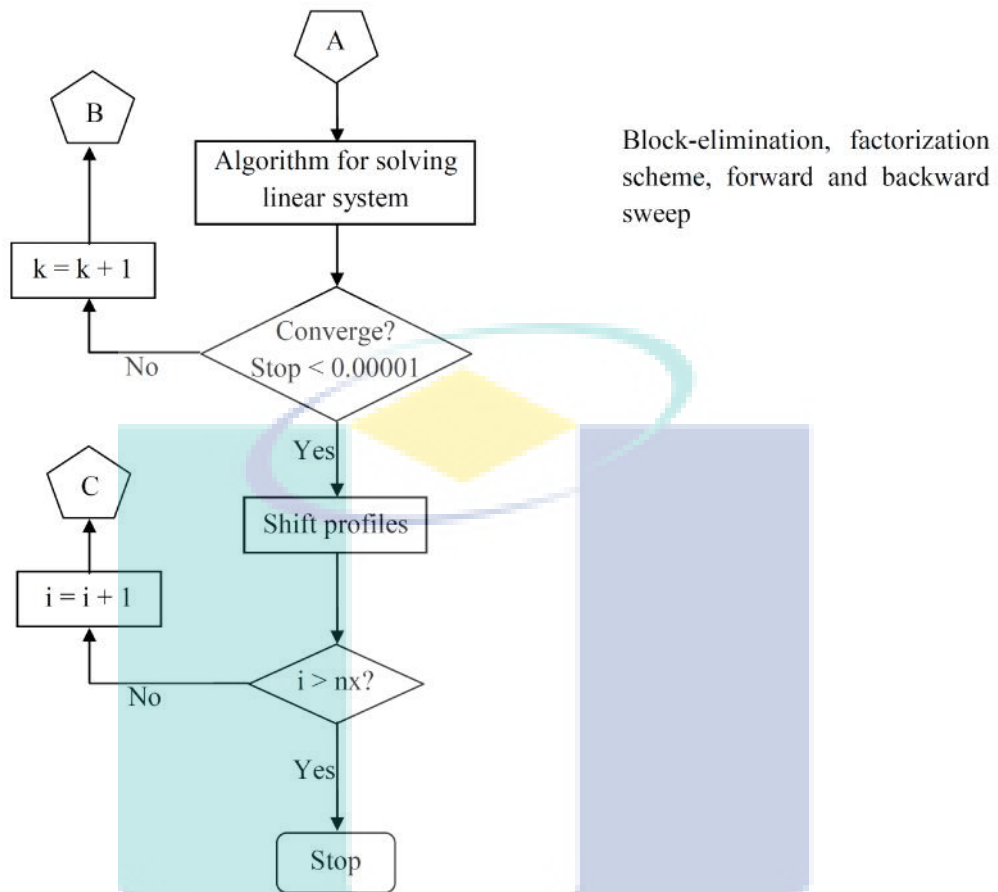


Figure 2.3: Flow diagram for the Keller-box method (continued)

UMP

## CHAPTER 3

### STAGNATION POINT FLOW AND HEAT TRANSFER TOWARDS AN EXPONENTIALLY STRETCHING/SHRINKING SHEET

#### 3.1 INTRODUCTION

In this chapter, two dimensional boundary layer stagnation point flow and heat transfer over an exponentially stretching/shrinking sheet are considered. This problem is studied with three cases of boundary conditions, which are prescribed wall temperature, prescribed surface heat flux and convective boundary conditions. The problem with prescribed wall temperature is compared with that done by Bhattacharyya and Vajravelu (2012).

The boundary layer flow and heat transfer over a stretching surface has many applications in industries and technologies. Therefore many researchers have been interested in studying boundary layer flow and heat transfer in a large number of applications. Some of these applications are drawing of plastic films, glass fiber production, hot rolling, wire drawing, artificial fibers, aerodynamic extrusion of plastic sheets, paper and metal production, polymer extrusion, metal spinning and many others industrial manufacturing processes. The final product with the requested characteristics depends on the cooling liquid used and the rate of stretching (Bachok et al., 2012).

Furthermore, Hiemenz (1911) was the first to investigated the two dimensional stagnation point flow over a stationary plat. The stagnation point flow towards a shrinking sheet was investigated by Wang (2008). The results obtained both a dual and unique solutions for the specific range of the velocity-ratio parameter in two-dimensional and asymmetric cases. Recently, Bhattacharyya (2013) and Bachok et al.

(2013) investigated the unsteady and steady boundary layer stagnation point flow over stretching/shrinking sheet with constant wall temperature and convective boundary conditions, respectively.

The constant/prescribed wall temperature, constant/prescribed surface heat flux, Newtonian heating and convective/conjugate boundary conditions are four general heating processes on the wall temperature distribution, which are considered by Merkin (1994). Commonly, in most research on the boundary layer flow and heat transfer, the constant wall temperature is used as the boundary conditions. For example the stagnation point flow over an exponentially stretching or shrinking sheet was investigated by Wong et al. (2011). They found the unique solutions for case of stretching sheet and dual solutions was obtained in the case of shrinking sheet. Makinde and Aziz (2011) investigated nanofluid flow over a stretching sheet with convection boundary condition. Recently, Nadeem et al. (2014) investigated the water-based nanofluid over an exponentially stretching sheet. In this study three boundary conditions are considered.

Hence, we study the stagnation flow over exponentially stretching/shrinking sheet with prescribed wall temperature, prescribed surface heat flux and with convective boundary conditions. Mathematical formulations of the problems are discussed in section 3.2. Section 3.3 is the results and discussion and is divided in three sub-sections. Sub-section 3.3.1 is about stagnation point flow over an exponentially stretching/shrinking sheet with prescribed wall temperature. Stagnation point flow with surface heat flux is discussed in sub-section 3.3.2. Sub-section 3.3.3 considered the case of convective boundary conditions. The conclusion is discussed in the section 3.4.

### **3.2 MATHEMATICAL FORMULATION**

Let us consider the steady viscous, laminar and two-dimensional boundary layer stagnation point flow (of an incompressible fluid) and heat transfer over an exponentially stretching/shrinking sheet as shown in Figure 2.1. The governing equations are written as follows,

$$f''' + ff'' - 2f'^2 + 2 = 0, \quad (3.1)$$

$$\theta'' + \text{Pr}(f\theta' - \theta f') = 0. \quad (3.2)$$

where  $\text{Pr} = \epsilon/\gamma$  is the Prandtl number. The boundary conditions are,

$$\begin{aligned} f(0) &= 0, \quad f'(0) = v, \quad \text{at } y = 0, \\ \theta(0) &= 1 \text{ (PWT)}, \quad \text{at } y = 0, \\ \theta'(0) &= -1 \text{ (PHF)}, \quad \text{at } y = 0, \\ \theta'(0) &= -x(1 - \theta(0)) \text{ (CBC)}, \quad \text{at } y = 0, \\ f'(y) &= 1, \quad \theta(y) = 0, \quad \text{as } y \rightarrow \infty, \end{aligned} \quad (3.3)$$

where  $v = b/a$  is the stretching/shrinking parameter, can be noted that  $v < 0$  is for shrinking,  $v > 0$  is valid for stretching and  $v = 0$  corresponds to a fixed sheet. The physical quantities of interest are the skin friction coefficient  $C_f$  and local Nusselt number  $Nu_x$  which are defined as:

$$C_f = \frac{\tau_w}{\rho U_e^2(x)}, \quad (3.4)$$

$$Nu_x = \frac{xq_w}{k(T_w - T_\infty)}, \quad (3.5)$$

where  $\rho$  is the fluid density,  $\tau_w$  is the surface shear stress and  $q_w$  represents the surface heat flux. Let

$$\tau_w = \mu \left( \frac{\partial u}{\partial y} \right)_{y=0}, \quad (3.6)$$

$$q_w = -k \left( \frac{\partial T}{\partial y} \right)_{y=0}, \quad (3.7)$$

where  $\mu$  and  $k$  are the dynamic viscosity and thermal conductivity, respectively. By substituting Eq. (2.23) and Eq. (2.21) into Eq. (3.6) and Eq. (3.4) respectively, the reduced skin friction coefficient is defined as:

$$\begin{aligned}
C_f &= \frac{\sim a e^{\frac{3x}{2L}} f''(y) \sqrt{\frac{a}{2\nu L}}}{\dots a^2 e^{\frac{2x}{L}}}, \\
C_f &= \frac{\sim f''(y)}{\dots \sqrt{a 2\nu L e^{\frac{x}{L}}}}, \\
C_{fx} &= C_f \sqrt{\frac{2L}{x}} \text{Re}_x = f''(y).
\end{aligned} \tag{3.8}$$

By substituting the boundary conditions Eq. (2.5) to Eq. (2.7) and similarity transformation Eq. (2.27), (2.28) and (2.15) respectively into Eq. (3.5), the reduced Nusselt number are as,

a. Prescribed wall temperature (PWT)

$$\begin{aligned}
Nu_x &= \frac{-kx \left( T_0 e^{\frac{x}{L}} \theta''(y) \sqrt{\frac{a}{2\nu L}} \right)}{k \left( T_\infty + T_0 e^{\frac{x}{L}} - T_\infty \right)}, \\
Nu_x &= - \frac{\theta''(y) \sqrt{x e^{\frac{x}{L}} a \frac{x}{\nu}}}{\sqrt{2L}}, \\
\frac{Nu_x}{\sqrt{\text{Re}_x}} \sqrt{\frac{2L}{x}} &= -\theta''(y).
\end{aligned} \tag{3.9}$$

b. Prescribed heat flux (PHF)

$$\begin{aligned}
Nu_x &= - \frac{-kx \left( \frac{q_{w_0}}{k} \sqrt{\frac{a}{2\nu L}} e^{\frac{x}{L}} \right)}{k \left( T_\infty + \left( \frac{q_{w_0}}{k} \right) \theta''(y) e^{\frac{x}{L}} - T_\infty \right)}, \\
Nu_x &= \frac{\sqrt{x e^{\frac{x}{L}} a \frac{x}{\nu}}}{\theta''(y) \sqrt{2L}}, \\
\frac{Nu_x}{\sqrt{\text{Re}_x}} \sqrt{\frac{2L}{x}} &= \frac{1}{\theta''(y)}.
\end{aligned} \tag{3.10}$$

c. Convective boundary condition (CBC)

$$Nu_x = \frac{-kx \left( -\frac{h}{k} T_0 e^{\frac{x}{2L}} (1 - \theta(y)) \right)}{k T_0 e^{\frac{x}{2L}}},$$

$$Nu_x = (1 - \theta(y)) h k^{-1} x \sqrt{\frac{a}{v}} e^{\frac{x}{2L}} \sqrt{\frac{v}{a}} e^{-\frac{x}{2L}},$$

$$\sqrt{\frac{2L}{x}} \frac{Nu_x}{\sqrt{Re_x}} = x (1 - \theta(y)). \quad (3.11)$$

where  $Re_x = \frac{u_e x}{\nu}$  is the local Reynolds number.

### 3.3 RESULTS AND DISCUSSION

#### 3.3.1 Prescribed Wall Temperature (PWT)

Eqs. (3.1) and (3.2) are subject to boundary conditions (3.3) which have been numerically solved using Keller-box method for the stretching/shrinking parameter and Prandtl number. The effects of governing parameter on the reduced skin friction coefficient, the reduced Nusselt number and velocity and temperature profile are presented in tabular form and graphically. The results for the reduced skin friction coefficient and reduced Nusselt number are compared with that reported results by Bhattacharyya and Vajravelu (2012). The reduced Nusselt number is presented in the Table 3.1 with various values of Prandtl number  $Pr$  and stretching/shrinking parameter  $\nu$ . It shows that the reduced Nusselt number increases with an increase in the value of  $Pr$  and  $\nu$ .

Furthermore, the reduced skin friction coefficient  $f''(0)$  and reduced Nusselt number  $-\theta'(0)$  are plotted in Figures 3.1 and 3.2 respectively. These figures show dual and unique solutions. The aforementioned problem has a dual solution for  $-1.487068 \leq \nu \leq -0.9734$ , a unique solution exists for  $\nu > -0.9734$  and for  $\nu < -1.487068$  there is no similarity solution. Figures 3.3 and 3.4 explain the

temperature profile  $\theta(y)$  with various values of  $Pr$  and  $v$ , respectively. The finding shows that the temperature profiles decreases, when the Prandtl number and stretching/shrinking parameter increase.

**Table 3.1:** The various value reduced Nusselt number  $-\theta'(0)$  with different values of  $Pr$  and  $v$ .

		$-\theta'(0)$				
		0.2	0.5	0.7	0.9	1
$v$	$Pr$					
-0.7		0.3543	0.4488	0.4772	0.4933	0.4983
-0.5		0.3866	0.5176	0.5676	0.6041	0.6190
-0.3		0.4156	0.5793	0.6484	0.7029	0.7263
0.1		0.4665	0.6874	0.7898	0.8751	0.9134
0.5		0.5111	0.7817	0.9126	1.0244	1.0751
1		0.5605	0.8862	1.0486	1.1889	1.2533
3		0.7185	1.2199	1.48067	1.7099	1.8159

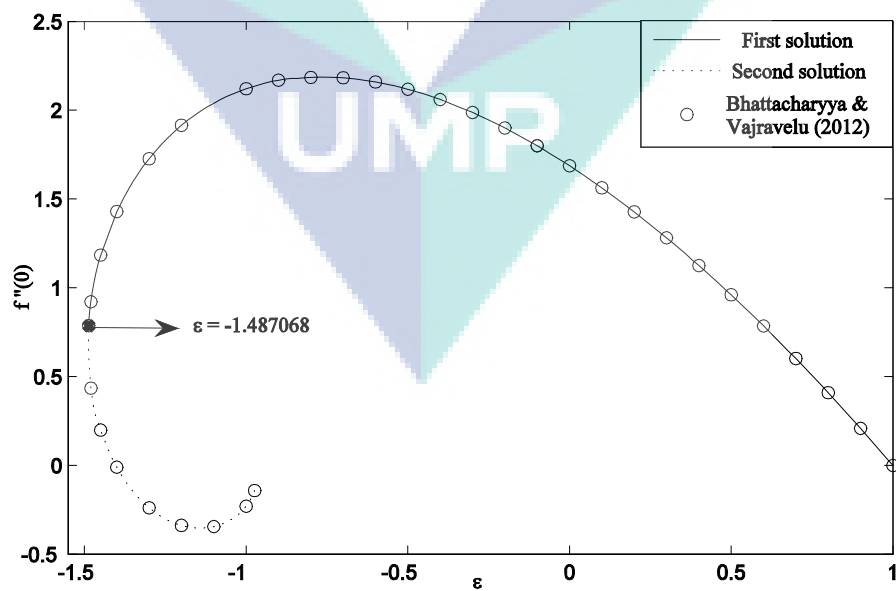


**Figure 3.1:** Comparison of the reduced skin friction coefficient  $f''(0)$  with different values of  $v$

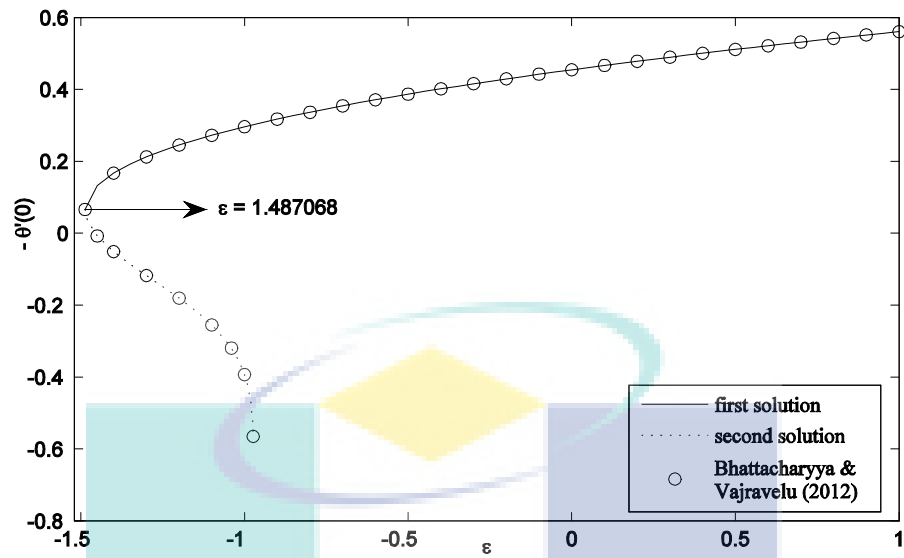


**Figure 3.2:** Comparison of the reduced Nusselt number  $-\theta'(0)$  with different values of  $\nu$  when  $Pr = 0.2$

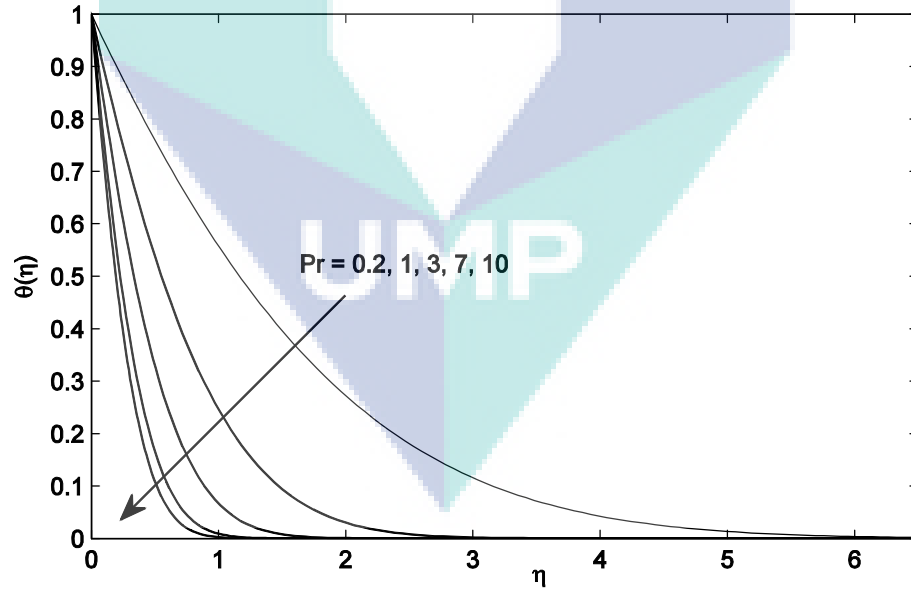


**Figure 3.3:** Variation of temperature profile  $\theta(\eta)$  with different values of  $Pr = 0.2, 1, 3, 7, 10$  when  $\nu = 0.5$

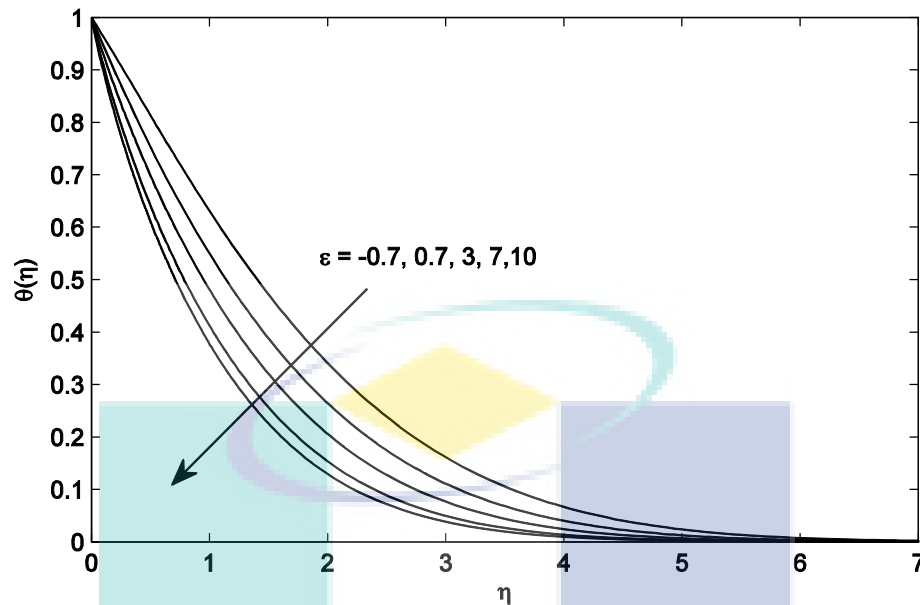


**Figure 3.4:** Variation of temperature profile  $\theta(\eta)$  with different values of  $\epsilon = -0.7, 0.7, 3, 7, 10$  when  $Pr = 0.2$

### 3.3.2 Prescribed Surface Heat Flux (PHF)

The problem of the stagnation point over an exponentially stretching/shrinking sheet with prescribed surface heat flux (PHF) has been numerically solved using Keller-box method. The results obtained are consistent with that have been reported by Bhattacharyya and Vajravelu (2012) in Figure 3.1. This confirms the dual existence and uniqueness of the solution to the aforementioned problem. Figure 3.5 illustrates the  $\sqrt{2L/x} Nu_x / Re_x^{1/2}$  as a function of  $v$  and it shows that a dual solution exists for  $-1.487068 \leq v \leq -0.9734$ , while no similar solution exists for  $v < -1.487068$  and a unique solution exists for  $v > -0.9734$ . These findings show a good agreement with Bhattacharyya and Vajravelu (2012). It can be concluded that this method works well for the present problem, and the results presented here are accurate. Also this figure shows that when  $v$  decreases the  $\sqrt{2L/x} Nu_x / Re_x^{1/2}$  slightly decreases in the first solution but increases in the second solution. As  $v$  decreasing, the temperature increases and it is found that  $\sqrt{2L/x} Nu_x / Re_x^{1/2}$  decreases.

Figure 3.6 illustrates the first and second solutions of the velocity profiles  $f'(y)$  for different values of  $\nu$  and with  $Pr=0.2$ . From this figure, it is found that the boundary thickness of the second solution is thicker than that of the first solution. Moreover, the velocity at a point increases with an increasing  $\nu$  for first solution and decreases for second solution. Finally, Figures 3.7 and 3.8 illustrate the temperature profiles  $\theta(y)$  for different values of  $\nu$  and  $Pr$ , respectively. It can be seen that, as  $Pr$  and  $\nu$  decreases, the temperature increases and the thermal boundary layer thickness also increases. This is because for small values of  $Pr$ , the fluid is highly conductive. Physically, if  $Pr$  increases, the thermal diffusivity decreases and this phenomenon lead to the decreasing of energy transfer ability that reduces the thermal boundary layer. The velocity profiles  $f'(y)$  with various values of velocity ratio parameter  $\nu$  are presented in Figures 3.9 and 3.10. The velocity  $f'(y)$  for different values of  $\nu > 1$  and  $\nu < 1$  increase, when the value of  $\nu$  is increased.

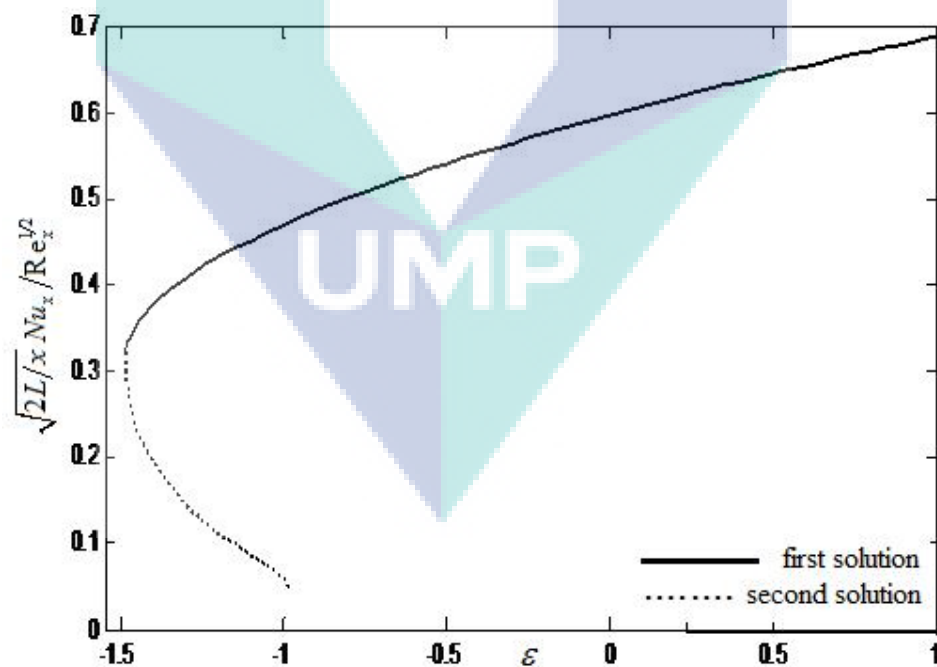
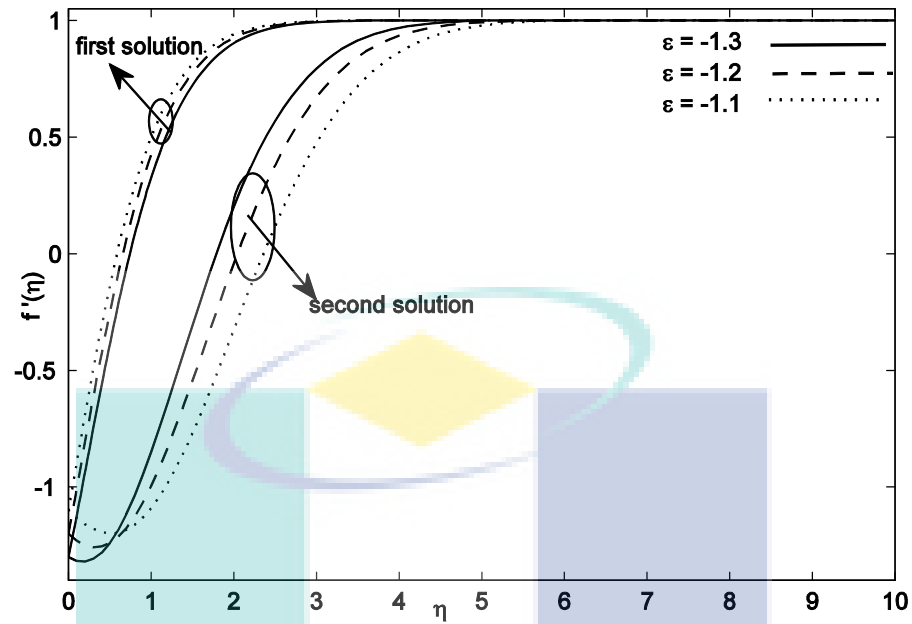
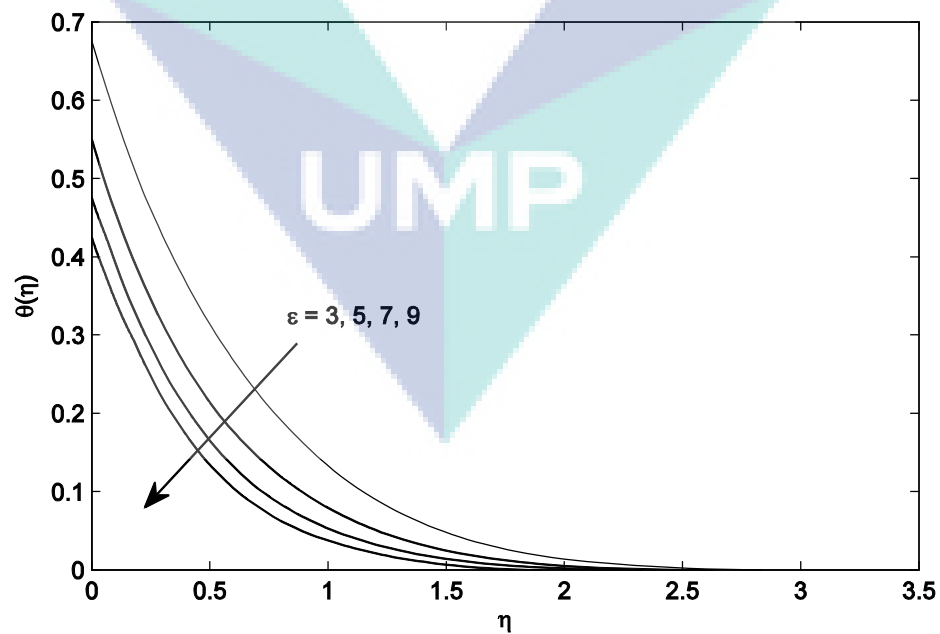


Figure 3.5: The value of  $\sqrt{2L/x} Nu_x / Re_x^{1/2}$  with  $\nu$



**Figure 3.6:** Variation of velocity profiles  $f'(y)$  with various values of  $v$  when  $Pr = 0.2$



**Figure 3.7:** Variation of temperature profiles  $\theta(y)$  with different values of  $v = 3, 5, 7, 9$  when  $Pr = 0.7$

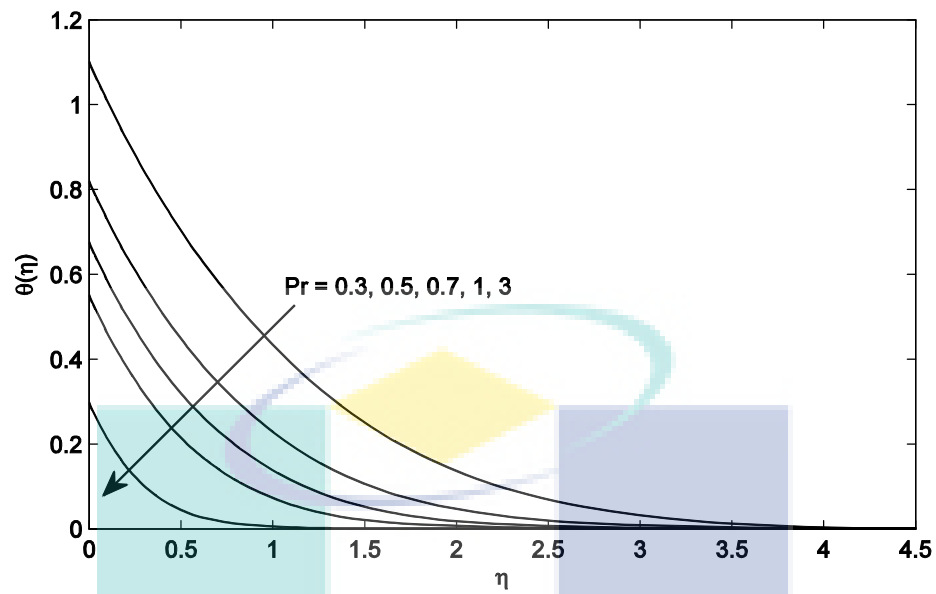


**Figure 3.8:** Variation of temperature profile  $\theta(\eta)$  with different values of  $Pr = 0.3, 0.5, 0.7, 1, 3$  when  $\nu = 3$

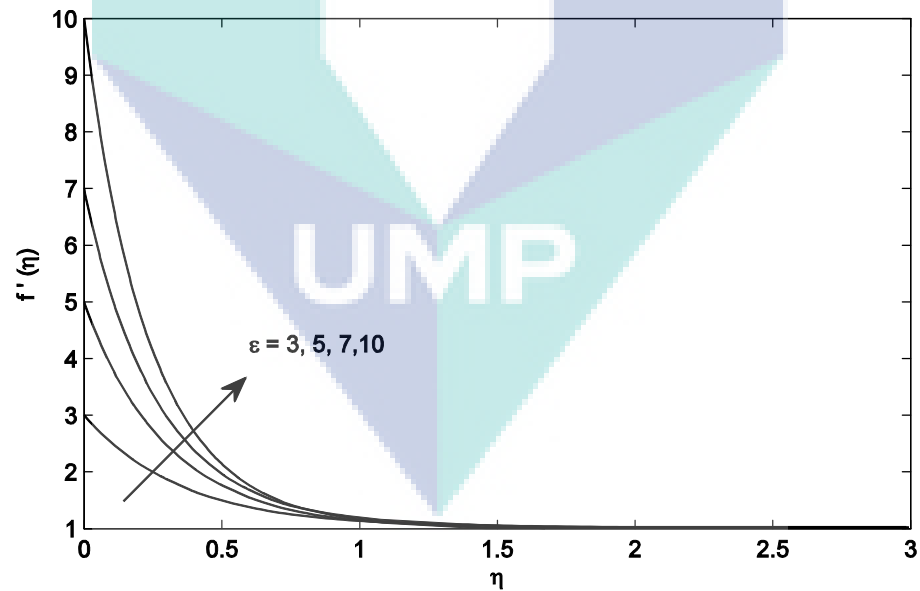


**Figure 3.9:** Variation of velocity profile  $f'(\eta)$  with different values of  $\nu = 3, 5, 7, 10$  when  $Pr = 0.7$

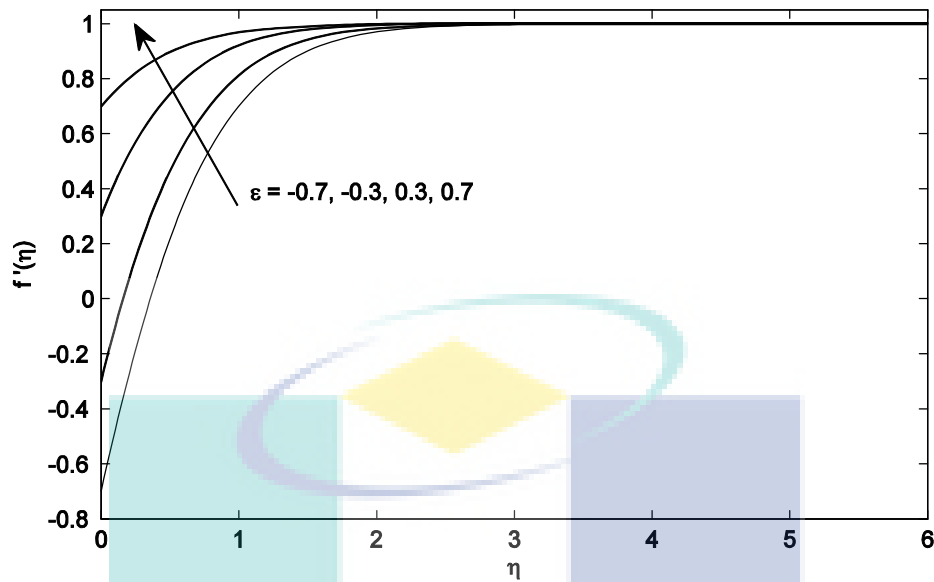


**Figure 3.10:** Variation of velocity profile  $f'(y)$  with different values of  $v = -0.7, -0.3, 0.3, 0.7$  when  $Pr = 0.7$

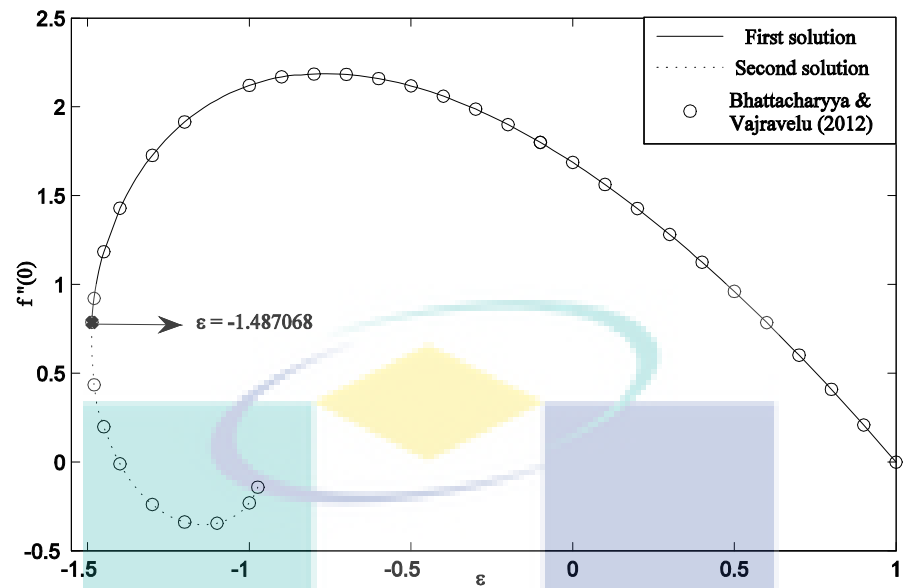
### 3.3.3 Convective Boundary Conditions (CBC)

Figures 3.12, 3.13 and 3.14 illustrate the reduced skin friction coefficient  $f''(0)$ , reduced Nusselt number  $-n'(0)$ , and the temperature  $n(0)$ , respectively, with various values of stretching/shrinking parameter  $v$ . From Figures 3.11 and 3.12 it was found that they are in a good agreement with the results reported by Bhattacharyya and Vajravelu (2012). It confirms the dual solution and unique solution of the aforementioned problem. In addition, it is found that the unique solution is for stretching case, while the dual solution is for shrinking case. These figures show that the dual solution exists, when  $-1.487068 \leq v \leq -0.9734$ . The unique solution exists when  $v > -0.9734$  and no solutions exist for  $v < -1.487068$ . Figure 3.13 illustrates that the stretching/shrinking parameter  $v$  increase with the increase in value of  $n(0)$  in the second solution. Meanwhile for the first solution  $v$  it decreases with the increasing value of  $n(0)$ .

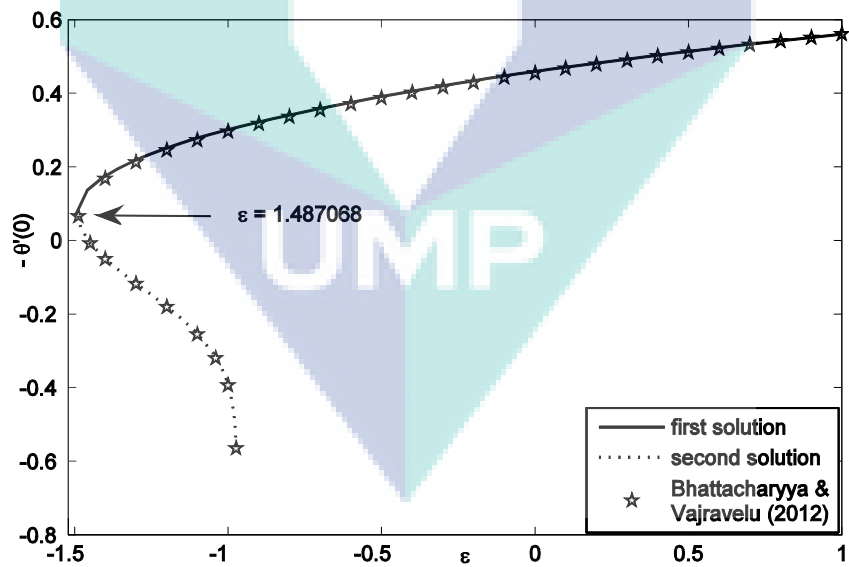
Figures 3.14 and 3.15 illustrate the temperature  $\theta(0)$  with  $Pr$  and  $\chi$  when  $\chi = 0.5, 1$  and  $Pr = 0.2$ , respectively. Figure 3.16 shows  $Pr$  must be less than some critical value, i.e.  $Pr_{c1} = 0.35$  and  $Pr_{c2} = 0.56$  when  $\chi = 0.5$  and  $\chi = 1$ , respectively. The value of  $\chi$  must be greater than some critical value, i.e.  $\chi_c = 0.186$  when  $\nu = -1.2$  and  $Pr = 0.2$  seen from Figure 3.15.

Figures 3.16 to 3.18 display the temperature profile  $\theta(y)$  for several values of  $\nu$ ,  $Pr$  and  $\chi$ , respectively. Figure 3.16 shows that the thermal boundary layer thickness for the second solution which is thicker than the case of the first solution in the temperature profile. In the first solution, magnitude of  $\nu$  at a point increase of the temperature  $\theta(y)$ . However temperature  $\theta(y)$  at the same point increases with the decrease in the magnitude of  $\nu$  in the second solution. The variation of the temperature profiles for same values of Prandtl number is visible in Figure 3.17. This shows that for a case of stretching/shrinking parameter, the temperature  $\theta(y)$  sharply increases initially with an increased value of the Prandtl number in the second solution. The Prandtl number decreases when the temperature  $\theta(y)$  increases in the first solution. Figure 3.18 shows the temperature profile with various values of  $\chi$ . It is observed that the temperature  $\theta(y)$  increases, with the increase in the value of conjugate parameter  $\chi$ , in the first solution, while for second solution it decreases.

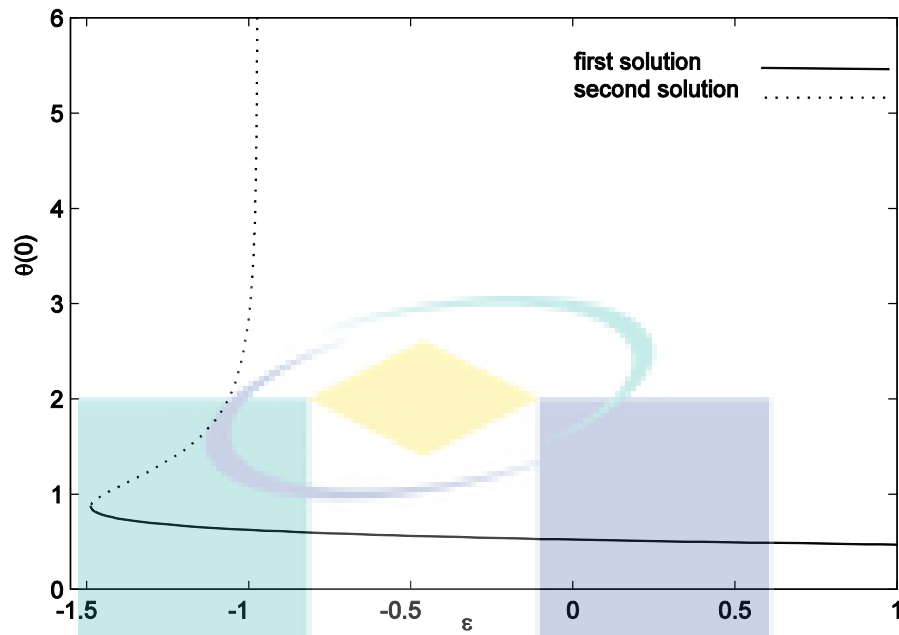
The dual and unique solutions of the velocity profile with various values of  $\nu$  are shown in Figures 3.19 and 3.20, respectively. From Figure 3.19 exhibits that in second solution the velocity increases with the decrease in the value of  $\nu$  except for a very small  $y$ . However, the velocity increases with the increase in the value of  $\nu$  in the case of first solution. Finally the velocity increases with the increase in the value of stretching parameter as illustrated in Figure 3.20. Lastly Table 3.2 shows the comparison velocity and temperature profile with three cases of boundary condition. It is found that, in three cases of boundary condition the behavior of velocity are same. The velocity increases by increasing the value of  $\nu$ , while the temperature decreases with increasing values of  $\nu$ . From this table, it is clear; the physical graphs of temperature are different which verified the boundary condition.



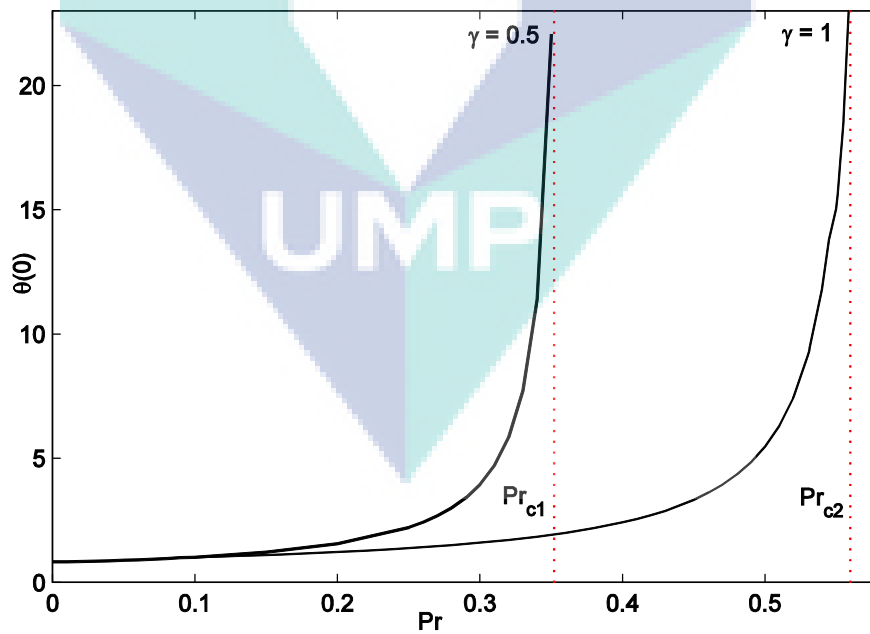
**Figure 3.11:** Variation of the reduced skin friction coefficient  $f''(0)$  with  $v$  when  $Pr = 0.2$  and  $\chi = 0.5$



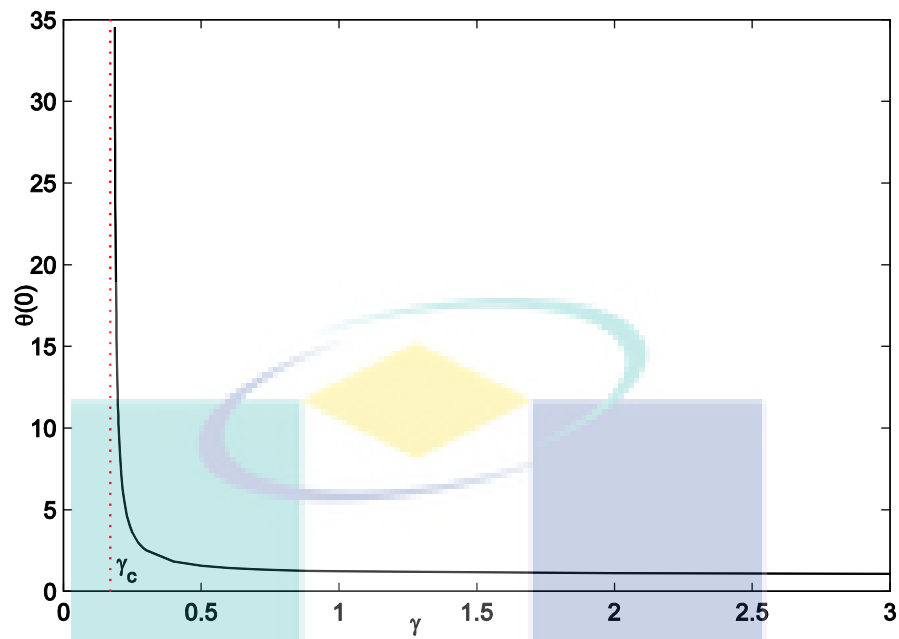
**Figure 3.12:** Comparison of the reduced Nusselt number  $-\theta'(0)$  with different values of  $v$  when  $Pr = 0.2$ ,  $\chi \rightarrow \infty$



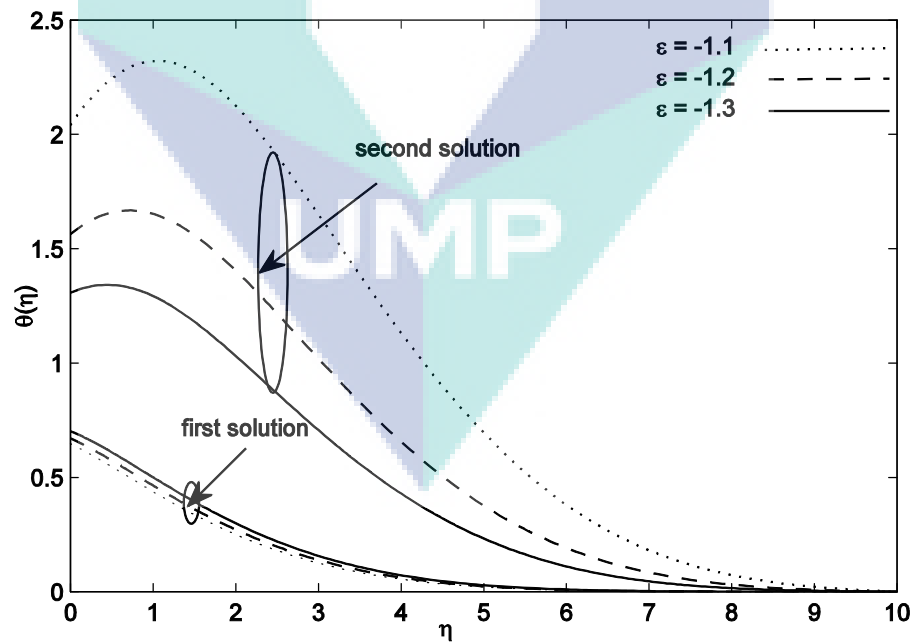
**Figure 3.13:** Variation of the temperature  $\theta(0)$  with  $v$  when  $Pr = 0.2$  and  $\chi = 0.5$



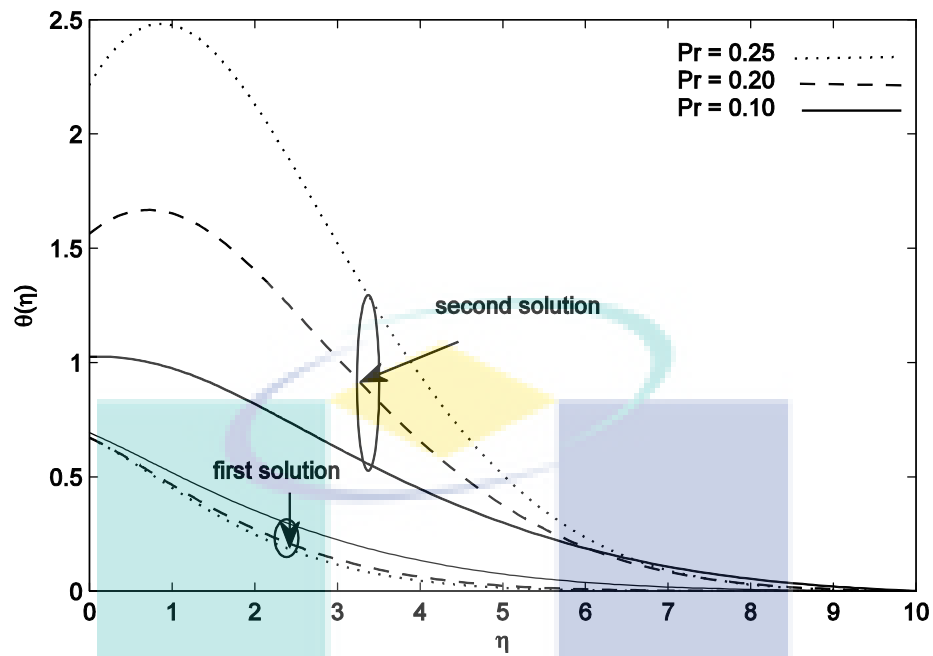
**Figure 3.14:** Variation of the temperature  $\theta(0)$  with  $Pr$  when  $\chi = 0.5, 1$  and  $v = -1.2$



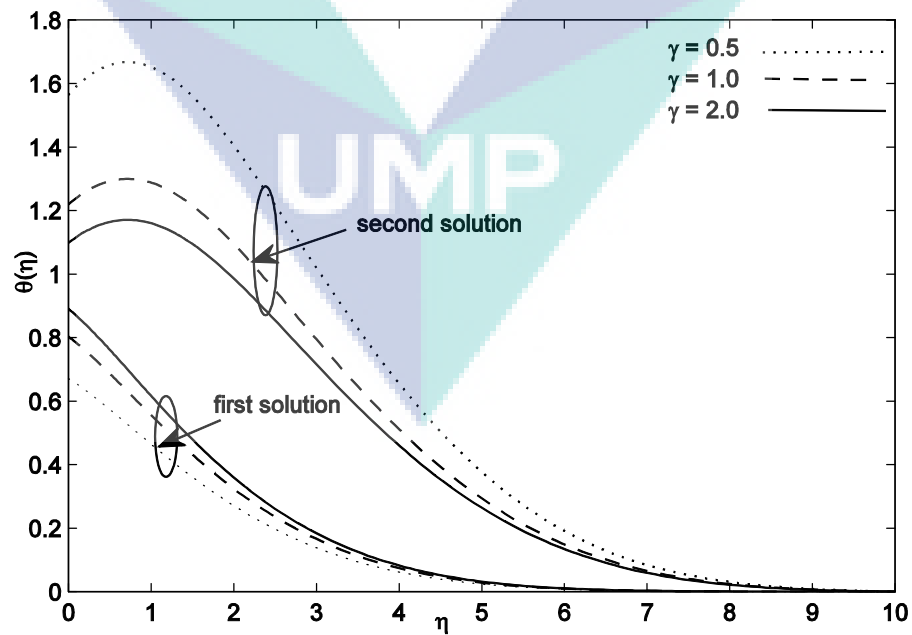
**Figure 3.15:** Variation of the temperature  $\theta(0)$  with  $\chi$  when  $Pr = 0.2$  and  $\nu = -1.2$



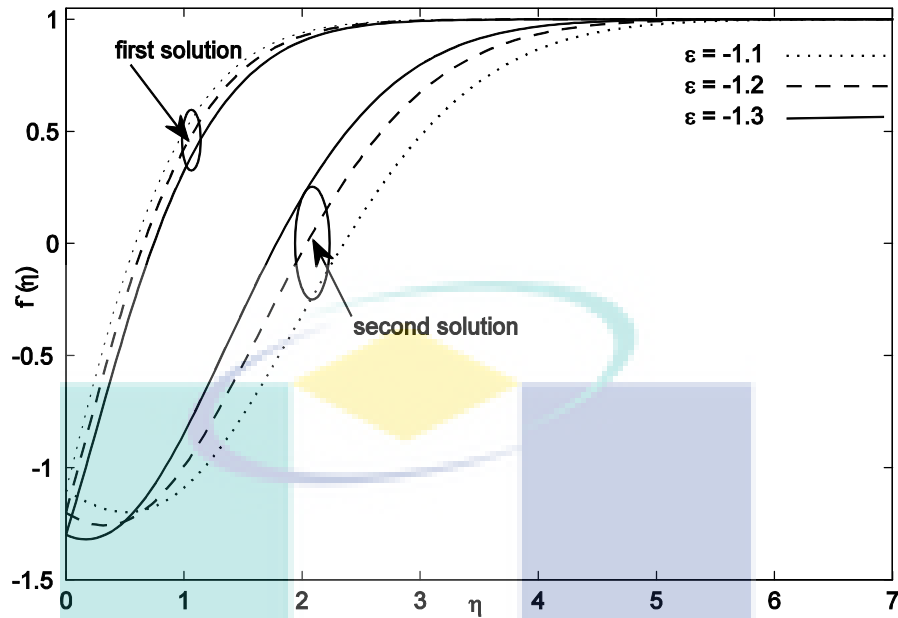
**Figure 3.16:** Temperature profile  $\theta(\eta)$  for various values of  $\nu = -1.1, -1.2, -1.3$  when  $Pr = 0.2$  and  $\chi = 0.5$



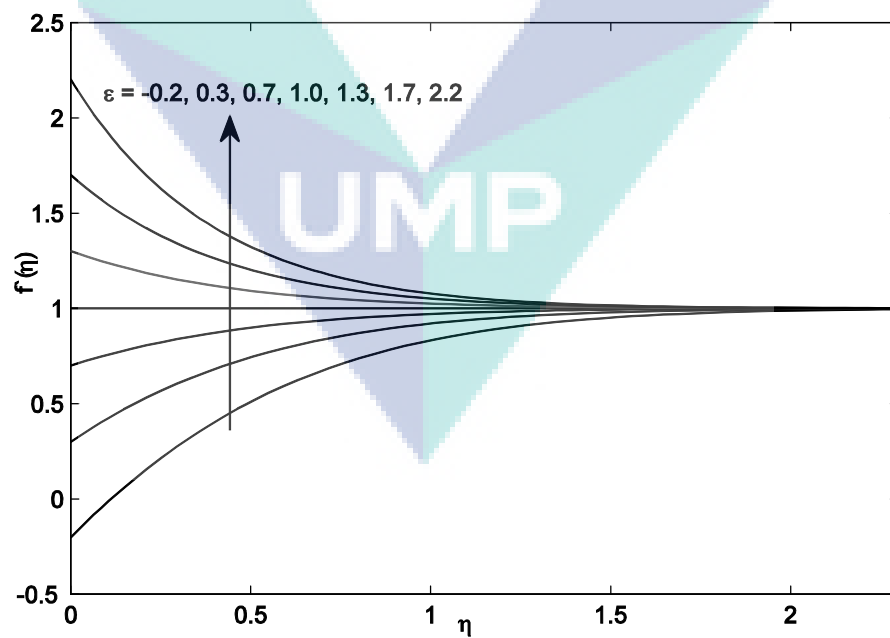
**Figure 3.17:** Temperature profile  $\theta(\eta)$  for various values of  $Pr = 0.1, 0.2, 0.25$  when  $v = -1.2$  and  $x = 0.5$



**Figure 3.18:** Temperature profile  $\theta(\eta)$  for various values of  $x = 0.5, 1, 2$  when  $Pr = 0.2$  and  $v = -1.2$



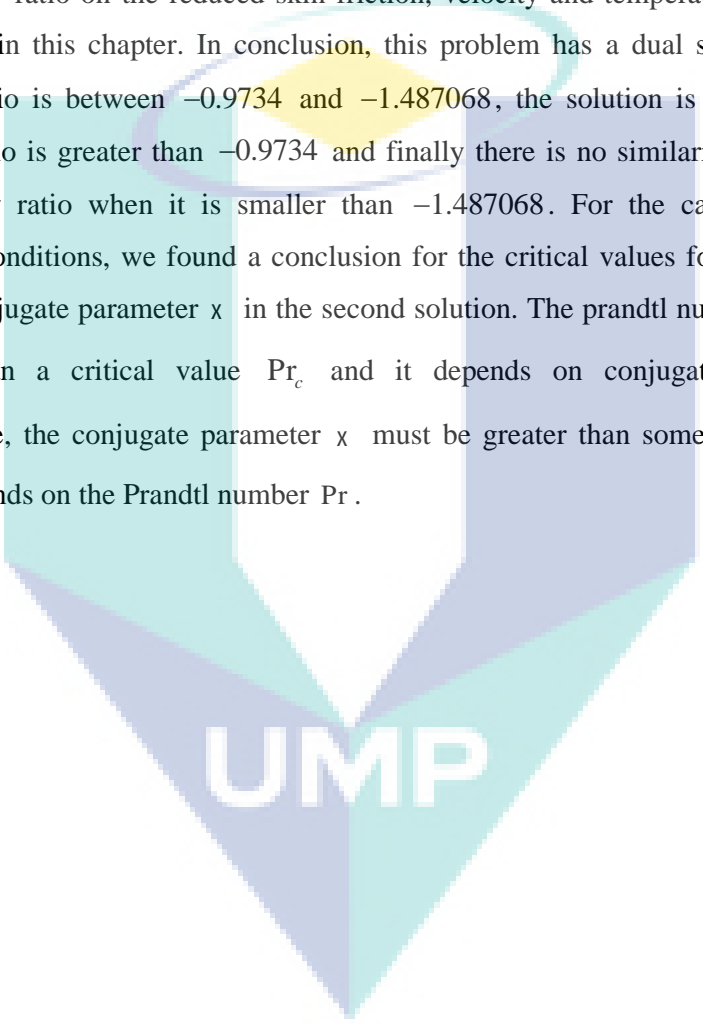
**Figure 3.19:** Velocity profiles  $f'(y)$  for different values of  $v = -1.1, -1.2, -1.3$  when  $Pr = 0.2$  and  $x = 0.5$



**Figure 3.20:** Velocity profiles  $f'(y)$  for different values of  $v = -0.2, 0.3, 0.7, 1.0, 1.3, 1.7, 2.2$  when  $Pr = 0.2$  and  $x = 0.5$

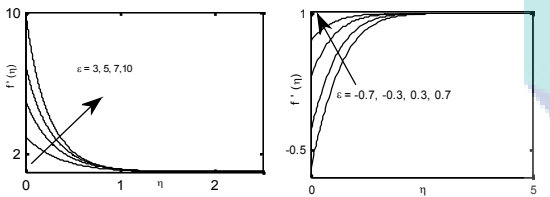
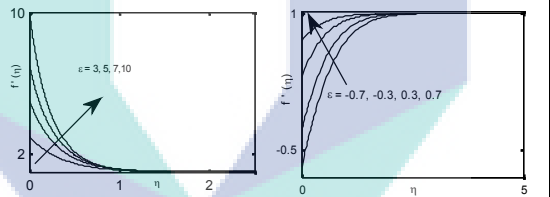
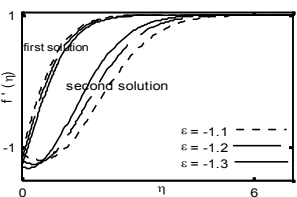
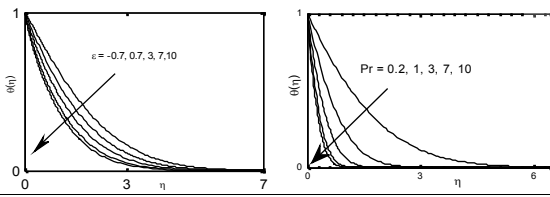
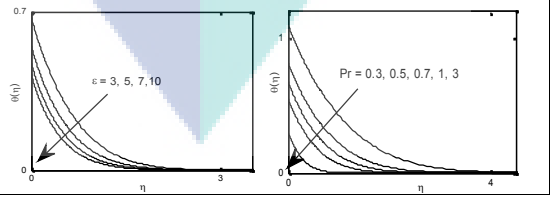
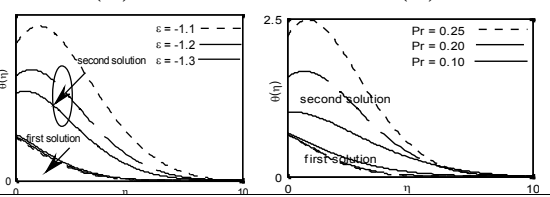
### 3.4 CONCLUSION

Two-dimensional boundary layer flow and heat transfer over an exponentially stretching/shrinking sheet is subjected to boundary conditions namely prescribed wall temperature, prescribed surface heat flux and convective boundary conditions were studied numerically in this chapter. The effects of Prandtl number, conjugate parameter and velocity ratio on the reduced skin friction, velocity and temperature profiles were considered in this chapter. In conclusion, this problem has a dual solution when the velocity ratio is between  $-0.9734$  and  $-1.487068$ , the solution is unique when the velocity ratio is greater than  $-0.9734$  and finally there is no similarity solution exists for velocity ratio when it is smaller than  $-1.487068$ . For the case of convective boundary conditions, we found a conclusion for the critical values for prandtl number  $Pr$  and conjugate parameter  $\chi$  in the second solution. The prandtl number  $Pr$  must be smaller than a critical value  $Pr_c$  and it depends on conjugate parameter  $\chi$ . Furthermore, the conjugate parameter  $\chi$  must be greater than some critical value  $\chi_c$  which depends on the Prandtl number  $Pr$ .

The logo of UMP (Universitas Muhammadiyah Purwokerto) is a large, stylized downward-pointing arrow. The arrow is composed of several overlapping geometric shapes in shades of teal and light blue. The letters 'UMP' are written in a bold, white, sans-serif font across the center of the arrow's shaft.

UMP

**Table 3.2:** The comparison velocity and temperature profiles with three boundary conditions PWT, PHF and CBC

	PWT	PHF	CBC
Boundary conditions	$u = U_w(x), v = 0, T = T_\infty + T_0 e^{\left(\frac{x}{2L}\right)}$ at $y = 0$ , $u = U_e(x), T \rightarrow T_\infty$ as $y \rightarrow \infty$ , and $f(0) = 0, f'(0) = v, \theta(0) = 1$ , $f'(\infty) = 1, \theta(\infty) = 0$ ,	$u = U_w(x), v = 0, \frac{\partial T}{\partial y} = -\frac{q_w}{k}$ at $y = 0$ , $u = U_e(x), T \rightarrow T_\infty$ as $y \rightarrow \infty$ , and $f(0) = 0, f'(0) = v, \theta'(0) = -1$ , $f'(\infty) = 1, \theta(\infty) = 0$ ,	$u = U_w(x), v = 0, -k \frac{\partial T}{\partial y} = h(T_\infty - T)$ at $y = 0$ , $u = U_e(x), T \rightarrow T_\infty$ as $y \rightarrow \infty$ , and $f(0) = 0, f'(0) = v, \theta'(0) = -x(1 - \theta(0))$ , $f'(\infty) = 1, \theta(\infty) = 0$ ,
Velocity Profile	$\uparrow v, \uparrow f'(y), v > 1$ $\uparrow v, \uparrow f'(y), v < 1$ 	$\uparrow v, \uparrow f'(y), v > 1$ $\uparrow v, \uparrow f'(y), v < 1$ 	$\uparrow v, \uparrow f'(y)$ FS ; $\uparrow v, \downarrow f'(y)$ , SS 
Temperature Profile	$\uparrow v, \downarrow \theta(y)$ $\uparrow Pr, \downarrow \theta(y)$ 	$\uparrow v, \downarrow \theta(y)$ $\uparrow Pr, \downarrow \theta(y)$ 	$\uparrow v, \downarrow \theta(y)$ , FS $\uparrow v, \uparrow \theta(y)$ , SS $\uparrow Pr, \downarrow \theta(y)$ , FS $\uparrow Pr, \uparrow \theta(y)$ , SS 

Not: FS=first solution and SS=second solution

## CHAPTER 4

### RADIATION EFFECT ON MHD STAGNATION POINT FLOW AND HEAT TRANSFER TOWARDS AN EXPONENTIALLY STRETCHING SHEET

#### 4.1 INTRODUCTION

The influence of thermal radiation on magnetohydrodynamic (MHD) stagnation point flow over an exponentially stretching sheet is considered in this chapter. This topic has received attention from many researchers due to its application in industrial and manufacturing processes. Elbashbeshy (2001), Khan (2006) and Sajid and Hayat (2008) have studied the two-dimensional boundary layer flow in a viscous fluid and viscoelastic fluid over an exponentially stretching sheet with suction and thermal radiation effects, respectively.

This problem was solved numerically using the Keller-box method. The numerical results were compared with the results obtained by Magyari and Keller (1999), Bidin and Nazar (2009), Ishak (2011), Mukhopadhyay (2013), Mabood et al. (2014) and Mustafa et al. (2013).

#### 4.2 MATHEMATICAL FORMULATION

Consider the problem of radiation effects of MHD boundary layer stagnation point and heat transfer over an exponentially stretching/shrinking sheet as shown in Figure 4.1. The Cartesian coordinate system is used in such a way that the  $x$ -axis is along the surface of the sheet and the  $y$ -axis is normal to it. Her  $U_e(x) = be^{x/L}$  is the free stream velocity and  $b > 0$  is the straining velocity rate, the velocity stretching velocity is  $U_w(x) = ae^{x/L}$ ,  $a$  is the stretching velocity rate and  $T_w = T_\infty + T_0e^{x/2L}$  is the surface

temperature,  $T_\infty$  is the stream temperature assumed to be constant,  $T_0$  is a constant which measures the rate of temperature increase along the sheet,  $L$  is the reference length,  $B(x)$  is the magnetic field and the thermal radiation parameter is  $q_r$ .

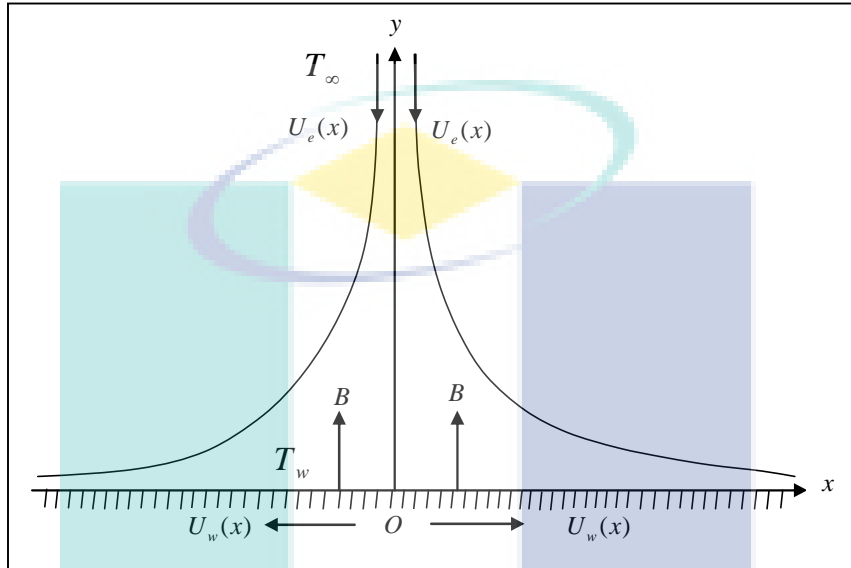


**Figure 4.1:** Physical model and coordinate system

The boundary layer equations are written as

$$\frac{\partial u}{\partial x} + \frac{\partial v}{\partial y} = 0, \quad (4.1)$$

$$u \frac{\partial u}{\partial x} + v \frac{\partial u}{\partial y} = U_e \frac{dU_e}{dx} + \nu \frac{\partial^2 u}{\partial y^2} - \frac{\sigma B^2}{\rho} u, \quad (4.2)$$

$$u \frac{\partial T}{\partial x} + v \frac{\partial T}{\partial y} = \frac{k}{\rho c_p} \frac{\partial^2 T}{\partial y^2} - \frac{1}{\rho c_p} \frac{\partial q_r}{\partial y}, \quad (4.3)$$

where  $u$  and  $v$  are the components of velocity in  $x$ - and  $y$ - axes, respectively.  $T$  is the temperature,  $\nu$  is the kinematic fluid viscosity,  $\sigma$  is the electric conductivity and  $k$  is the thermal conductivity. Subject to the boundary conditions (Bachok et al., 2012):

$$u = U_w(x), \quad v = 0, \quad \text{at } y = 0, \quad (4.4)$$

$$T = T_w = T_\infty + T_0 e^{\frac{x}{2L}} \text{ (PWT), at } y = 0, \quad (4.5)$$

$$\frac{\partial T}{\partial y} = -\frac{q_w}{k} \text{ (PHF), at } y = 0, \quad (4.6)$$

$$-k \frac{\partial T}{\partial y} = h(T_f - T) \text{ (CBC), at } y = 0, \quad (4.7)$$

$$u = U_e(x), T \rightarrow T_\infty, \text{ as } y \rightarrow \infty. \quad (4.8)$$

where  $q_w(x) = q_{w_0} \sqrt{a/2\nu L} e^{x/L}$  is the variable surface heat flux. According to Rosseland approximation, the radiative heat flux  $q_r$  is defined as

$$q_r = -\frac{4\uparrow^*}{3k^*} \frac{\partial T^4}{\partial y}, \quad (4.9)$$

where  $\uparrow^*$  and  $k^*$  the Stefan – Boltzmann and are constant and the mean absorption coefficient, respectively. It is assumed the temperature differences within the flow as such in that the term  $T^4$  in Taylor series toward  $T_\infty$  is given by

$$T^4 \approx 4T_\infty^3 T - 3T_\infty^4. \quad (4.10)$$

In view of Eqs. (4.9) and (4.10),

$$\frac{\partial q_r}{\partial y} = -\frac{16\uparrow^* T_\infty^3}{3k^*} \frac{\partial^2 T}{\partial y^2}. \quad (4.11)$$

Substituting Eq. (4.11) into Eq. (4.3) yields,

$$u \frac{\partial T}{\partial x} + v \frac{\partial T}{\partial y} = \left( \frac{k}{\dots c} + \frac{16\uparrow^* T_\infty^3}{3 \dots c k^*} \right) \frac{\partial^2 T}{\partial y^2}. \quad (4.12)$$

In order to satisfy the similarity solution, the magnetic field  $B(x)$  is assumed as

$$B = B_0 e^{\frac{x}{2L}}, \quad (2.13)$$

where  $B_0$  is the constant magnetic field.

A particularly useful similarity transformation is adopted from Sajid and Hayat (2008);

$$\Xi = \sqrt{(2avL)} e^{\frac{x}{2L}} f(y), \quad (4.14)$$

$$y = y \sqrt{\left(\frac{a}{2vL}\right)} e^{\frac{x}{2L}}, \quad (4.15)$$

$$\theta(y) = \frac{T - T_\infty}{T_w - T_\infty} \quad (\text{PWT}), \quad (4.16)$$

$$\theta(y) = \left(\frac{k}{q_w}\right) (T - T_\infty) \sqrt{\left(\frac{a}{2vL}\right)} e^{\frac{x}{2L}} \quad (\text{PHF}), \quad (4.17)$$

$$\theta(y) = \frac{T - T_\infty}{T_f - T_\infty} \quad (\text{CBC}), \quad (4.18)$$

where  $y$  is the similarity variable,  $f(y)$  is the dimensionless stream function and  $\theta(y)$  is the dimensionless temperature. The velocity component  $u$  and  $v$  are as

$$u = a e^{\frac{x}{2L}} f'(y). \quad (4.19)$$

$$v = -\sqrt{\frac{va}{2L}} e^{\frac{x}{2L}} \{f(y) + y f'(y)\}. \quad (4.20)$$

The stretching velocity  $U_w$  and straining velocity  $U_e$  are written as,

$$U_w = b e^{\frac{x}{2L}}, \quad (4.21)$$

$$U_e = a e^{\frac{x}{2L}}, \quad (4.22)$$

By substituting Eq. (2.22) to Eq. (2.24) and velocity components Eq. (4.19) and Eq. (4.20) into Eq. (4.2), the momentum equation derives as,

$$\begin{aligned}
& ae^{\frac{x}{L}} f'(\eta) \left( \frac{a}{L} e^{\frac{x}{L}} f'(\eta) + e^{\frac{x}{L}} f''(\eta) \frac{\eta a}{2L} \right) - \sqrt{\frac{va}{2L}} e^{\frac{x}{2L}} \{ f(\eta) + \eta f'(\eta) \} \\
& \left( ae^{\frac{x}{L}} f''(\eta) \sqrt{\frac{a}{2\nu L}} e^{\frac{x}{2L}} \right) = be^{\frac{x}{L}} \frac{b}{L} e^{\frac{x}{L}} + \epsilon \frac{a^2}{2\nu L} e^{\frac{2x}{L}} f'''(\eta) - \frac{\dagger S_0^2}{\dots} e^{\frac{x}{L}} ae^{\frac{x}{L}} f'(\eta), \\
& 2 \frac{a^2}{2L} e^{\frac{2x}{L}} (f'(\eta))^2 - \frac{a^2}{2L} e^{\frac{2x}{L}} f(\eta) f''(\eta) \\
& = 2 \frac{b^2}{2L} e^{\frac{2x}{L}} + \frac{a^2}{2L} e^{\frac{2x}{L}} f'''(\eta) - \left( \frac{2\dagger S_0^2 L}{\dots a^2} \right) \frac{a^2}{2L} e^{\frac{2x}{L}} f'(\eta), \\
& 2f'^2 - ff'' = 2\nu^2 + f''' - Mf', \\
& f''' + f f'' - 2f'^2 + 2\nu^2 - Mf' = 0, \tag{4.23}
\end{aligned}$$

where  $M = 2\dagger B_0^2 L / \dots a$  is the magnetic parameter

By substituting Eq. (2.27) to Eq. (2.29) into Eq. (4.12), the energy equation derives as,

a. Prescribed wall temperature

$$\begin{aligned}
& \left( ae^{\frac{x}{L}} f'(\eta) \right) \left( \frac{T_0}{2L} \eta'(\eta) \right) - \sqrt{\frac{va}{2L}} e^{\frac{x}{2L}} \{ f(\eta) + \eta f'(\eta) \}, \\
& T_0 e^{\frac{x}{2L}} \eta'(\eta) \sqrt{\frac{a}{2\nu L}} e^{\frac{x}{2L}} = \frac{k}{\dots c} \left( 1 + \frac{4}{3} \frac{4\dagger T_\infty^3}{k.k^*} \right) \frac{a T_0}{2\nu L} e^{\frac{3x}{2L}} \eta''(\eta), \tag{4.24}
\end{aligned}$$

b. Prescribed surface heat flux

$$\begin{aligned}
& \left( ae^{\frac{x}{L}} f'(\eta) \right) \left( \frac{q_{w_0}}{k} \frac{1}{2L} \eta''(\eta) e^{\frac{x}{2L}} \right) - \sqrt{\frac{va}{2L}} e^{\frac{x}{2L}} \{ f(\eta) + \eta f'(\eta) \}, \\
& \frac{q_{w_0}}{k} e^{\frac{x}{2L}} \eta''(\eta) \sqrt{\frac{a}{2\nu L}} = \frac{k}{\dots c} \left( 1 + \frac{4}{3} \frac{4\dagger T_\infty^3}{k.k^*} \right) \frac{q_{w_0}}{k} e^{\frac{3x}{2L}} \eta''(\eta) \frac{a}{2\nu L}, \tag{4.25}
\end{aligned}$$

c. Convective boundary condition

$$\begin{aligned}
& \left( ae^{\frac{x}{L}} f'(\eta) \right) \left( \frac{T_0}{2L} e^{\frac{x}{2L}} \eta''(\eta) \right) - \sqrt{\frac{va}{2L}} e^{\frac{x}{2L}} \{ f(\eta) + \eta f'(\eta) \} \\
& \left( T_0 e^{\frac{x}{2L}} \eta''(\eta) \sqrt{\frac{a}{2\nu L}} \right) = \frac{k}{\dots c} \left( 1 + \frac{4}{3} \frac{4\dagger T_\infty^3}{k.k^*} \right) T_0 e^{\frac{x}{2L}} \eta''(\eta) \frac{a}{2\nu L} e^{\frac{x}{2L}}, \tag{4.26}
\end{aligned}$$

The resulting of Eq. (4.24) to (4.26) are,

$$\left(1 + \frac{4}{3}N_R\right)\theta'' + \text{Pr}(f\theta' - f'\theta) = 0, \quad (4.27)$$

where  $N_R = \frac{4\ddagger^*T_\infty^3}{k^*k}$  is the radiation parameter and  $\text{Pr} = \dots v c_p / k$  is the Prandtl number.

The boundary conditions Eqs. (4.4) to (4.8) become,

$$\begin{aligned} f(0) &= 0, \quad f'(0) = 1 \text{ at } y = 0, \\ \theta(0) &= 1 \text{ (CWT), at } y = 0, \\ \theta'(0) &= -1 \text{ (CHF), at } y = 0, \\ \theta'(0) &= -\chi(1 - \theta(0)) \text{ (CBC) at } y = 0, \\ f'(y) &\rightarrow v, \quad \theta(y) = 0 \text{ as } y \rightarrow \infty. \end{aligned} \quad (4.28)$$

where  $v = a/b$  is the velocity ratio parameter.

The physical quantities of interest are the skin friction coefficient  $C_f$  and local Nusselt number  $Nu_x$  which are introduced in Eqs. (3.4) and (3.5) and the surface shear stress  $\ddagger_w$  is in Eq. (3.6), but the surface heat flux  $q_w$  is defined as:

$$q_w = -k \left( \left( k + \frac{16\ddagger^*T_\infty^3}{3k^*} \right) \frac{\partial T}{\partial y} \right)_{y=0}, \quad (4.29)$$

The reduced skin friction is defined as,

$$C_{fx} = C_f \sqrt{\frac{2L}{x} \text{Re}_x} = f''(y).$$

By using the boundary conditions Eq. (4.5) to Eq. (4.7) and similarity transformation Eq. (4.16) to Eq. (4.18), the reduced Nusselt number for three cases of boundary conditions are,

- a. Prescribed wall temperature,

$$\begin{aligned}
 Nu_x &= \frac{-kx \left( \left( 1 + \frac{16\ddagger T_\infty^3}{3k^*k} \right) T_0 e^{\frac{x}{2L}} \prime(y) \sqrt{\frac{a}{2\nu L}} \right)}{k \left( T_\infty + T_0 e^{\frac{x}{2L}} - T_\infty \right)}, \\
 Nu_x &= - \frac{\left( 1 + \frac{4}{3} N_R \right) \prime(y) \sqrt{x e^{\frac{x}{2L}} a \frac{x}{\nu}}}{\sqrt{2L}}, \\
 \frac{Nu_x}{\left( 1 + \frac{4}{3} N_R \right) \sqrt{Re_x}} \sqrt{\frac{2L}{x}} &= - \prime(y). \tag{4.30}
 \end{aligned}$$

b. Prescribed heat flux,

$$\begin{aligned}
 Nu_x &= - \frac{-kx \left( \left( 1 + \frac{16\ddagger T_\infty^3}{3k^*k} \right) \frac{q_{w_0}}{k} \sqrt{\frac{a}{2\nu L}} e^{\frac{x}{2L}} \right)}{k \left( T_\infty + \left( \frac{q_{w_0}}{k} \right) \prime(y) e^{\frac{x}{2L}} - T_\infty \right)}, \\
 Nu_x &= \frac{\left( 1 + \frac{4}{3} N_R \right) \sqrt{x e^{\frac{x}{2L}} a \frac{x}{\nu}}}{\prime(y) \sqrt{2L}}, \\
 \frac{Nu_x}{\left( 1 + \frac{4}{3} N_R \right) \sqrt{Re_x}} \sqrt{\frac{2L}{x}} &= \frac{1}{\prime(y)}. \tag{4.31}
 \end{aligned}$$

c. Convective boundary condition,

$$\begin{aligned}
 Nu_x &= \frac{-kx \left( - \left( 1 + \frac{16\ddagger T_\infty^3}{3k^*k} \right) \frac{h}{k} T_0 e^{\frac{x}{2L}} (1 - \prime(y)) \right)}{k T_0 e^{\frac{x}{2L}}}, \\
 Nu_x &= \left( 1 + \frac{4}{3} \frac{4\ddagger T_\infty^3}{k^*k} \right) (1 - \prime(y)) h k^{-1} x \sqrt{\frac{a}{\nu}} e^{\frac{x}{2L}} \sqrt{\frac{\nu}{a}} e^{-\frac{x}{2L}}, \\
 \sqrt{\frac{2L}{x}} \frac{Nu_x}{\left( 1 + \frac{4}{3} N_R \right) \sqrt{Re_x}} &= x (1 - \prime(y)). \tag{4.32}
 \end{aligned}$$

where  $Re_x = \frac{u_e x}{\nu}$  is the local Reynolds number.

### 4.3 RESULTS AND DISCUSSION

Eqs. (4.23) and (4.27) are subject to the boundary conditions (4.28) were numerically solved for the three cases namely, the prescribed wall temperature (PWT), prescribed surface heat flux (PHF) and convective boundary conditions (CBC). In this section the effect of governing parameters on reduced skin friction coefficient, heat transfer coefficient and velocity and temperature profile are discussed in tabular form and graphically.

#### 4.3.1 Prescribed Wall Temperature (PWT)

In this subsection, the prescribed wall temperature with the effects of governing parameters on the reduced skin friction coefficient and heat transfer coefficient are discussed. The results compared with the existing results from Magyari and Keller (1999), Bidin and Nazar (2009), Ishak (2011), Mukhopadhyay (2013), Mabood et al. (2014) and Mustafa et al. (2013). The numerical comparison of existing results and previous results show good agreement, as illustrated in Tables 4.1 and 4.2. The numerical results without velocity ratio  $v$  are in good agreement with the previous results. The comparison results for various values of heat transfer coefficient  $-_{\theta}'(0)$  with radiation parameter  $N_R$ , magnetic parameter  $M$  and Prandtl number  $Pr$  are shown in Table 4.1. We notice that from Table 4.1, when  $N_R = M = 0$  (in the absence of radiation and magnetic field effects), the result is close towards the results reported by Magyari and Keller (1999), Bidin and Nazar (2009), Ishak (2011), Mukhopadhyay (2013) and Mabood et al. (2014). Moreover, when the parameters  $N_R$ ,  $M$  and  $Pr$  are presence, the present results good agreement with the results of Ishak (2011), Mukhopadhyay (2013) and Mabood et al. (2014).

Table 4.2 presents the value of reduced skin friction coefficient  $f''(0)$  with different values of velocity ratio parameter  $v$ . The results are compared with results of Mustafa et al. (2013). The various values of the reduced skin friction coefficient  $f''(0)$  and heat transfer coefficient  $-_{\theta}'(0)$  with different values of governing parameter are presented in Tables 4.3 to 4.6. In addition, the various values of the reduced skin

friction coefficient  $f''(0)$  and heat transfer coefficient  $-_\theta'(0)$  with different values of  $M$  when  $\text{Pr}, N_R = 1$  and  $\nu = 0.2$  are shown in Table 4.3. From this table we can see that the values of  $f''(0)$  and  $-_\theta'(0)$  reduces with increasing values of  $M$  when  $\text{Pr}, N_R$  and  $\nu$  are fixed.

Tables 4.4 and 4.5 present the different values of  $f''(0)$  and  $-_\theta'(0)$  with various values of  $N_R$  and  $\text{Pr}$ , respectively, when the others governing parameters are fixed. Increasing values of  $N_R$  with the values of  $-_\theta'(0)$  decrease, when  $\text{Pr}, M$  and  $\nu$  are fixed, visible in Table 4.4. Also, it can be seen clearly that the radiation parameter  $N_R$  does not effect on the reduced skin friction coefficient  $f''(0)$ . Table 4.5 shows that the values of  $f''(0)$  and  $-_\theta'(0)$  increase as the values of  $\text{Pr}$  increases when  $M = N_R = 1$  and  $\nu = 0.5$ . Table 4.6 illustrates the reduced skin friction coefficient  $f''(0)$  and heat transfer coefficient  $-_\theta'(0)$  with the various values of  $\nu$  when other parameters are fixed. The value of the reduced skin friction coefficient and heat transfer coefficient increase with increasing values of velocity ratio parameter  $\nu$ .

The velocity profile  $f'(y)$  for different values of velocity ratio parameter  $\nu$  is illustrated in Figures 4.2. It can be observed from this figure that the velocity increases with increasing values of  $\nu$ . Figure (4.3) shows the velocity profiles  $f'(y)$  for various values of the magnetic parameter  $M$ . The velocity  $f'(y)$  is found to increases with increasing values of  $M$  when  $\nu < 1$ , while a reverse effect is observed for the case of  $\nu > 1$  when  $\text{Pr} = N_R = 1$ . Furthermore, it is also clearly seen from these figures, that the velocity satisfies the given boundary condition (4.3) which ensures the accuracy of our results.

Figures 4.4 to 4.7 show the temperature profiles  $_\theta(y)$  with different values of  $\nu$ ,  $\text{Pr}$ ,  $N_R$  and  $M$ , respectively. Figure 4.4 discusses the variation of temperature field for different values of the velocity ratio parameter  $\nu$ . The temperature  $_\theta(y)$  decreases with increasing values of  $\nu$ . The influence of the Prandtl number  $\text{Pr}$  on the temperature field is shown in Figure 4.5. It can be observed from this figure that the temperature of

the fluid decreases, as  $Pr$  increases. This situation corresponds to the physical observation of the fluids with large Prandtl number which has high viscosity and small thermal conductivity. Consequently this makes the fluid thick. Naturally it causes a decrease in the velocity of the fluid.

On the other hand, from Figures 4.6, it is clear that when the radiation parameter  $N_R$  increases, the temperature also increases. The effect of the magnetic parameter  $M$  on the temperature profile is presented in Figure 4.7. Physically,  $M = 0$  means that there is no magnetic effect and the flow. Moreover, it is found from this figure that the temperature increases with increasing values of  $M$ . In addition, it can be concluded from the above graphs that the temperature is at a maximum near the plate and it decreased away from the plate and finally asymptotically approaches zero in the free stream region.

**Table 4.1:** The comparison heat transfer coefficient  $-u''(0)$  when  $v = 0$

$N_R$	$M$	$Pr$	Magyari and Keller (1999)	Bidin and Nazar (2009)	Ishak (2011)	Mukhopadh yay (2013)	Mabood et al. (2014)	Present Results
0	0	1	0.9548	0.9548	0.9548	0.9547	0.95478	0.9547
0	0	2	-----	1.4714	1.4715	1.4714	1.47151	1.4715
0	0	3	1.8691	1.8691	1.8691	1.8691	1.86909	1.8691
0	0	5	2.5001	-----	2.5001	2.5001	2.50012	2.5003
0	0	10	3.6604	-----	3.6604	3.6603	3.66039	3.6635
1	0	1	-----	0.5315	0.5312	0.5312	0.53121	0.5322
0	1	1	-----	-----	0.8611	0.8610	0.86113	0.8614
0.5	0	2	-----	1.0735	-----	1.0734	1.07352	1.0735
0.5	0	3	-----	1.3807	-----	1.3807	1.38075	1.3807
1	0	3	-----	1.1214	-----	1.1213	1.12142	1.1214
1	1	1	-----	-----	0.4505	-----	0.45052	0.4515

**Table 4.2:** Comparison skin friction coefficient  $f''(0)$  when  $M = 0$ 

$\nu$	$f''(0)$	
	Mustafa <i>et al.</i> (2013)	Present results
0	-1.281809	-1.2819
0.1	-1.253580	-1.2535
0.2	-1.195118	-1.1951
0.5	-0.879833	-0.8800
0.8	-0.397767	-0.3979
1.2	0.451568	0.4520

**Table 4.3:** Values of the reduced skin friction coefficient  $f''(0)$  and heat transfer coefficient  $-n'(0)$  for several values of  $M$  when  $\text{Pr} = N_R = 1$  and  $\nu = 0.2$ 

$M$	$f''(0)$	$-n'(0)$
0	-1.1950	0.6027
0.3	-1.3212	0.5712
0.5	-1.3982	0.5519
0.7	-1.4704	0.5343
1	-1.5715	0.5109
3	-2.1185	0.4054
5	-2.5481	0.3481
7	-2.9145	0.2857
10	-3.3904	0.2411

**Table 4.4:** Values of the reduced skin friction coefficient  $f''(0)$  and heat transfer coefficient  $-n'(0)$  for different values on  $N_R$  when  $Pr = M = 1$  and  $\nu = 0.2$

$N_R$	$f''(0)$	$-n'(0)$
0	-1.5713	0.9068
0.3	-1.5715	0.7248
0.5	-1.5715	0.6441
0.7	-1.5715	0.5818
1	-1.5715	0.5109
3	-1.5715	0.2702

**Table 4.5:** Values of the reduced skin friction coefficient  $f''(0)$  and heat transfer coefficient  $-n'(0)$  for various values of  $Pr$  when  $N_R = M = 1$  and  $\nu = 0.5$

$Pr$	$f''(0)$	$-n'(0)$
0.3	-1.3011	0.3083
0.5	-1.3011	0.4140
0.7	-1.3010	0.5037
1	-1.3010	0.6201
3	-1.2994	1.1751
5	-1.2970	1.5739
7	-1.2904	1.9079
10	-1.2833	2.3265

**Table 4.6:** Values of the reduced skin friction coefficient  $f''(0)$  and heat transfer coefficient  $-_{\eta}'(0)$  with various values of  $\nu$  when  $N_R = M = 1$  and  $Pr = 1$

$\nu$	$f''(0)$	$-_{\eta}'(0)$
0.1	-1.6142	0.4727
0.3	-1.5034	0.5499
0.5	-1.3010	0.6201
0.7	-1.0227	0.6822
0.9	-0.6790	0.7385
1	-0.4851	0.7648
3	5.7300	1.1700
5	15.2003	1.4663

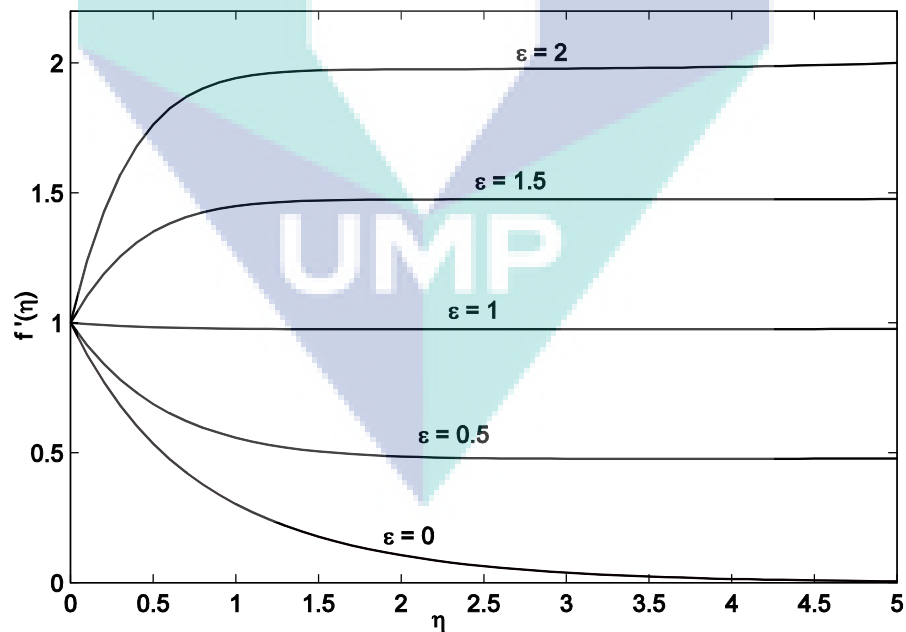


**Figure 4.2:** The velocity profile  $f'(\eta)$  with  $\eta$  for different values of  $\nu = 0, 0.5, 1, 1.5, 2$  when  $Pr = N_R = 1$  and  $M = 0.1$

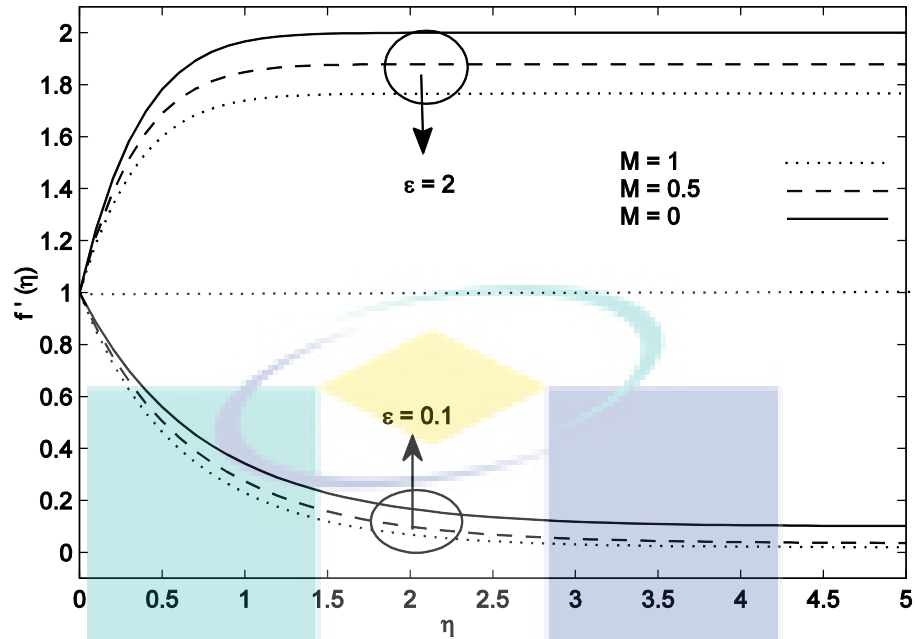


**Figure 4.3:** The velocity profile  $f'(y)$  with  $y$  for different values of  $M = 0, 0.5, 1$  when  $\nu = 0.1, 2$  and  $\text{Pr} = N_R = 1$

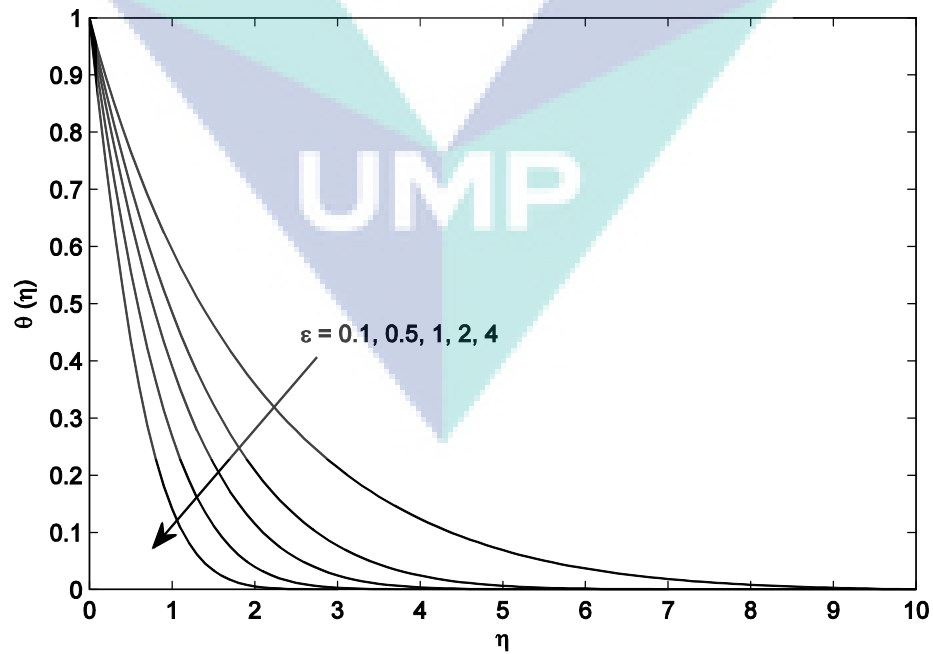


**Figure 4.4:** The temperature profile  $\theta(y)$  with  $y$  for different values of  $\nu = 0.1, 0.5, 1, 2, 4$  when  $\text{Pr} = N_R = 1$  and  $M = 1$

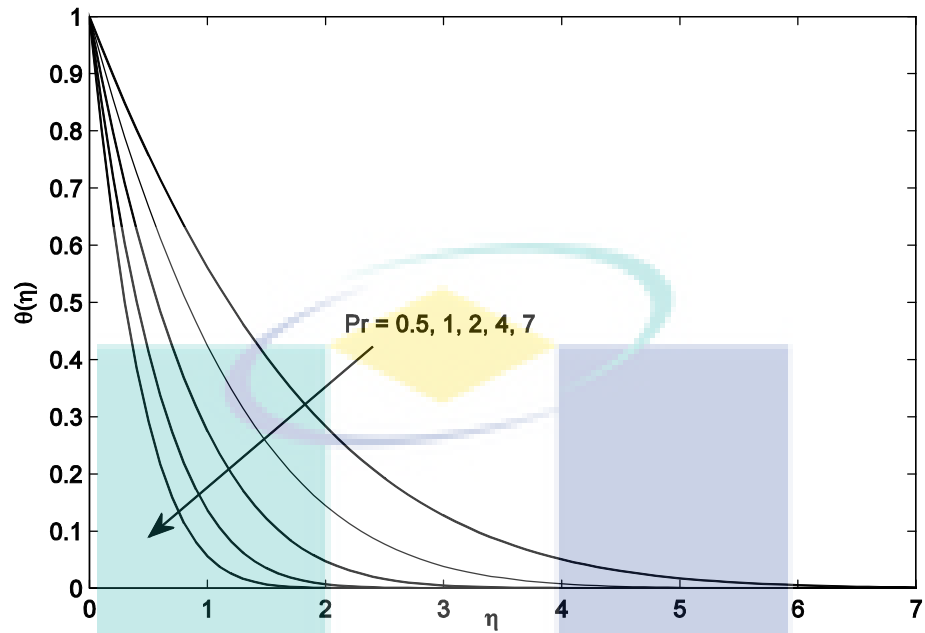


**Figure 4.5:** The temperature profile  $\theta(\eta)$  with  $\eta$  for different values of  $Pr = 0.5, 1, 2, 4, 7$  when  $\nu = N_R = 1$  and  $M = 1$

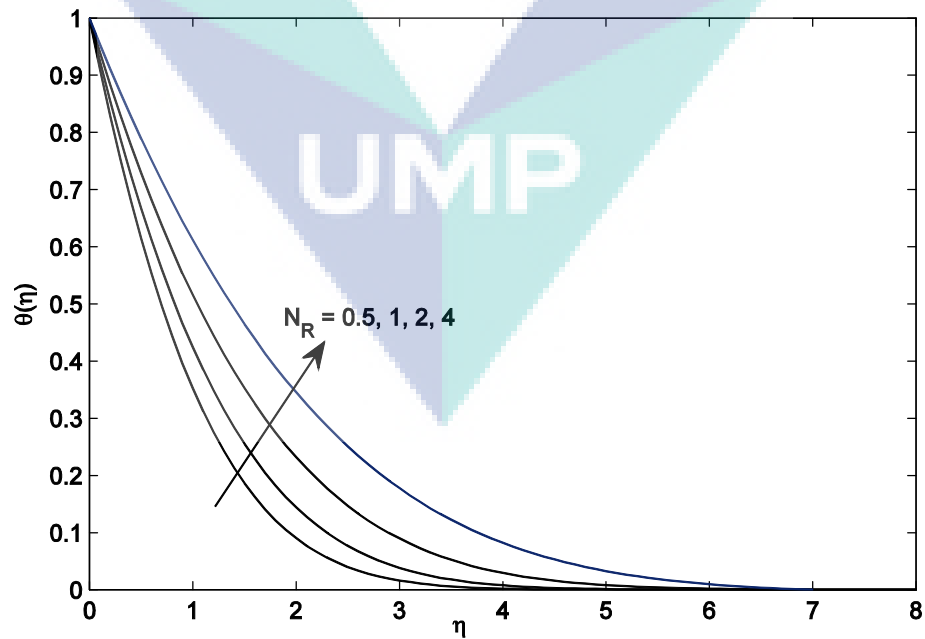


**Figure 4.6:** The temperature profile  $\theta(\eta)$  with  $\eta$  for different values of  $N_R = 0.5, 1, 2, 4$  when  $Pr = \nu = 1$  and  $M = 1$

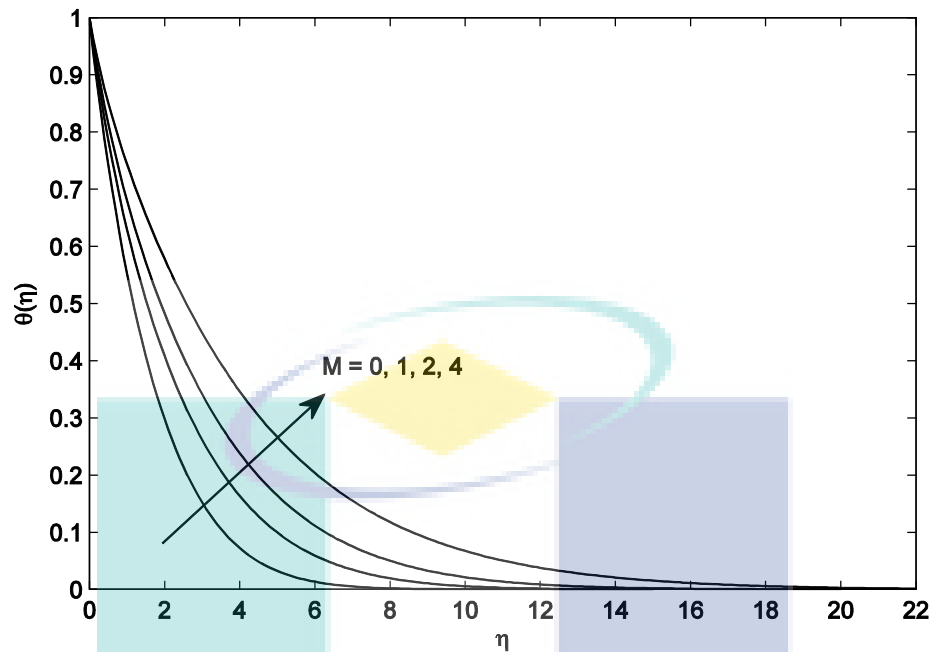


**Figure 4.7:** The temperature profile  $\theta(\eta)$  with  $\eta$  for different values of  $M = 0, 1, 2, 4$  when  $Pr = N_R = 1$  and  $\nu = 0.2$

### 4.3.2 Prescribed Surface Heat Flux (PHF)

Eqs. (4.23) and (4.27) with prescribed surface heat flux are solved numerically. Tables 4.7 and 4.8 illustrate the reduced Nusselt number with governing parameter namely, radiation effects parameter  $N_R$ , velocity ratio parameter  $\nu$ , Prandtl number  $Pr$  and magnetic parameter  $M$ . From Table 4.7 it can be clearly seen that the reduced Nusselt number increases with an increase in the values of velocity ratio parameter, while it decreases when the values of radiation parameter increases. Table 4.8 illustrates the reduced Nusselt number with magnetic parameter  $M$  and Prandtl number  $Pr$ . The table shows that in decreasing manner of the reduced Nusselt number, which represents the heat transfer rate at the surface, by increasing in values of magnetic parameter  $M$ , but the reduced Nusselt number increases with increasing values of Prandtl number.

The temperatures profiles  $\theta(\eta)$  with  $\nu$ ,  $Pr$ ,  $M$  and  $N_R$  are presented in Figures 4.8 to 4.11, respectively. Figure 4.8 presents by the variation of temperature profiles

$\theta(y)$  for different values of the velocity ratio parameter  $v$ . The temperature reduces with enhancing values of  $v$ . Figure 4.9 shows the effects of Prandtl number on the temperature profile  $\theta(y)$ , when others parameter are fixed. It is observed from this figure that the temperature of the fluid decreases with increasing values of  $Pr$ . In addition, the influence of magnetic parameter  $M$  on the temperature profile  $\theta(y)$  is presented in Figure 4.10. It is clear from this figure that due to increased in value of magnetic field, the temperature increases. Temperature profile with radiation parameter is shown in Figure 4.11. The temperature increases as the values of radiation parameter  $N_R$  increases.

Figure 4.12 illustrates the velocity profiles  $f'(y)$  for different values of velocity ratio parameter  $v$ . It can be seen from the Figure that the velocity is increasing with the increasing values of  $v$ . Figure 4.13 shows the velocity profiles  $f'(y)$  for various values of the magnetic parameter  $M$ . The velocity  $f'(y)$  is found to increase with increasing values of  $M$  when  $v < 1$ , while a reverse effect is observed for the case of  $v > 1$  when  $Pr = N_R = 1$ .

**Table 4.7:** Various values of the reduced Nusselt number for various values of  $v$  and  $N_R$  when  $M = 1$  and  $Pr = 1$

		$1/\theta'(0)$				
		0	0.5	1	2	3
$v$	$N_R$					
0.1		0.8393	0.4921	0.2703	0.1142	0.0503
0.5		1.0101	0.7361	0.5743	0.3821	0.2799
0.9		1.1533	0.8816	0.7370	0.5787	0.4850
2		1.4701	1.1580	0.9889	0.7989	0.6866
3		1.7099	1.3690	1.1698	0.9433	0.7184

**Table 4.8:** Various values of the reduced Nusselt number for various values of Pr and  $M$  when  $N_R = 1$  and  $\nu = 0.5$

		$1/\theta'(0)$				
$M$	Pr	0.5	0.7	1	3	5
1		0.3489	0.4492	0.5813	1.1351	1.5452
3		0.1869	0.2651	0.3499	0.8758	1.2949
5		0.1216	0.1804	0.2322	0.6578	1.0207
7		0.0955	0.1266	0.1929	0.5332	0.7204
10		0.0678	0.0736	0.1122	0.2799	0.6040

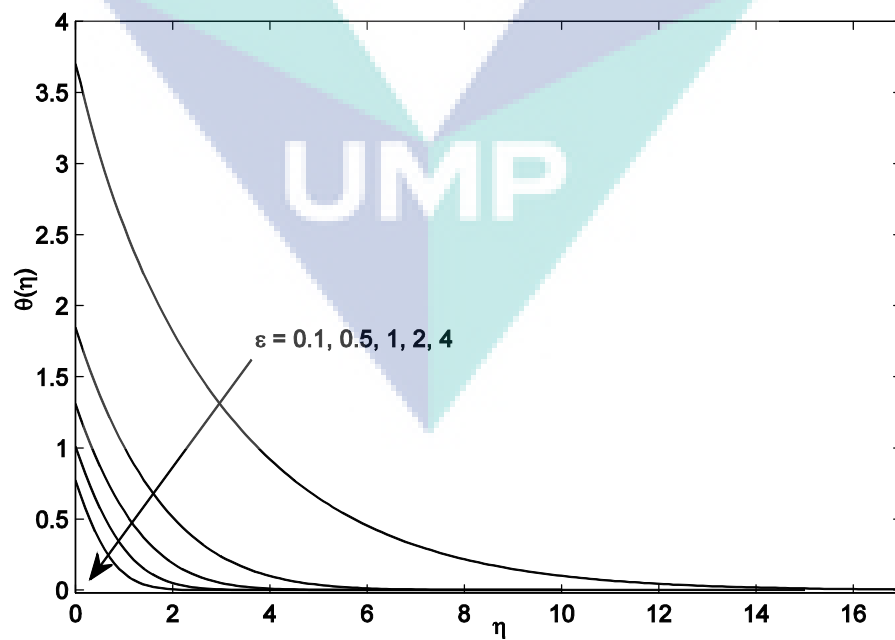


**Figure 4.8:** The temperature profile  $\theta(y)$  with  $y$  for different values of  $\nu = 0.1, 0.5, 1, 2$  when  $Pr = N_R = 1$  and  $M = 1$

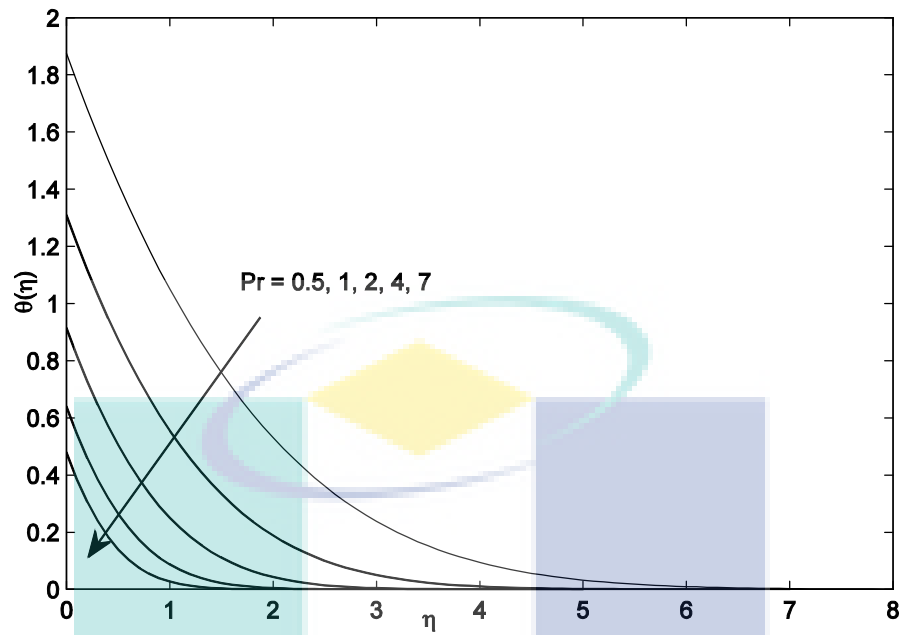


**Figure 4.9:** The temperature profile  $\theta(\eta)$  with  $\eta$  for different values of  $Pr = 0.5, 1, 2, 4, 7$  when  $N_R = \nu = 1$  and  $M = 1$

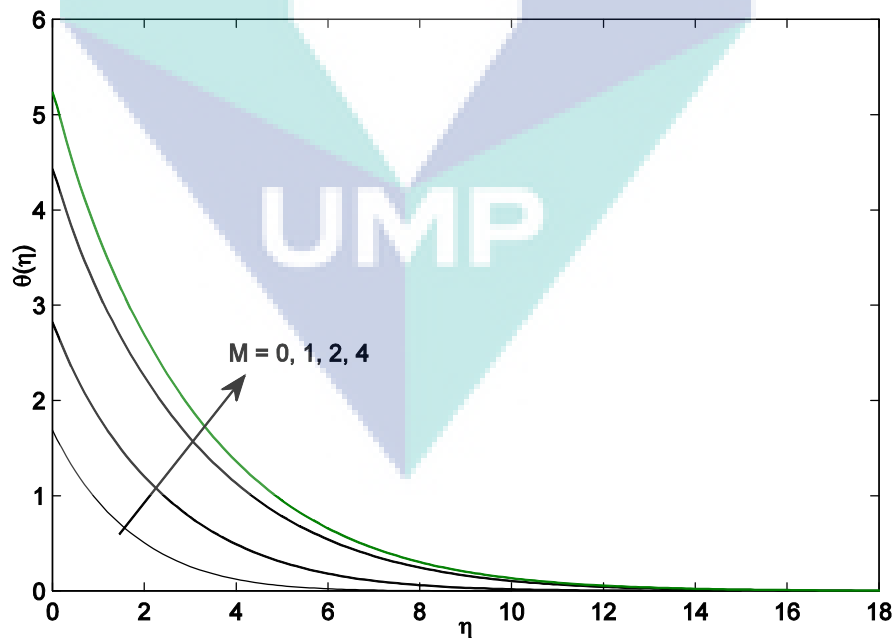


**Figure 4.10:** The temperature profile  $\theta(\eta)$  with  $\eta$  for different values of  $M = 0, 1, 2, 4$  when  $Pr = N_R = 1$  and  $\nu = 0.2$

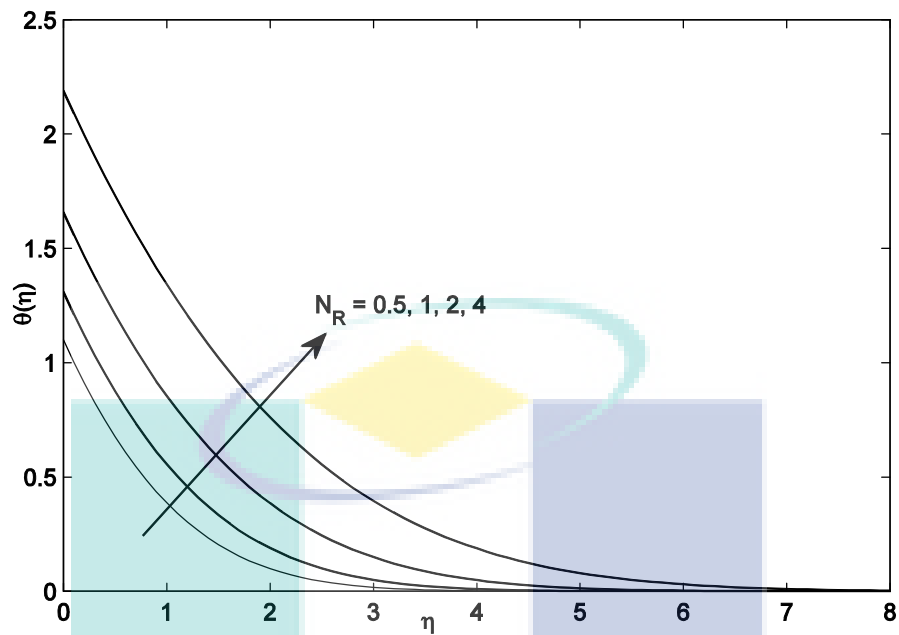


**Figure 4.11:** The temperature profile  $\theta(\eta)$  with  $\eta$  for different values of  $N_R = 0.5, 1, 2, 4$  when  $Pr = \nu = 1$  and  $M = 1$

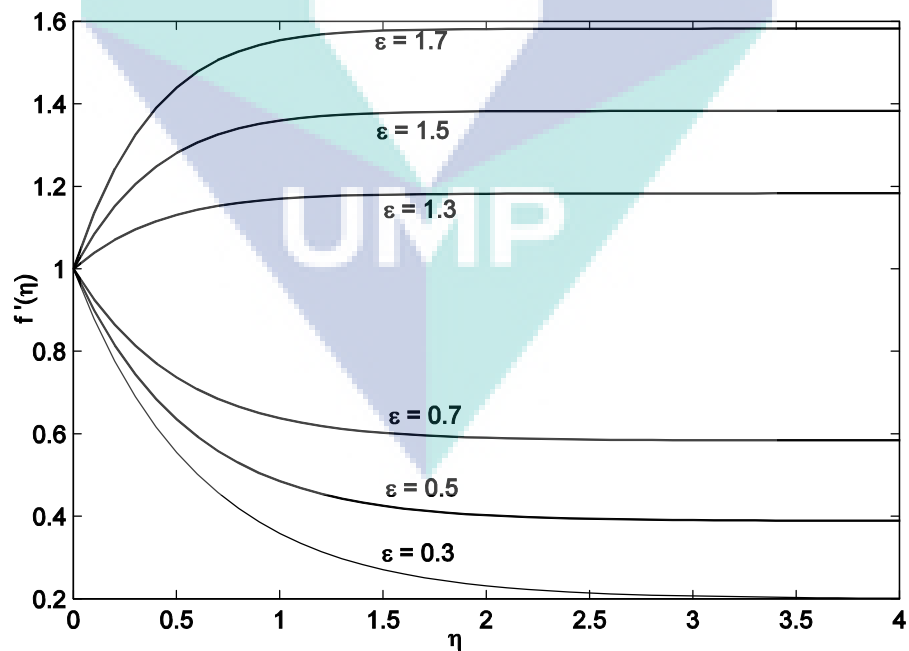


**Figure 4.12:** The velocity profile  $f'(\eta)$  with  $\eta$  for different values of  $\nu = 0.3, 0.5, 0.7, 1.3, 1.5, 1.7$  when  $Pr = N_R = 1$  and  $M = 0.5$

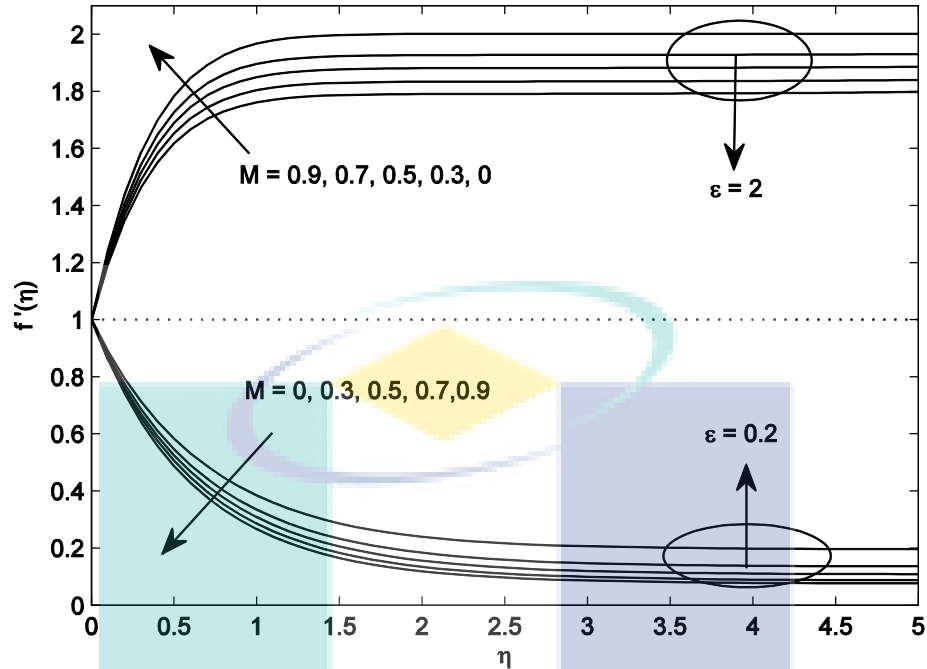


**Figure 4.13:** The velocity profile  $f'(y)$  with  $y$  for different values of  $M = 0.0, 0.3, 0.5, 0.7, 0.9$  when  $v = 0.2, 2$  and  $Pr = N_R = 1$

### 4.3.3 Convective Boundary Conditions (CBC)

The Eqs. (4.23) and (4.27) with boundary condition (4.28) are numerically solved for the case of convective boundary conditions with five parameters considered, namely, the magnetic parameter  $M$ , radiation parameter  $N_R$ , velocity ratio parameter  $v$ , Prandtl number  $Pr$  and conjugate parameter  $\chi$ . Table 4.9 presents the comparison results for convective boundary conditions (CBC) corresponding to the value of heat transfer coefficient  $-u'(0)$  without the velocity ratio parameter when  $\chi \rightarrow \infty$  with the available published results of Magyari and Keller (1999) and Ishak (2011). The new results shows good agreement with previous results reported by Magyari and Keller (1999) and Ishak (2011).

Tables 4.10 to 4.14 exhibit the reduced skin friction coefficient and heat transfer coefficient  $-u'(0)$  with various values of magnetic parameter  $M$ , radiation parameter

$N_R$ , velocity ratio parameter  $v$ , Prandtl number  $Pr$ , and conjugate parameter  $\chi$  respectively. Table 4.10 shows the reduced skin friction coefficient  $f''(0)$  and heat transfer coefficient  $-_{\theta}'(0)$  with various values of  $M$  when  $v = \chi = N_R = 0.5$  and  $Pr = 10$ . It demonstrates that with strong magnetic field the reduced skin friction coefficient and heat transfer coefficient are reduced. The reduced skin friction coefficient  $f''(0)$  and heat transfer coefficient  $-_{\theta}'(0)$  with various values of  $N_R$  when  $v = \chi = M = 0.5$  and  $Pr = 10$  are provided in Table 4.11. The value of the reduced skin friction coefficient  $f''(0)$  and heat transfer coefficient  $-_{\theta}'(0)$  decreases with increasing values of radiation parameter  $N_R$ .

Table 4.12 shows the reduced skin friction coefficient  $f''(0)$  and heat transfer coefficient  $-_{\theta}'(0)$  with various values of  $v$ , when other governing parameters are fixed. This table illustrates the reduced skin friction coefficient  $f''(0)$  and heat transfer coefficient  $-_{\theta}'(0)$  increases with increasing values of  $v$ . The effects of Prandtl number on the reduced skin friction coefficient  $f''(0)$  and heat transfer coefficient  $-_{\theta}'(0)$  are presented in Table 4.13. From this table it should be noted that by increasing the values of Prandtl number  $Pr$ , it will increase the reduced skin friction coefficient  $f''(0)$  and heat transfer coefficient  $-_{\theta}'(0)$ . Finally, the effect of the reduced skin friction coefficient  $f''(0)$  and heat transfer coefficient  $-_{\theta}'(0)$  with various values of  $\chi$  when  $v = M = N_R = 0.5$  and  $Pr = 10$  are shown in Table 4.12. It shows the conjugate parameter  $\chi$  has no effect on the reduced skin friction coefficient  $f''(0)$ , but, heat transfer coefficient  $-_{\theta}'(0)$  increases with increasing the values of conjugate parameter  $\chi$ .

In addition, temperature profiles  $\theta(y)$  with governing parameters are plotted in Figures 4.14 to 4.18. Figure 4.14 shows the temperature profiles  $\theta(y)$  for various values of  $M = 0.2, 0.5, 1, 2$  when  $Pr = N_R = v = 0.5$  and  $\chi = 0.5$ . It can be seen that temperature  $\theta(y)$  increases with increasing of magnetic field  $M$ . Moreover, the temperature profile  $\theta(y)$  for different values of  $N_R = 0.2, 0.5, 1, 2$  is shown in Figure 4.15. It shows that,

$\theta(\eta)$  increases with increasing values of  $N_R$  and fixed values of  $Pr, M, \nu$  and  $\chi$ . Figure 4.16 illustrates the effect of  $\theta(\eta)$  with various values of  $\chi = 0.2, 0.5, 1, 2$  and fixed value of  $Pr = M = N_R = 0.5$  and  $\nu = 0.5$ . Temperature  $\theta(\eta)$  increases with increasing in the values of  $\chi$ .

On the other hand, Figure 4.17 shows that the temperature  $\theta(\eta)$  increases with the decreasing values of  $Pr$ . Finally, figure 4.18 presents the temperature profile  $\theta(\eta)$  with  $\nu = 0.2, 0.5, 1, 2$  and fixed values of  $Pr = M = N_R = 0.5$  and  $\chi = 0.5$ . It shows the values of  $\nu$  decreases with increasing values of the temperature  $\theta(\eta)$ . The velocity profiles  $f'(\eta)$  for different values of velocity ratio parameter  $\nu$  are illustrated in Figure 4.19. It can be observed from the figure that, the velocity increases with increasing values of  $\nu$ . Figure 4.20 shows the velocity profiles  $f'(\eta)$  for various values of the magnetic parameter  $M$ . The velocity  $f'(\eta)$  is found to be increased with increasing values of  $M$  and for  $\nu < 1$ . While a reverse effect is observed for the case of  $\nu > 1$  and  $Pr = N_R = 1$ .

Table 4.15 displays the comparison velocity and temperature profiles with three cases of boundary conditions. From this table, it's found that, in three cases of boundary conditions the behavior of velocity profile are the same. The velocity increases by increasing the value of  $M$  when  $\nu < 1$ , while a reverse effect is observed for the case of  $\nu > 1$ . Furtherer, the temperature increase with increasing the value of magnetic parameter, but it increases by decreasing  $\nu$ . Just the physical graphs of temperature confirm the boundary conditions.

**Table 4.9:** The comparison of  $-u'(0)$  with various values of  $N_R$ ,  $M$  and  $Pr$  when  $v = 0$  and  $x \rightarrow \infty$

$N_R$	$M$	$Pr$	Magyari and Keller, 1999	Ishak (2011)	Present results
0	0	10	3.660379	3.6604	3.6604
0	0	5	2.500135	2.5001	2.5001
0	0	3	1.869075	1.8691	1.8691
0	0	1	0.954782	0.9548	0.9548
0	1	1	-----	0.8611	0.8611
1	0	1	-----	0.5312	0.5312
1	1	1	-----	0.4505	0.4505

**Table 4.10:** The values of  $-u'(0)$  and  $f''(0)$  with different values of  $M$  when  $v = x = N_R = 0.5$  and  $Pr = 10$

$M$	$-u'(0)$	$f''(0)$
0.3	0.4255	-1.0097
0.5	0.4251	-1.0918
0.7	0.4247	-1.1706
1	0.4241	-1.2831
3	0.4204	-1.9011
5	0.4173	-2.3732
7	0.4145	-2.7652
10	0.4106	-3.2657
15	0.4049	-3.9579

**Table 4.11:** The values of  $-u'(0)$  and  $f''(0)$  with different values of  $N_R$  when  $v = x = M = 0.5$  and  $Pr = 10$

$N_R$	$-u'(0)$	$f''(0)$
0.3	0.4308	-1.0962
0.5	0.4251	-1.0918
0.7	0.4198	-1.0918
1.0	0.4128	-1.0918
3.0	0.3786	-1.0962
5.0	0.3553	-1.1007
7.0	0.3375	-1.1025
10.0	0.3166	-1.1033
15.0	0.2908	-1.1038

**Table 4.12:** The values of  $-u'(0)$  and  $f''(0)$  with different values of  $v$  when  $N_R = x = M = 0.5$  and  $Pr = 10$

$v$	$-u'(0)$	$f''(0)$
0.1	0.4226	-1.4430
0.2	0.4230	-1.3898
0.3	0.4236	-1.3132
0.5	0.4250	-1.0962
0.7	0.4266	-0.8049
1.0	0.4291	-0.2493
3.0	0.4419	6.0538
5.0	0.4498	15.5428
7.0	0.4552	27.4143

**Table 4.13:** The values of  $-u'(0)$  and  $f''(0)$  with different values of Pr when  $N_R = v = M = 0.5$  and  $\chi = 0.5$

Pr	$-u'(0)$	$f''(0)$
0.3	0.2226	-1.1040
0.5	0.2584	-1.1040
0.7	0.2821	-1.1038
1.0	0.3065	-1.1036
3.0	0.3730	-1.1007
5.0	0.3979	-1.0962
7.0	0.4120	-1.0918
10.0	0.4251	-1.0850
15.0	0.4379	-1.0850

**Table 4.14:** The values of  $-u'(0)$  and  $f''(0)$  with different values of  $\chi$  when  $N_R = v = M = 0.5$  and Pr = 10

$\chi$	$-u'(0)$	$f''(0)$
0.1	0.0966	-1.0850
0.2	0.1868	-1.0850
0.3	0.2713	-1.0850
0.5	0.4251	-1.0850
0.7	0.5615	-1.0850
1.0	0.7395	-1.0850
3.0	1.4586	-1.0850
5.0	1.8107	-1.0850
7.0	2.0196	-1.0850

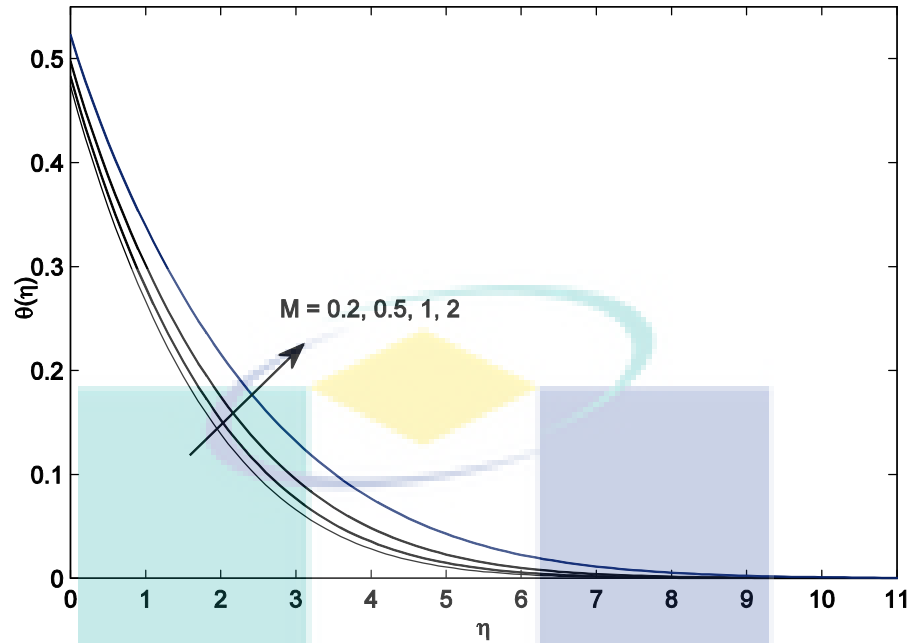


**Figure 4.14:** The temperature profiles  $\theta(\eta)$  for several values of  $M = 0.2, 0.5, 1, 2$  when  $\text{Pr} = N_R = v = 0.5$  and  $\chi = 0.5$

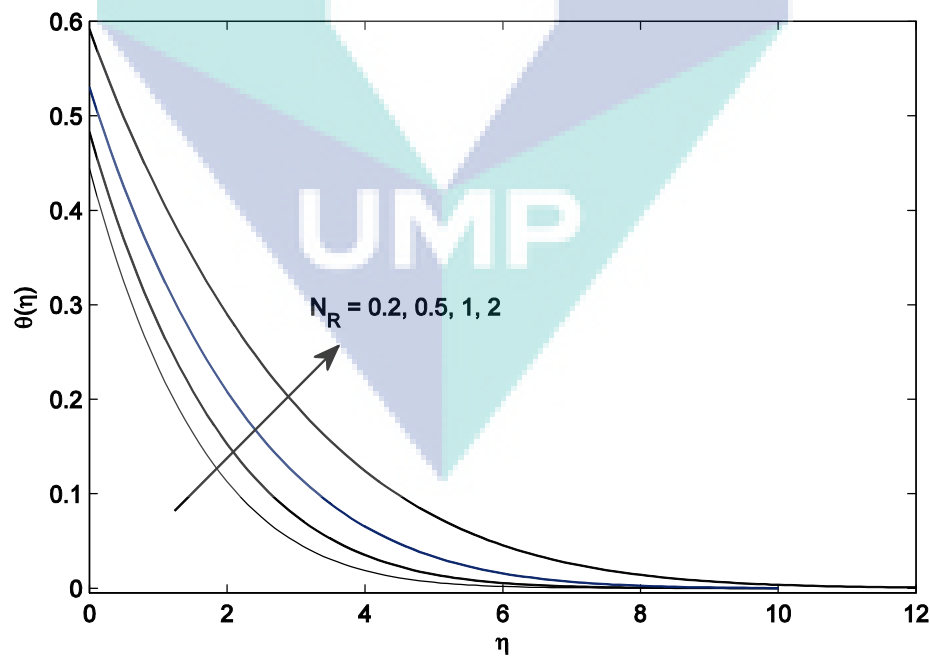


**Figure 4.15:** The temperature profiles  $\theta(\eta)$  for several values of  $N_R = 0.2, 0.5, 1, 2$  when  $\text{Pr} = M = v = 0.5$  and  $\chi = 0.5$

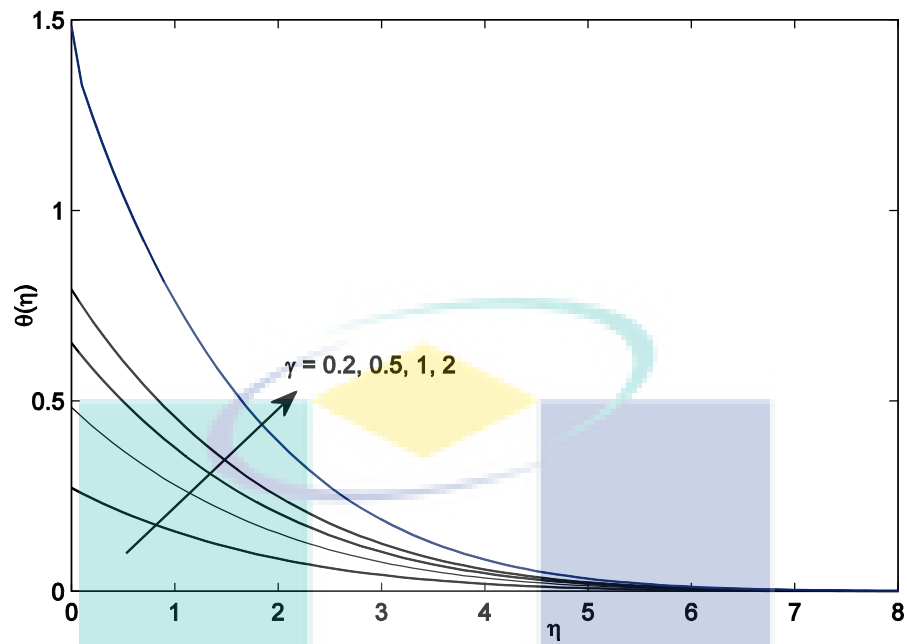


**Figure 4.16:** The temperature profiles  $\theta(\eta)$  for several values of  $\gamma = 0, 2, 0.5, 1, 2$  when  $Pr = M = \nu = 0.5$  and  $N_R = 0.5$

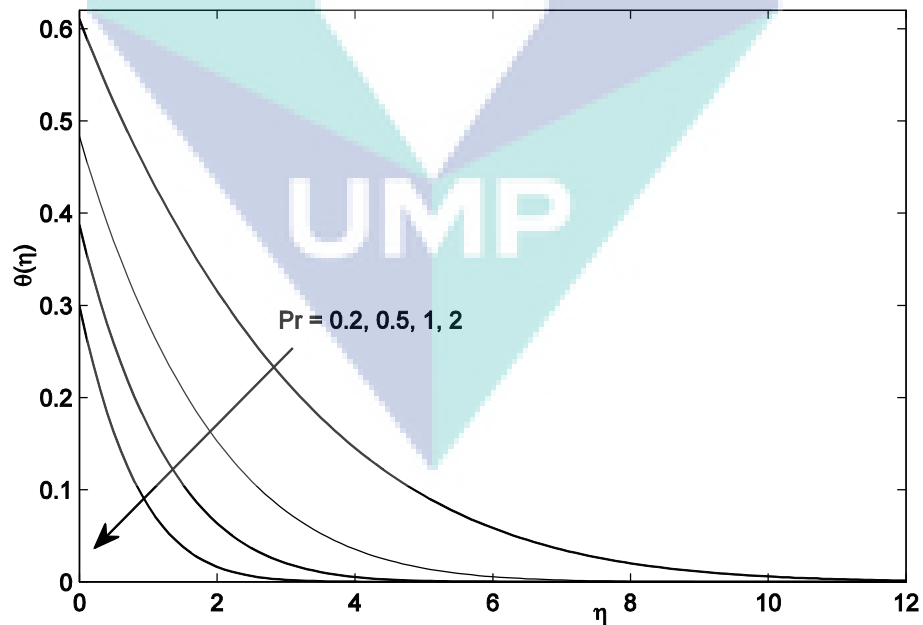


**Figure 4.17:** The temperature profiles  $\theta(\eta)$  for several values of  $Pr = 0, 2, 0.5, 1, 2$  when  $N_R = M = \nu = 0.5$  and  $\chi = 0.5$

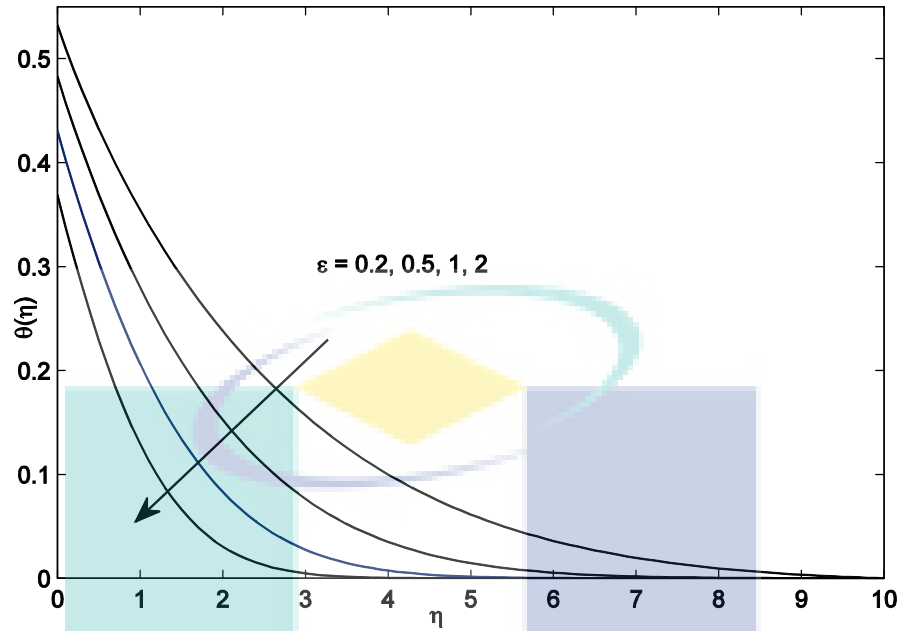


**Figure 4.18:** The temperature profiles  $\theta(\eta)$  for several values of  $\nu = 0.2, 0.5, 1, 2$  when  $N_R = M = \text{Pr} = 0.5$  and  $\chi = 0.5$

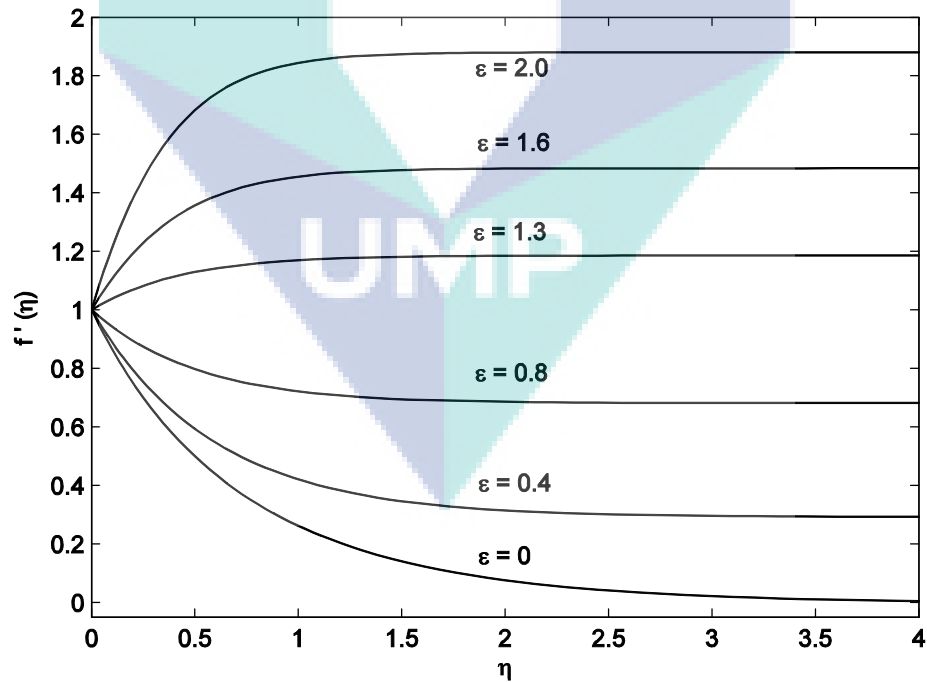


**Figure 4.19:** The velocity profiles  $f'(\eta)$  for several values of  $\nu = 0, 0.4, 0.8, 1.3, 1.6, 2.0$  when  $N_R = M = \text{Pr} = 0.5$  and  $\chi = 0.5$

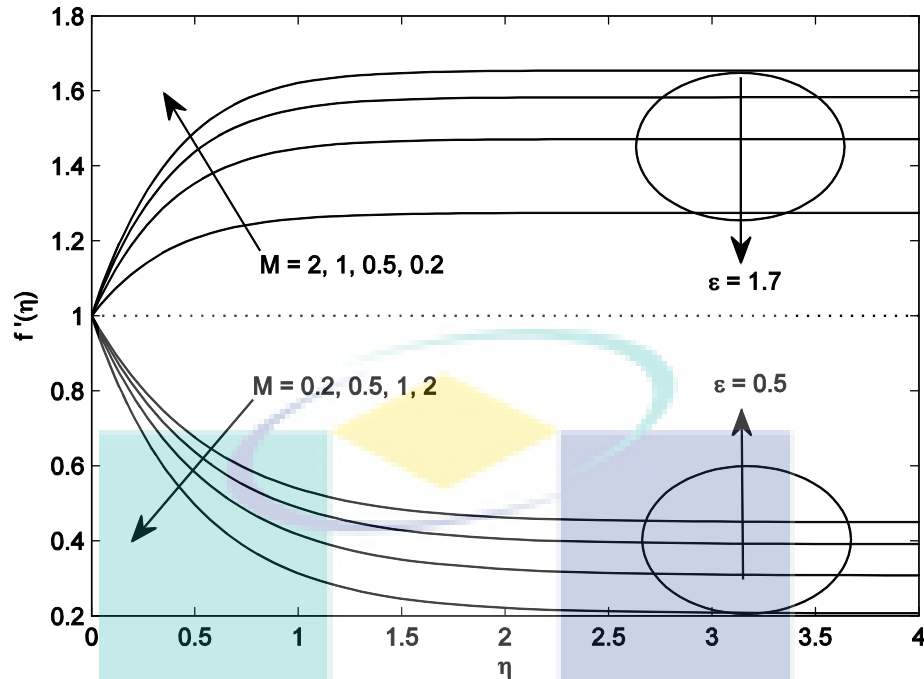


**Figure 4.20:** The velocity profiles  $f'(y)$  for several values of  $M = 0.2, 0.5, 1, 2$  when  $N_R = \chi = Pr = 0.5$  and  $v = 0.5, 1.7$

#### 4.4 CONCLUSION

This chapter investigates the effect of radiation on stagnation point flow and heat transfer toward an exponentially stretching sheet in hydrodynamic field with three cases boundary conditions namely prescribed wall temperature, prescribed surface heat flux and convective boundary conditions are considered. In this investigation, the effect of velocity ratio parameter  $v$ , radiation parameter  $N_R$ , magnetic parameter  $M$ , prandtl number  $Pr$  and conjugate parameter  $\chi$  on reduced skin friction coefficient, local Nusselt number, velocity and temperature profile are discussed.

Temperature profile increases when the values of the radiation parameter and magnetic parameter increase, but with an increase in temperature profile, the values of the Prandtl number and velocity ration parameter are decreased. The temperature profile and velocity profile increases with increasing values of the conjugate parameter and velocity ratio parameter, respectively.

**Table 4.15:** The comparison velocity and temperature profiles with three boundary conditions PWT, PHF and CBC

	PWT	PHF	CBC
Boundary conditions	$u = U_w(x), v = 0, T = T_\infty + T_0 e^{\left(\frac{x}{2L}\right)}$ at $y = 0$ , $u = U_e(x), T \rightarrow T_\infty$ as $y \rightarrow \infty$ , and $f(0) = 0, f'(0) = 1, \theta(0) = 1,$ $f'(\infty) = v, \theta(\infty) = 0,$	$u = U_w(x), v = 0, \frac{\partial T}{\partial y} = -\frac{q_w}{k}$ at $y = 0$ , $u = U_e(x), T \rightarrow T_\infty$ as $y \rightarrow \infty$ , and $f(0) = 0, f'(0) = 1, \theta'(0) = -1,$ $f'(\infty) = v, \theta(\infty) = 0,$	$u = U_w(x), v = 0, -k \frac{\partial T}{\partial y} = h(T_\infty - T)$ at $y = 0$ , $u = U_e(x), T \rightarrow T_\infty$ as $y \rightarrow \infty$ , and $f(0) = 0, f'(0) = 1, \theta'(0) = -\lambda(1 - \theta(0)),$ $f'(\infty) = v, \theta(\infty) = 0,$
Velocity Profile	$\uparrow M, \uparrow f'(y), v > 1$ $\uparrow M, \downarrow f'(y), v < 1$ 	$\uparrow M, \uparrow f'(y), v > 1$ $\uparrow M, \downarrow f'(y), v < 1$ $\uparrow v, \uparrow f'(y),$ $v > 1$ and $v < 1$ 	$\uparrow M, \uparrow f'(y), v > 1$ $\uparrow M, \downarrow f'(y), v < 1$ $\uparrow v, \uparrow f'(y),$ $v > 1$ and $v < 1$ 
Temperature profile	$\uparrow v, \downarrow \theta(y)$ $\uparrow M, \uparrow \theta(y)$ 	$\uparrow v, \downarrow \theta(y)$ $\uparrow M, \uparrow \theta(y)$ 	$\uparrow v, \downarrow \theta(y)$ $\uparrow M, \uparrow \theta(y)$ 

## CHAPTER 5

### CONCLUSIONS

#### 5.1 SUMMARY AND CONCLUSION

This research project considers two main problems. The first problem is that of the boundary layer stagnation point flow and heat transfer over an exponentially stretching sheet. This problem considers three cases of boundary conditions namely, prescribed wall temperature, prescribed surface heat flux and convective boundary conditions. The second problem is the radiation effects on the MHD stagnation point and heat transfer towards an exponentially stretching sheet. This problem also, considers three cases of boundary conditions, prescribed wall temperature, prescribed surface heat flux and convective boundary conditions. We derive the mathematical models of these problems. First of all, the nonlinear partial differential equations are transformed to nonlinear ordinary differential equations by similarity transformation. The nonlinear ordinary differential equations have being numerically solved by using the Keller-box method.

General introductions, the boundary layer theory, boundary conditions, research objective, research scope, literature review, significant of the research and thesis outline are presented in Chapter 1. The governing equation and detailed numerical method are discussed in Chapter 2. In this chapter, the Keller-box method is considered for a particular problem of the boundary layer stagnation point flow and heat transfer over an exponentially stretching sheet with prescribed wall temperature. This method involves several steps. Firstly, the ordinary differential equation is reduced to a system of first-order equations. Then, the system rewrites in finite difference forms using central difference. Next, Newton's method is used for linearization. The linear system is solved

by using the block triadiagonal elimination technique, the Keller-box method is programmed in MATLAB. The complete program is given in Appendix B.

Chapter 3 discusses the first problem of stagnation point flow and heat transfer towards an exponentially stretching/shrinking sheet. The problem considers three cases of boundary conditions, namely prescribed wall temperature, prescribed surface heat flux and convective boundary conditions. The results of this problem were compared with the existing results from literature and the results obtained are consistent with previous reported results. The effects of the governing parameter namely the Prandtl number and stretching/shrinking parameter on the momentum and energy equations are discussed. The equations have dual, unique and non-similarity solution and which is dependent on the velocity ratio parameter. When  $-0.9734 \leq v \leq -1.487068$  the equations have dual solution, the unique solution exists for  $v > -0.9734$  and non-similarity solution is found for  $v < -1.487068$ . For the case of convective boundary conditions, we found that the critical values for prandtl number  $Pr$  and conjugate parameter  $\chi$  in second solution. The prandtl number  $Pr$  must be smaller than a critical value  $Pr_c$  and it depends on conjugate parameter  $\chi$ . Furthermore, the conjugate parameter  $\chi$  must be greater than some critical value  $\chi_c$  which depends on the Prandtl number  $Pr$ .

The radiation effect on the magnetohydrodynamic (MHD) stagnation point flow and heat transfer over an exponentially stretching sheet is presented in chapter 4. This chapter studied the effect of the radiation parameter, magnetic parameter, Prandtl number and stretching parameter on the reduced skin friction coefficient, local Nusselt number as well as velocity and temperature profiles. We consider three cases of boundary conditions namely prescribed wall temperature, prescribed surface heat flux and convective boundary conditions. The problem is then reduced to a system of nonlinear ordinary differential equation. The results are also compared with the existing results in the literature. The results are presented in the tabular form and graphically. It can be concluded that we have added two parameters namely the radiation parameter, the magnetic parameter in second problem, so we can compare these two problem, it is

important to know the effects of these two parameter on skin friction coefficient, heat transfer coefficient, velocity profile and temperature.

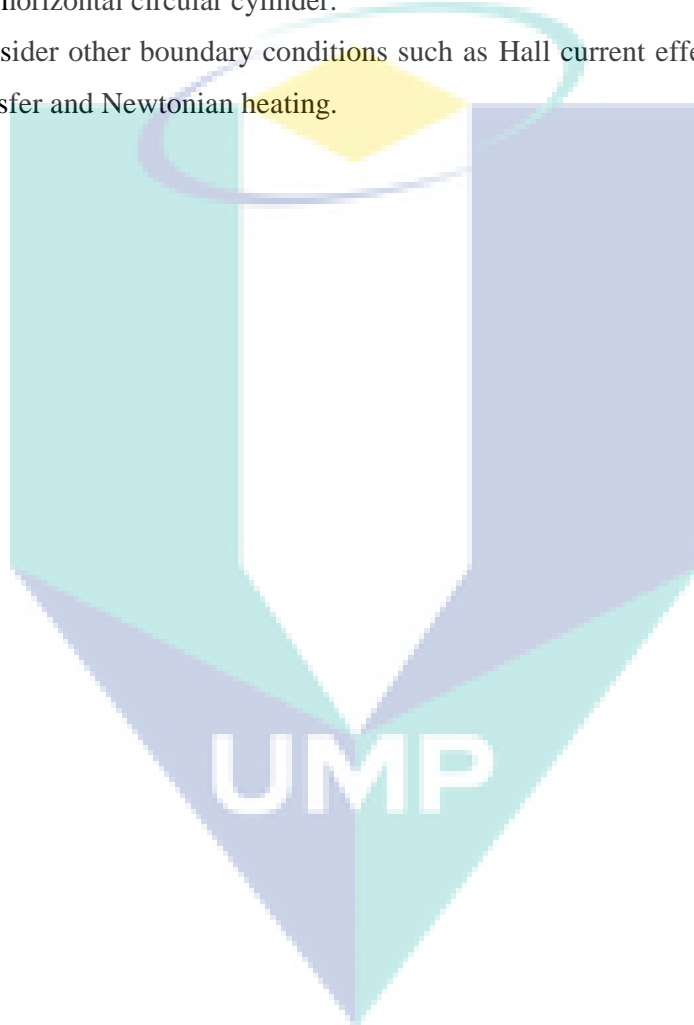
In comparison we can write, the heat transfer coefficient increased with increasing values of the velocity ratio parameter and Prandtl number in both problems, meanwhile it decreases with the increasing values of the magnetic parameter and radiation parameter in second problem. In these three cases of boundary conditions the behavior of temperature are the same. In both problems, the temperature profiles decrease with the increase in the values of Prandtl number and the velocity ratio parameter. But in second problem, the temperature increases with increasing values of radiation parameter and magnetic parameter. The temperature increases with the increase in the values of conjugate parameter for case of convective boundary conditions in both problems. In comparison, the radiation parameter has negative effects on heat transfer, but the magnetic parameter has positive effects in velocity of flow. In addition, it can be concluded from the graphs that temperature is highest near the plate, decreases when further away from the plate and asymptotically approaches zero in the free stream region.

The contributions in this thesis are presented in the form of reduced skin friction coefficient, heat transfer coefficient, local Nusselt number, and dimensionless velocity and temperature profiles for various values of velocity ratio parameter, Prandtl number, magnetic parameter, radiation parameter and conjugate parameter.

## **5.2 SUGGESTION FOR FUTURE STUDIES**

There are number of interesting investigations regarding the problem of boundary layer flow. The problem of boundary layer stagnation point flow towards an exponentially stretching sheet is presented in this thesis. This problem concentrates on three types of boundary conditions which are prescribed wall temperature, prescribed surface heat flux and convective boundary conditions. This problem might be extended for future studies as follows

1. Include other effects such as chemical reaction, slip effects and sores/dufour which are also important in industrial applications.
2. Consider the nanosize particles (nanofluid) and viscoelastic due to its important applications such as in cooling of a large metallic plate in a bath and glass fiber production.
3. Consider other geometrics such as vertical plate inclined stretching plate, sphere and horizontal circular cylinder.
4. Consider other boundary conditions such as Hall current effect convective heat transfer and Newtonian heating.



## REFERENCES

- Abd El-Aziz, M. 2009. Viscous dissipation effect on mixed convection flow of a micropolar fluid over an exponentially stretching sheet. *Canadian Journal of Physics*, **87** (4): 359-368.
- Ahmad, S. 2009. *Convection Boundary Layer Flows over Needles and Cylinders in Viscous Fluids*. Ph. D Thesis, Universiti Putra Malaysia, Malaysia.
- Aman, F., Ishak, A., and Pop, I. 2013. Magneto hydrodynamic stagnation-point flow towards a stretching/shrinking sheet with slip effects. *International Communications in Heat and Mass Transfer*, **47**: 68-72.
- Anwar, M., Khan, I., Sharidan, S., and Salleh, M. Z. 2012. Conjugate effects of heat and mass transfer of nanofluids over a nonlinear stretching sheet. *International Journal of Physical Sciences*, **7** (26): 4081-4092.
- Aziz, A. 2009. A similarity solution for laminar thermal boundary layer over a flat plate with a convective surface boundary condition. *Communications in Nonlinear Science and Numerical Simulation*, **14** (4): 1064-1068.
- Bachok, N., Ishak, A., Nazar, R., and Senu, N. 2013. Stagnation-point flow over a permeable stretching/shrinking sheet in a copper-water nanofluid. *Boundary Value Problems*, **2013** (1): 1-10.
- Bachok, N., Ishak, A., and Pop, I. 2012. Boundary layer stagnation-point flow and heat transfer over an exponentially stretching/shrinking sheet in a nanofluid. *International Journal of Heat and Mass Transfer*, **55** (25): 8122-8128.
- Bachok, N., Ishak, A., and Pop, I. 2013. Stagnation point flow toward a stretching/shrinking sheet with a convective surface boundary condition. *Journal of the Franklin Institute*, **350** (9): 2736-2744.
- Baehr, H. D., and Stephan, K. 1994. *Heat and Mass Transfer*. Berlin Heidelberg: Springer Verlag.
- Bejan, A. 1984. *Convection Heat Transfer (second edition)*. New York: John Wiley & Sons.
- Bejan, A., and Kraus, A. D. 2003. *Heat Transfer Handbook*. (Vol. 1), New York: John Wiley & Sons.

- Bhattacharyya, K. 2011a. Boundary layer flow and heat transfer over an exponentially shrinking sheet. *Chinese Physics Letters*, **28** (7): 074701.
- Bhattacharyya, K. 2011b. Dual solutions in boundary layer stagnation-point flow and mass transfer with chemical reaction past a stretching/shrinking sheet. *International Communications in Heat and Mass Transfer*, **38** (7): 917-922.
- Bhattacharyya, K. 2012. Steady boundary layer flow and reactive mass transfer past an exponentially stretching surface in an exponentially moving free stream. *Journal of the Egyptian Mathematical Society*, **20** (3): 223-228.
- Bhattacharyya, K. 2013. Heat transfer analysis in unsteady boundary layer stagnation-point flow towards a shrinking/stretching sheet. *Ain Shams Engineering Journal*, **4** (2): 259-264.
- Bhattacharyya, K., and Vajravelu, K. 2012. Stagnation-point flow and heat transfer over an exponentially shrinking sheet. *Communications in Nonlinear Science and Numerical Simulation*, **17** (7): 2728-2734.
- Bidin, B., and Nazar, R. 2009. Numerical solution of the boundary layer flow over an exponentially stretching sheet with thermal radiation. *European Journal of Scientific Research*, **33** (4): 710-717.
- Burmeister, L. C. 1983. *Convective Heat Transfer*. New York: John Wiley & Sons.
- Cebeci, T., and Bradshaw, P. 1988. *Physical and Computational Aspects of Convective Heat Transfer*. New York: Springer.
- Cebeci, T., and Cousteix, J. (2005). *Modeling and Computing of Boundary-Layer Flows*; New York: Springer
- Chen, C. K., and Char, M. I. 1988. Heat transfer of a continuous, stretching surface with suction or blowing. *Journal of Mathematical Analysis and Applications*, **135** (2): 568-580.
- Chiam, T. 1994. Stagnation-point flow towards a stretching plate. *Journal of the Physical Society of Japan*, **63** (6): 2443-2444.
- Crane, L. J. 1970. Flow past a stretching plate. *Zeitschrift für angewandte Mathematik und Physik ZAMP*, **21** (4): 645-647.
- Davidson, P. A. 2001. *An Introduction to Magnetohydrodynamics*. (Vol. 25) United Kingdom : Cambridge University Press.

- Elbashbeshy, E. 2001. Heat transfer over an exponentially stretching continuous surface with suction. *Archives of Mechanics*, **53** (6): 643-651.
- Elbashbeshy, E., and Bazid, M. 2002. The mixed convection along a vertical plate with variable surface heat flux embedded in porous medium. *Applied Mathematics and Computation*, **125** (2): 317-324.
- Elbashbeshy, E. M. A., and Aldawody, D. A. 2010. Heat transfer over an unsteady stretching surface with variable heat flux in the presence of a heat source or sink. *Computers & Mathematics with Applications*, **60** (10): 2806-2811.
- Elbashbeshy, E. M. A., Emam, T. G., and Abdelgaber, K. M. 2012. Effects of thermal radiation and magnetic field on unsteady mixed convection flow and heat transfer over an exponentially stretching surface with suction in the presence of internal heat generation/absorption. *Journal of the Egyptian Mathematical Society*, **20** (3): 215-222.
- Gupta, P., and Gupta, A. 1977. Heat and mass transfer on a stretching sheet with suction or blowing. *The Canadian Journal of Chemical Engineering*, **55** (6): 744-746.
- Hamad, M. 2011. Analytical solution of natural convection flow of a nanofluid over a linearly stretching sheet in the presence of magnetic field. *International Communications in Heat and Mass Transfer*, **38** (4): 487-492.
- Hayat, T., Javed, T., and Abbas, Z. 2009. MHD flow of a micropolar fluid near a stagnation-point towards a non-linear stretching surface. *Nonlinear Analysis: Real World Applications*, **10** (3): 1514-1526.
- Hiemenz, K. 1911. Boundary layer for a homogeneous flow around a dropping cylinder. *Dinglers Polytech. J.*, **326**: 321-410.
- Incropera, F. P. 2011. *Introduction to Heat Transfer*. New York: John Wiley & Sons.
- Ishak, A. 2010. Similarity solutions for flow and heat transfer over a permeable surface with convective boundary condition. *Applied Mathematics and Computation*, **217** (2): 837-842.
- Ishak, A. 2011. MHD boundary layer flow due to an exponentially stretching sheet with radiation effect. *Sains Malaysiana*, **40** (4): 391-395.
- Ishak, A., Jafar, K., Nazar, R., and Pop, I. 2009. MHD stagnation point flow towards a stretching sheet. *Physica A: Statistical Mechanics and its Applications*, **388** (17): 3377-3383.

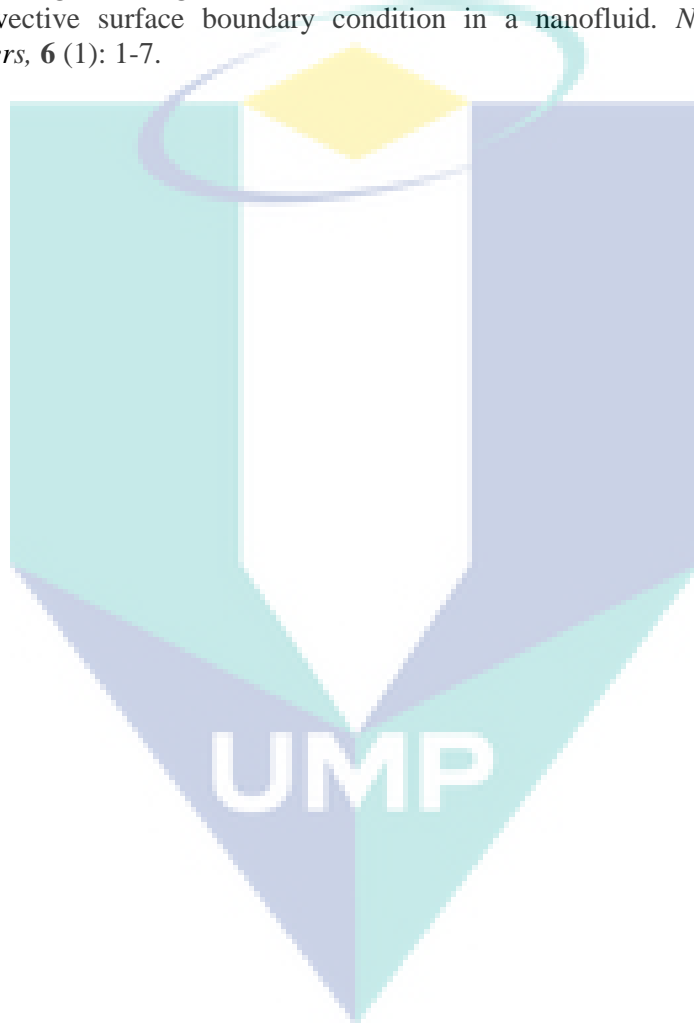
- Ishak, A., Lok, Y. Y., and Pop, I. 2010. Stagnation-point flow over a shrinking sheet in a micropolar fluid. *Chemical Engineering Communications*, **197** (11): 1417-1427.
- Ishak, A., Nazar, R., and Pop, I. 2006. Mixed convection boundary layers in the stagnation-point flow toward a stretching vertical sheet. *Meccanica*, **41** (5): 509-518.
- Ishak, A., Nazar, R., and Pop, I. 2008a. Magnetohydrodynamic (MHD) flow of a micropolar fluid towards a stagnation point on a vertical surface. *Computers & Mathematics with Applications*, **56** (12): 3188-3194.
- Ishak, A., Nazar, R., and Pop, I. 2008b. Mixed convection stagnation point flow of a micropolar fluid towards a stretching sheet. *Meccanica*, **43** (4): 411-418.
- Jafar, K., Ishak, A., and Nazar, R. 2011. MHD Stagnation-Point Flow over a Nonlinearly Stretching/Shrinking Sheet. *Journal of Aerospace Engineering*, **26** (4): 829-834.
- Kakac, S., Yener, Y., and Pramuanjaroenkij, A. 2013. *Convective Heat Transfer*. Boca Raton: CRC Press.
- Keller, H. B. 1970. A New Difference Scheme for Parabolic Problems *Dalam: Bramble, Numerical Solution of Partial Differential Equations*. New York: Academic Press.
- Keller, H. B., and Cebeci, T. 1972. Accurate Numerical Methods for Boundary-Layer Flows. II: Two Dimensional Turbulent Flows. *AIAA Journal*, **10** (9): 1193-1199.
- Khan, S. K. 2006. Boundary layer viscoelastic fluid flow over an exponentially stretching sheet. *Applied Mechanics and Engineering*, **11** (2): 321.
- Khan, S. K., and Sanjayanand, E. 2005. Viscoelastic boundary layer flow and heat transfer over an exponential stretching sheet. *International Journal of Heat and Mass Transfer*, **48** (8): 1534-1542.
- Kumari, M., and Nath, G. 1989. Unsteady mixed convection with double diffusion over a horizontal cylinder and a sphere within a porous medium. *Wärme-und Stoffübertragung*, **24** (2): 103-109.
- Kumari, M., Takhar, H. S., and Nath, G. 1990. MHD flow and heat transfer over a stretching surface with prescribed wall temperature or heat flux. *Wärme-und Stoffübertragung*, **25** (6): 331-336.
- Lin, C. R., and Chen, C. K. 1998. Exact solution of heat transfer from a stretching surface with variable heat flux. *Heat and Mass Transfer*, **33** (5-6): 477-480.

- Lok, Y. Y. 2008. *Mathematical Modelling of a Micropolar Fluid Boundary Layer near a Stagnation-point*. Ph.D. Thesis, Universiti Teknologi Malaysia.
- Luikov, A., Aleksashenko, V., and Aleksashenko, A. 1971. Analytical methods of solution of conjugated problems in convective heat transfer. *International Journal of Heat and Mass Transfer*, **14** (8): 1047-1056.
- Mabood, F., Khan, W. A., and Ismail, A. I. M. 2014. MHD flow over exponential radiating stretching sheet using homotopy analysis method. *Journal of King Saud University - Engineering Sciences*.
- Magyari, E., and Keller, B. 1999. Heat and mass transfer in the boundary layers on an exponentially stretching continuous surface. *Journal of Physics D: Applied Physics*, **32** (5): 577-585.
- Mahapatra, T. R., and Gupta, A. 2001. Magnetohydrodynamic stagnation-point flow towards a stretching sheet. *Acta Mechanica*, **152** (1-4): 191-196.
- Makinde, O. 2010. MHD mixed-convection interaction with thermal radiation and nth order chemical reaction past a vertical porous plate embedded in a porous medium. *Chemical Engineering Communications*, **198** (4): 590-608.
- Makinde, O., and Aziz, A. 2010. MHD mixed convection from a vertical plate embedded in a porous medium with a convective boundary condition. *International Journal of Thermal Sciences*, **49** (9): 1813-1820.
- Makinde, O. D., and Aziz, A. 2011. Boundary layer flow of a nanofluid past a stretching sheet with a convective boundary condition. *International Journal of Thermal Sciences*, **50** (7): 1326-1332.
- Malvandi, A., Hedayati, F., and Domairry, G. 2013. Stagnation point flow of a nanofluid toward an exponentially stretching sheet with nonuniform heat generation/absorption. *Journal of Thermodynamics*, **2013**.
- Mandal, I. C., and Mukhopadhyay, S. 2013. Heat transfer analysis for fluid flow over an exponentially stretching porous sheet with surface heat flux in porous medium. *Ain Shams Engineering Journal*, **4** (1): 103-110.
- Merkin, J. 1994. Natural-convection boundary-layer flow on a vertical surface with Newtonian heating. *International journal of heat and fluid flow*, **15** (5): 392-398.
- Merkin, J., and Pop, I. 2011. The forced convection flow of a uniform stream over a flat surface with a convective surface boundary condition. *Communications in Nonlinear Science and Numerical Simulation*, **16** (9): 3602-3609.

- Mohamed, M. K. A., Salleh, M. Z., Nazar, R., and Ishak, A. 2013. Numerical investigation of stagnation point flow over a stretching sheet with convective boundary conditions. *Boundary Value Problems*, **2013** (1): 1-10.
- Mohamed, M. K. A. 2013. *Mathematical modeling for the convection boundary layer flow in a viscous fluid with newtonian heating and convective boundary conditions*. MSc. Thesis. Universiti Malaysia Pahang.
- Mukhopadhyay, S. 2013. Slip effects on MHD boundary layer flow over an exponentially stretching sheet with suction/blowing and thermal radiation. *Ain Shams Engineering Journal*, **4** (3): 485-491.
- Mustafa, M., Farooq, M. A., Hayat, T., and Alsaedi, A. 2013. Numerical and Series Solutions for Stagnation-Point Flow of Nanofluid over an Exponentially Stretching Sheet. *PloS one*, **8** (5): e61859.
- Na, T. 1979. *Computational Methods in Engineering Boundary Value Problems*. New York: Academic Press.
- Nadeem, S., and Lee, C. 2012. Boundary layer flow of nanofluid over an exponentially stretching surface. *Nanoscale research letters*, **7** (1): 1-6.
- Nadeem, S., Ul Haq, R., and Khan, Z. H. 2014. Heat transfer analysis of water-based nanofluid over an exponentially stretching sheet. *Alexandria Engineering Journal*, **53** (1): 219-224.
- Nazar, R. 2003. *Mathematical Models for Free and Mixed Convection Boundary Layers flow of Micropolar Fluids*. Ph.D. Thesis, Universiti Teknologi Malaysia.
- Nazar, R., Amin, N., Filip, D., and Pop, I. 2004. Unsteady boundary layer flow in the region of the stagnation point on a stretching sheet. *International Journal of Engineering Science*, **42** (11): 1241-1253.
- Nazar, R., Amin, N., and Pop, I. 2002. Free convection boundary layer on an isothermal horizontal circular cylinder in a micropolar fluid. *Heat Transfer*, **2**: 525-530.
- Pavithra, G. M., and Giresha, B. J. 2014. Unsteady flow and heat transfer of a fluid-particle suspension over an exponentially stretching sheet. *Ain Shams Engineering Journal*, **5** (2): 613-624.
- Pramanik, S. 2014. Casson fluid flow and heat transfer past an exponentially porous stretching surface in presence of thermal radiation. *Ain Shams Engineering Journal*, **5** (1): 205-212.
- Rolle, K. C. 2014. *Heat & Mass Transfer (2nd Edition)*. United States of America, Boston: Cl-Engineering.

- Rosali, H., Ishak, A., and Pop, I. 2011. Stagnation point flow and heat transfer over a stretching/shrinking sheet in a porous medium. *International Communications in Heat and Mass Transfer*, **38** (8): 1029-1032.
- Ro ca, N. C., Ro ca, A. V., and Pop, I. 2014. Stagnation point flow and heat transfer over a non-linearly moving flat plate in a parallel free stream with slip. *Communications in Nonlinear Science and Numerical Simulation*, **19** (6): 1822-1835.
- Sajid, M., and Hayat, T. 2008. Influence of thermal radiation on the boundary layer flow due to an exponentially stretching sheet. *International Communications in Heat and Mass Transfer*, **35** (3): 347-356.
- Sakiadis, B. 1961. Boundary-layer behavior on continuous solid surfaces: I. Boundary-layer equations for two-dimensional and axisymmetric flow. *AIChE Journal*, **7** (1): 26-28.
- Salleh, M. Z., Nazar, R., and Pop, I. 2010a. Boundary layer flow and heat transfer over a stretching sheet with Newtonian heating. *Journal of the Taiwan Institute of Chemical Engineers*, **41** (6): 651-655.
- Salleh, M. Z., Nazar, R., and Pop, I. 2009. Forced convection boundary layer flow at a forward stagnation point with Newtonian heating. *Chemical Engineering Communications*, **196** (9): 987-996.
- Salleh, M. Z., Nazar, R., and Pop, I. 2010b. Mixed convection boundary layer flow about a solid sphere with Newtonian heating. *Archives of Mechanics*, **62** (4): 283-303.
- Schlichting, H. 1979. *Boundary Layer Theory. (7th Edition)*. New York: McGraw-Hill Inc.
- Shu, J.-J., and Pop, I. 1998. On thermal boundary layers on a flat plate subjected to a variable heat flux. *International journal of heat and fluid flow*, **19** (1): 79-84.
- Suali, M., Long, N., and Ishak, A. 2012. Unsteady stagnation point flow and heat transfer over a stretching/shrinking sheet with prescribed surface heat flux. *Applied Mathematics and Computational Intelligence*, **1** (1): 1-11.
- Tilley, B., and Weidman, P. 1998. Oblique two-fluid stagnation-point flow. *European Journal of Mechanics-B/Fluids*, **17** (2): 205-217.
- Tsou, F., Sparrow, E., and Goldstein, R. J. 1967. Flow and heat transfer in the boundary layer on a continuous moving surface. *International Journal of Heat and Mass Transfer*, **10** (2): 219-235.

- Wang, C. 2008. Stagnation flow towards a shrinking sheet. *International Journal of Non-Linear Mechanics*, **43** (5): 377-382.
- Wong, S. W., Awang, M. O., and Ishak, A. 2011. Stagnation-Point Flow over an Exponentially Shrinking/Stretching Sheet. *Zeitschrift fur Naturforschung A-Journal of Physical Sciences*, **66** (12): 705.
- Yacob, N. A., Ishak, A., Pop, I., and Vajravelu, K. 2011. Boundary layer flow past a stretching/shrinking surface beneath an external uniform shear flow with a convective surface boundary condition in a nanofluid. *Nanoscale research letters*, **6** (1): 1-7.



## APPENDIX A

## LIST OF SYMBOLS IN MATLAB PROGRAM

MATLAB	KELLER-BOX
np	$J$
eta, etainf, deleta	$y, y_{\infty}, \Delta y$
f, u, v, s, t	$f, f', f'', u, u'$
cfb, cub, cvb, csb, ctb	$f_{j-1/2}^{n-1}, u_{j-1/2}^{n-1}, v_{j-1/2}^{n-1}, s_{j-1/2}^{n-1}, t_{j-1/2}^{n-1}$
cuub, cfvb, cftb, cusb	$(u_{j-1/2}^{n-1})^2, f_{j-1/2}^{n-1}v_{j-1/2}^{n-1}, f_{j-1/2}^{n-1}t_{j-1/2}^{n-1}, u_{j-1/2}^{n-1}s_{j-1/2}^{n-1}$
cdervb, cdertb	$(v_j^{n-1} - v_{j-1}^{n-1})h_j^{-1}, (t_j^{n-1} - t_{j-1}^{n-1})h_j^{-1}$
fb, ub, vb, sb, tb	$f_{j-1/2}, u_{j-1/2}, v_{j-1/2}, s_{j-1/2}, t_{j-1/2}$
uub, fvb, ftb, usb	$(u_{j-1/2})^2, f_{j-1/2}v_{j-1/2}, f_{j-1/2}t_{j-1/2}, u_{j-1/2}s_{j-1/2}$
dervb, dertb	$(v_j - v_{j-1})h_j^{-1}, (t_j - t_{j-1})h_j^{-1}$
a1 to a6	$(a_1)_j$ to $(a_6)_j$
b1 to b8	$(b_1)_j$ to $(b_8)_j$
r1 to r5	$(r_1)_j$ to $(r_5)_j$
r1, r2	$(R_1)_{j-1/2}^{n-1}, (R_2)_{j-1/2}^{n-1}$
a, b, c	$[A_j], [B_j], [C_j]$
alfa, gamma	$[r_j], [\Gamma_j]$
ww, rr, dell	$[W_j], [r_j], [u_j]$
delf, delu, delv, dels, delt	$u f, u u, u v, u s, u t$



```

etaul5 = 1 / eta(np,1);
etanp = eta(np,1);
for j = 1:np
deta(j,k) = deleta;
etab = eta(j,1) / eta(np,1);
etabl = (1-etab);
etab2 = (1-etab)^2;
etau = eta(j,1);

% initial guess used for Eqs. (2.116)-(2.120)

f(j,1) = etau * (ee + 0.5 * etab * (1-ee));
u(j,1) = etab + eeetabl;
v(j,1) = etaul5 * (1 - ee);
s(j,1) = etab2;
t(j,1) = -2* etabl * etaul5;
end

% Present station
% Eqs. (2.51)- (2.53)

for j = 2: np

fb(j,k) = 0.5 * (f(j,k) + f(j-1,k));
ub(j,k) = 0.5 * (u(j,k) + u(j-1,k));
vb(j,k) = 0.5 * (v(j,k) + v(j-1,k));
sb(j,k) = 0.5 * (s(j,k) + s(j-1,k));
tb(j,k) = 0.5 * (t(j,k) + t(j-1,k));
fvb(j,k) = fb(j,k) * vb(j,k);
uub(j,k) = ub(j,k) * ub(j,k);
ftb(j,k) = fb(j,k) * tb(j,k);
sub(j,k) = sb(j,k) * ub(j,k);

%coefficients of the difference momentum equation (2.89)

a1(j,k) = 1.0 + ( 0.5 * deta(j,k) * fb(j,k));
a2(j,k) = a1(j,k) - 2.0;
a3(j,k) = 0.5 * deta(j,k) * vb(j,k);
a4(j,k) = a3(j,k);
a5(j,k) = - deta(j,k) * ub(j,k);
a6(j,k) = a5(j,k);

%coefficients of the difference energy Eq (2.90)

b1(j,k) = 1 + 0.5 * pr * deta(j,k) * fb(j,k);
b2(j,k) = b1(j,k) - 2.0;
b3(j,k) = 0.5 * pr * deta(j,k) * tb(j,k);
b4(j,k) = b3(j,k);
b5(j,k) = -0.5 * pr * deta(j,k) * sb(j,k);
b6(j,k) = b5(j,k);
b7(j,k) = -0.5 * pr * deta(j,k) * ub(j,k);
b8(j,k) = b7(j,k);

% expressions of r(j-1/2) in Eq(2.91)

r1(j,k) = (f(j-1,k) - f(j,k)) + (deta(j,k) * ub(j,k));

```

```

r2(j,k) = (u(j-1,k) - u(j,k)) + (deta(j,k) * vb(j,k));
r3(j,k) = (s(j-1,k) - s(j,k)) + (deta(j,k) * tb(j,k));
r4(j,k) = (v(j-1,k) - v(j,k)) - deta(j,k) * (fvb(j,k)...
+ 2 - 2 * uub(j,k));
r5(j,k) = pr * deta(j,k) *(sub(j,k) - ftb(j,k))...
+(t(j-1,k) - t(j,k)) ;
end

% obtain the matrices

a{2,k} = [0 0 1 0 0; -0.5*deta(2,k) 0 0 -0.5*deta(2,k) 0;...
0 -0.5*deta(2,k) 0 0 -0.5*deta(2,k); a2(2,k) 0 a3(2,k)
a1(2,k) 0;...
0 b2(2,k) b3(2,k) 0 b1(2,k)];
for j= 3:np
a{j,k} = [-0.5*deta(j,k) 0 1 0 0; -1 0 0 -0.5*deta(j,k) 0;...
0 -1 0 0 -0.5*deta(j,k); a6(j,k) 0 a3(j,k) a1(j,k) 0;...
b6(j,k) b8(j,k) b3(j,k) 0 b1(j,k)];
b{j,k} = [0 0 -1 0 0; 0 0 0 -0.5*deta(j,k) 0;...
0 0 0 0 -0.5*deta(j,k); 0 0 a4(j,k) a2(j,k) 0;...
0 0 b4(j,k) 0 b2(j,k)];
end
for j=2: np-1
c{j,k} = [ -0.5*deta(j,k) 0 0 0 0; 1 0 0 0 0 ; 0 1 0 0 0;...
a5(j,k) 0 0 0 0; b5(j,k) b7(j,k) 0 0 0];
end

% The recursion formulas

alfa{2,k} = a{2,k};
for j = 3:np
gamma{j,k} = b{j,k} * inv(alfa{j-1,k});
alfa{j,k} = a{j,k} - gamma{j,k} * c{j-1,k};
end
for j = 2:np
rr{j,k} = [ r1(j,k); r2(j,k); r3(j,k); r4(j,k); r5(j,k)];
end
ww{2,k} = rr{2,k};
for j = 3:np
ww{j,k} = rr{j,k} - gamma{j,k} * ww{j-1,k};
end

% Eq. (2.92)

delf(1,k) = 0;
delu(1,k) = 0;
dels(1,k) = 0;
delu(np,k) = 0;
dels(np,k) = 0;
dell{np,k} = inv(alfa{np,k}) * ww{np,k};
for j = np-1:-1:2
dell{j,k} = inv(alfa{j,k}) * (ww{j,k} - (c{j,k} *
dell{j+1,k}));
end
delv(1,k) = dell{2,k}(1,1);
delt(1,k) = dell{2,k}(2,1);
delf(2,k) = dell{2,k}(3,1);

```

```

delv(2,k) = dell{2,k}(4,1);
delt(2,k) = dell{2,k}(5,1);
for j = np:-1:3
delu(j-1,k) = dell{j,k}(1,1);
dels(j-1,k) = dell{j,k}(2,1);
delf(j,k) = dell{j,k}(3,1);
delv(j,k) = dell{j,k}(4,1);
delt(j,k) = dell{j,k}(5,1);
end

% Newton's method

for j = 1:np
f(j,k+1) = f(j,k) + delf(j,k);
u(j,k+1) = u(j,k) + delu(j,k);
v(j,k+1) = v(j,k) + delv(j,k);
s(j,k+1) = s(j,k) + dels(j,k);
t(j,k+1) = t(j,k) + delt(j,k);
end

% Check for convergence of the derivatives

stop = abs(delv(1,k));
kmax = k;
k = k+1;
end
kmax
f_0=f(1,kmax)
u_0=u(1,kmax)
u_inf=u(np,kmax)
s_0=s(1,kmax)
f_inf=f(np,kmax)
s_inf=s(np,kmax)
t_0=-t(1,kmax)
v_0=v(1,kmax)

plot (eta,s(:,kmax),'r')
xlabel('\eta')
ylabel('\theta(\eta)')

hold on

```

**APPENDIX C****LIST OF PUBLICATIONS****A. Proceeding**Presented

1. Alavi, S. Q., Rosli, N., and Salleh, M. Z. (2015). Numerical Solutions of the Stagnation-Point Flow and Heat Transfer towards an Exponentially Stretching/Shrinking Sheet with Constant Heat Flux. *Paper Presented at the 2nd ISM International Statistical Conference 2014 (ISM-II): Empowering the Applications of Statistical and Mathematical Sciences*. 2015, 541-546.
2. Alavi, S. Q., Rosli, N., A. R. M. Kasim and Salleh, M. Z. (2015). Stagnation point Flow and Heat Transfer Towards an Exponentially Stretching/Shrinking Sheet with Convective Boundary Conditions. *The 3<sup>rd</sup> international Conference on computer Engineering and Mathematical Sciences (ICCEMS 2014): Science & Knowledge Research society*, 2015, 878-882.

**B. Journal**Submit

1. Alavi, S. Q., Abid, H., Rosli, N., and Salleh, M. Z. (2015). MHD Stagnation-Point Flow Towards an Exponentially Stretching Sheet with Prescribed Wall Temperature and Prescribed Heat Flux. *Malaysian Journal of Mathematical Sciences (MJMS)*.